

Study of the role of skin lymphatics in electrolyte and blood pressure regulation

Tore Reikvam

Avhandling for graden philosophiae doctor (ph.d.)
Universitetet i Bergen
2020

UNIVERSITETET I BERGEN



Study of the role of skin lymphatics in electrolyte and blood pressure regulation

Tore Reikvam



Avhandling for graden philosophiae doctor (ph.d.)
ved Universitetet i Bergen

Disputasdato: 21.02.2020

© Copyright Tore Reikvam

Materialet i denne publikasjonen er omfattet av åndsverkslovens bestemmelser.

År: 2020

Tittel: Study of the role of skin lymphatics in electrolyte and blood pressure regulation

Navn: Tore Reikvam

Trykk: Skipnes Kommunikasjon / Universitetet i Bergen

Study of the role of skin lymphatics in electrolyte and blood
pressure regulation

Thesis for the Degree of Philosophiae Doctor (Ph.D.) University
of Bergen

Tore Reikvam

September 2019

Scientific environment

The present work was carried out in The Cardiovascular Research Group at the Department of Biomedicine, University of Bergen during the years 2015-2019. Professor Helge Wiig M.D. Ph.D. was main supervisor, Associate Professor Tine V. Karlsen Ph.D. and Professor Olav Tenstad M.D. Ph.D. were co-supervisors. Financial support was received from The Norwegian Health Association.



Acknowledgments

I would like to express my sincere gratitude to my supervisor Professor Helge Wiig. Thank you for giving me the opportunity to work in your research group and for all your effort to help me during the work with this thesis. I am grateful for the expert advices, discussions, motivation, and encouragement throughout the last four years. Your great knowledge is both impressive and inspirational.

My extended gratitude goes to my supervisors Associated Professor Tine V. Karlsen and Professor Olav Tenstad for their advice and assistance throughout my Ph.D. I would like to thank Olav for technical support and guidance in the lab. This thesis would not have been possible without Tines excellent support and scientific assistance. Your optimism, shared knowledge and good mood are truly appreciated.

Thanks to present and former colleagues in the circulation group; Trude, Elham, Jianhua, Irene, Eli Sihh, Åse, Marek and Anne-Maj. I also would like to thank other colleagues at BBB, Hilde, Penny, Inga and my former office mate Pugaz. I am grateful for all the technical and scientific support for the last four years. The Ph.D. period would not have been the same without any of you.

A special thanks to my friend and former colleague, Miro. It was always a pleasure having you as a guest when you where in Bergen. Attending the wedding of Bettina and you in Switzerland, and meeting little Jonah was something both Ina and I truly appreciated. I hope I will see you in Bergen again soon; you and your family are always welcome.

I am grateful that former member of the group and colleague at the hospital, Øyvind Svendsen, introduced me to Helge, and thereby giving me the opportunity to start my Ph.D. project.

Thanks to Helge for letting me work part time at Håkonsvern during the last year, and thereby giving me the opportunity to learn more about the field of

diving medicine. A special thanks to Lin Hege for all the help at DFS, and to Jan and Rune for sheering their knowledge with me.

To my parents, Åse and Kjell-Olav – Thank you for all the support thorough this process. I can always count on your help and I am grateful for all the discussions we have had, and all the advices you have shared, even if I have not always followed them. Ida and Nora are lucky to have you as grandparents. To my sister and brother, Anne-Grete and Håkon, thanks for always being supportive. My sincere thanks go to my family in-law, Lise, Tore, Kaia, Anette, Terje and Jarl.

And finally, last but not least, my deepest thanks and gratitude goes to Ina. Thank you for always being there for me and all the encouragement and support you have given during this project and in life in general. With you by my side life is better than I ever could have hoped for. To Ida and Nora, the two most precious gifts in life. Thanks for your unconditional love and always helping me remember the important things in life.

Bergen, September 2019

Tore

Abstract

Cardiovascular diseases are the major cause of death worldwide and represent a dramatic socio-economic challenge. Hypertension accounts for 18% of cardiovascular disease deaths in the Western countries, and is a major risk factor for stroke, coronary heart disease and heart failure. Excessive dietary salt intake is known to be a risk factor for developing hypertension, but the pathophysiology of salt sensitive hypertension is poorly understood. The kidneys are the main regulators of Na^+ and water in the body. Salt sensitive hypertension has traditionally been explained by an impaired capacity of the kidneys to excrete Na^+ , resulting in water retention and thereby a progressive alteration in the filling of the vasculature, resulting in increased blood pressure. Recent studies have suggested that Na^+ can be retained or removed from the body without commensurate water, and that the skin may function as sodium reservoir. It has been shown that the Na^+ accumulation is controlled by immune cells and involves modification of the extracellular matrix and lymphangiogenesis in the skin. In this thesis we therefore addressed three major questions to clarify aspects of the new hypothesis proposing the skin as a contributor to Na^+ and blood pressure homeostasis; 1) What are the microcirculatory effects of increased lymphatic vasculature in the skin, 2) are new lymph vessels induced by Na^+ retention functional, and 3) does lymphatic vasculature in the skin affect Na^+ accumulation and blood pressure homeostasis.

To study the microcirculatory effects of a chronically expanded lymphatic vasculature in the skin we used K14-VEGF-C mice overexpressing vascular endothelial growth factor-C (VEGF-C), resulting in an expanded lymphatic network in skin. Acute and chronic inflammation resulted in increased interstitial fluid pressure and reduced lymph flow, but to the same extent in transgenic mice and WT controls. However, after local overhydration in the skin we observed increased lymph flow and fluid transport in the transgenic mice. Despite increased production of the immune cell chemoattractant CCL21 in K14-VEGF-C mice, local inflammation did not result in an increased number of migrating

immune cells from the skin to the draining lymph node. We concluded that lymphangiogenesis might enhance clearance of fluid in situations with increased fluid filtration.

Sodium accumulation in the skin is suggested to be regulated by macrophages that secrete VEGF-C in response to a hyperosmotic microenvironment thereby stimulating lymphangiogenesis. An important question is whether these newly formed vessels are functional. After salt loading in rats we measured lymph flow in skin and muscle with optical imaging and a newly developed PET-CT method. Increased lymph flow was observed in skin as well as muscle. A reduction of lymph flow was observed after macrophage depletion in the skin. Our findings suggest that newly formed lymphatic vessels are functional, and that macrophages may be involved in the regulation of lymph flow and thereby clearance of Na⁺ from tissues.

Previous studies have shown that mice lacking lymphatics in the skin develop higher blood pressure after salt loading. To address the question whether lymphatic vasculature in skin is important for Na⁺ accumulation and blood pressure homeostasis, we used genetically engineered mice with either increased or reduced lymphatic vasculature in the skin. Blood pressure was measured with telemetric recording before salt loading and at the termination of the experiment. Tissue samples from skin and muscle were harvested for analysis of Na⁺ and K⁺ concentration. We found no differences in Na⁺ accumulation or blood pressure response between genetically engineered mice and normal controls. Our results suggest that lymphatic vasculature in skin does not have an important role in electrolyte and blood pressure homeostasis in mice.

List of Publications

This thesis is a summary of the following papers, which is referred to by their roman numerals in the text.

- I. **Karlsen TV, Reikvam T, Tofteberg A, Nikpey E, Skogstrand T, Wagner M, Tenstad O, Wiig H (2017)**
Lymphangiogenesis Facilitates Initial Lymph Formation and Enhances the Dendritic Cell Mobilizing Chemokine CCL21 Without Affecting Migration.
Arterioscler Thromb Vasc Biol. 2017 Nov;37(11):2128-2135. doi: 10.1161/ATVBAHA.117.309883

- II. **Karlsen TV, Nikpey E, Han J, Reikvam T, Rakova N, Castorena-Gonzalez JA, Davis MJ, Titze JM, Tenstad O, Wiig H (2018)**
High-Salt Diet Causes Expansion of the Lymphatic Network and Increased Lymph Flow in Skin and Muscle of Rats.
Arterioscler Thromb Vasc Biol. 2018 Sep;38(9):2054-2064.
doi: 10.1161/ATVBAHA.118.311149.

- III. **Reikvam T, Karlsen TV, Thowsen IM, Skogstrand T, Samuelsson AM, Tenstad O, Wiig H**
No evidence for a role of lymphatics in skin in electrolyte and blood pressure homeostasis in mice.
Manuscript

The finale peer reviewed version of the later published papers is reprinted with permission from the publishers.

Table of Contents

1. Introduction	9
1.1 Preface	11
1.2 Blood pressure	12
1.2.1 Blood pressure regulation	12
1.2.2 Hypertension	14
1.2.3 Pathophysiology of hypertension	14
1.3 The Lymphatic system	16
1.3.1 Lymphatic vasculature	17
1.3.2 Lymph	19
1.3.3 Lymph flow	20
1.3.4 Lymphangiogenesis	21
1.4 Skin	23
1.4.1. The extracellular matrix of the skin	25
1.5 Immune system	26
1.5.1 Immune cells in skin	27
1.5.2 Lymph nodes	28
1.5.3 Immune cell migration from the skin to the lymph node	28
1.5.4 The immune system and hypertension	29
1.6 Sodium	30
1.6.1 Sodium and blood pressure	31
1.6.2 Sodium and the skin	31
2. Aims	34
3. Methods	35
3.1 Animal models	35
3.2 Inducing high blood pressure	36
3.3 Blood pressure measurements	36
3.4 Lymph flow in skin and muscle	37
3.5 Flow cytometry	38
3.6 Immunohistochemistry	39
3.7 Chemical analysis of tissue electrolytes	40
4. Summary of the results	42
5. Discussion	45
5.1 Methodological considerations	45
5.1.1. Animal models of hypertension	45
5.1.2. Inducing hypertension	46
5.1.3. Measuring blood pressure in rodents	47
5.1.4. Immunohistochemistry	49
5.1.5. Flow cytometry	50
5.1.6. Lymph flow	52
5.2 General discussion	53
5.2.1 Lymphangiogenesis and function	53
5.2.2 Blood pressure and lymphatics in the skin	55
5.2.3 Salt accumulation in tissue	57
6. Conclusion	59
7. Future perspectives	60
8. References	61

List of Abbreviations

ABP	Arterial blood pressure
ACE	Angiotensin-converting enzyme
ANG I and II	Angiotensin I and II
ANS	Autonomic nervous system
APC	Antigen presenting cell
AT ₁	Angiotensin II type 1 receptor
CCL21	Chemokine (C-C motif) ligand 21
CCR7	C-C chemokine receptor 7
CNS	Central nervous system
CO	Cardiac output
CT	Computer tomography
DC	Dendritic cell
DOCA	Deoxycorticosterone acetate
DPB	Diastolic blood pressure
DW	Dry weight
ECM	Extracellular matrix
FITC	Fluorescein isothiocyanate
FMO	Fluorescence minus one
GAGs	Glycosaminoglycans
HA	Hyaluronan
HPLC	High performance liquid chromatography
HSD	High salt diet
LC	Langerhans cell
LEC	Lymphatic endothelial cells
LMC	Lymphatic muscle cell
LSD	Low salt diet
MHC II	Major histocompatibility complex II
MMPs	Matrix metalloproteinase
MPS	Mononuclear phagocyte system

MR	Mineralocorticoid receptor
MRI	Magnetic resonance imaging
NSD	Normal salt diet
NO	Nitric oxide
PET	Positron emission tomography
PG	Proteoglycans
P_{if}	Interstitial fluid pressure
PLFG	Placenta growth factor
RAAS	Renin-angiotensin-aldosterone system
ROS	Reactive oxygen species
SBP	Systolic blood pressure
SNS	Sympathetic nervous system
sVEGF-R	Soluble vascular endothelial growth factor receptor
TonEBP	Tonicity-responsive enhancer-binding protein
TPR	Total peripheral resistance
TTW	Total tissue water
VEGF	Vascular endothelial growth factor
VEGFR	Vascular endothelial growth factor receptor
VPR	Volume pressure recording
WT	Wild type

1. Introduction

1.1 Preface

High blood pressure or hypertension is a major risk factor for developing cardiovascular diseases and kidney failure, and is ranked as the leading risk factor for premature deaths in the world. Worldwide over 1 billion people have high blood pressure, and it has been estimated that 9 million people die every year of diseases that are directly linked to hypertension (1).

The relationship between high blood pressure and risk of certain diseases has been known since the 18th century, but it was uncertain whether reducing blood pressure was useful in disease prevention. In 1932 Johan Hay stated that “the greatest danger to man with high blood pressure lies in its discovery, because then some fool is certain to try and reduce it” (2). Today the knowledge of the importance of lowering an elevated blood pressure to reduce the risk of developing diseases is undisputed (3).

Genetics, race, age, gender and behavioural (e.g. smoking, physical inactivity, unhealthy diet) are all factors that are known to predispose individuals for developing hypertension (4). Importantly, a reduction in dietary salt intake has been shown in several studies to lower blood pressure in individuals with hypertension (5).

In the 1960s Guyton et al. introduced the classical view on how salt affects the blood pressure. They stated that hypertension is the result of impaired excretion of sodium in the kidneys, which leads to a higher blood pressure to maintain the sodium excretion, so called pressure natriuresis (6). Here the kidneys were identified as the main regulators of long term blood pressure (7). This hypothesis has been discussed over the years, and it seems clear that the complex mechanisms that lead to hypertension are not exclusively found in the kidneys, but also involve other organ systems.

Titze et al. have shown in studies with mice, rats and humans that salt can be stored in the body without commensurate water and that the skin can be a reservoir for sodium (8-10). These findings have led to the hypothesis that skin might contribute as an extrarenal regulator of the sodium homeostasis in the body. This salt accumulation model seems to involve remodelling of the lymphatic network and activation of immune cells in the skin. Inhibition of the immune cells in the skin after salt loading appears to increase blood pressure (11-13).

In the introduction to my thesis I will briefly discuss the physiology of blood pressure and the pathophysiology that might lead to hypertension. The lymphatic system, the interstitium and the immune system, with a focus on the anatomy and function within the skin, will be described. Towards the end of the introduction I will discuss the role of sodium in fluid volume homeostasis in the body and present elements that seem to be central in the new model of salt storage in the skin.

1.2 Blood pressure

Arterial blood pressure (ABP), hereafter referred to as blood pressure, is an important clinical parameter. Because it is easy and fast to measure and gives important information about patient health, blood pressure is one of the most frequently used clinical parameters. Blood pressure is given with two values, a systolic blood pressure (SBP) and a diastolic blood pressure (DBP), where SBP is the pressure in the arteries during heart contraction and DBP is the pressure when the heart is relaxing.

1.2.1 Blood pressure regulation

In the simplest sense, blood pressure is defined as the product of two factors; cardiac output (CO) and total peripheral resistance (TPR): $ABP = CO \times TPR$. CO depends on the total blood volume in the vasculature, the contractility volume and heart rate, whereas TPR is determined by the contractile state of the

small arteries and arterioles and the viscosity of the blood (14). In the body there are many systems that regulate these factors and they work together in a complex way. The kidneys, nervous system and vasculature together with different hormonal regulators are all important contributors in blood pressure homeostasis (15). Two physiological systems that play an important role in this regulation are the renin-angiotensin-aldosterone system (RAAS) and the autonomic nervous system (ANS) (16, 17).

The RAAS is important for sodium and volume balance and thereby blood pressure regulation in the body. The enzyme renin is released from the kidneys in response to different stimuli, such as reduced perfusion pressure in the afferent arterioles of the kidney and low concentration of sodium and chloride in the tubule system in the kidney (18). Renin cleaves angiotensinogen, which is synthesized primarily in the liver, to the biologically inactive substrate angiotensin I (ANG I). ANG I is further cleaved to angiotensin 2 (ANG II), the main effector peptide of the RAAS, by the enzyme angiotensin-converting enzyme (ACE) which is found in different organs in the body and is particularly abundant on the surface of endothelial cell in the lungs (19). Via activation of the receptor angiotensin II Type 1 (AT₁), ANG II elicits most of the functions of the RAAS such as vasoconstriction, water retention and aldosterone production (20). Aldosterone is a mineralocorticoid that mainly regulates renal sodium retention in the kidneys, whereby an increased secretion of aldosterone leads to increased intravascular volume (21).

Baroreceptors that sense changes in blood pressure are located in various places in the arterial vasculature, a central location being the carotid sinus (14). These receptors sense when an increased blood pressure stretches the blood vessel wall, leading to nerve impulse messages to the brain and decrease of the sympathetic activity of the ANS and thereby lowering blood pressure (22).

By producing different vasoactive substances, vascular endothelial cells are also major contributors to blood pressure regulation (23). Nitric oxide (NO), being

the most important of these substances, is produced and released continuously by vascular endothelial cells in response to changes in shear stress induced by the blood flow (24). NO is a gas and once it is synthesized in the endothelial cell, it diffuses into the smooth muscle that surrounds blood vessels where it activates enzymes that produce substrates that reduce the tension of the smooth muscle (25).

1.2.2 Hypertension

Hypertension occurs when the pressure in the arteries is persistently elevated. Normal blood pressure in an adult is defined as a systolic blood pressure of 120 mmHg and a diastolic pressure of 80 mmHg. New guidelines from the American Heart Association define hypertension as an average SBP \geq 130mmHg or an average DBP \geq 80 (26). It is expected that these new guidelines will increase the prevalence of individuals diagnosed with hypertension by 14% compared with the old guidelines (average SBP \geq 140mmHg or an average DBP \geq 90).

In 90-95 % of patients with hypertension the cause of the elevated blood pressure is unknown, so-called idiopathic or essential hypertension (4). Hypertension caused by other medical conditions is termed secondary hypertension. Conditions that can lead to elevated blood pressure are diseases in the kidneys, heart, blood vessels and endocrine system. These underlying conditions are often correctable, and the blood pressure will normalize when patients are treated (27). Further discussion in this thesis will focus on essential hypertension.

1.2.3 Pathophysiology of hypertension

Since there are many systems involved in blood pressure regulation, the pathophysiological abnormalities associated with essential hypertension are also complex. Despite intensive research in the area of hypertension spanning several decades and new understanding of cellular and molecular biology, the pathophysiology is still poorly understood. Figure 1 shows some of the main organ systems involved in hypertension.

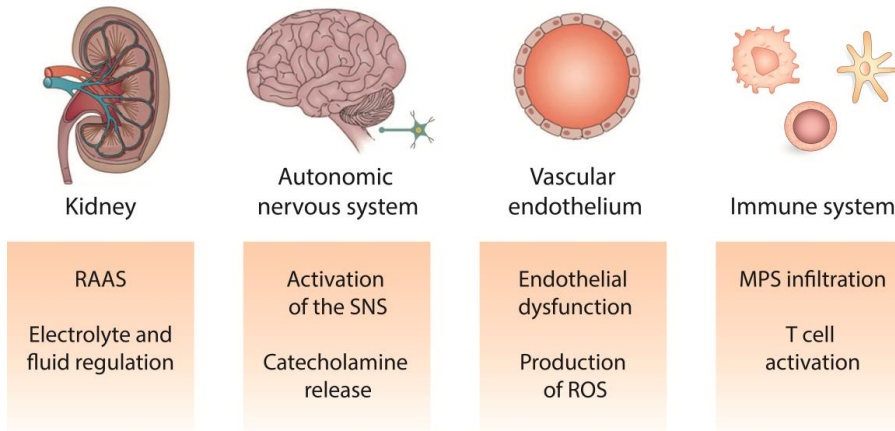


Figure 1. Organ systems involved in the pathophysiology of hypertension.

As discussed earlier is the RAAS important for blood pressure regulation. Impaired capacity of the kidneys to excrete fluid and sodium because of abnormalities in the RAAS seems to play an important role in hypertension, and ACE inhibitors and angiotensin receptor blockers are important drugs for treatment (28). Interestingly, kidney transplantation from a hypertensive animal (Dahl hypertensive rat), into a normotensive animal resulted in the development of hypertension in the normotensive animal (29). This indicates that the kidneys might have intrinsic functions that are important for development of hypertension.

In hypertension, the control of the ANS can be impaired, leading to an increase in activity in the sympathetic nervous system (SNS) which regulates the heart and peripheral vessels (30). The increased activity in SNS is relevant for both acute increases in blood pressure as well as the development of a persistently elevated blood pressure. Studies in patients with hypertension where SNS activity is measured with microneurography have shown that increasing levels of SNS activity correlate with increasing severity of hypertension (31, 32). The plasma concentration of norepinephrine, a catecholamine that is an important neurotransmitter in the SNS, is also found to be elevated in patients with hypertension (33).

Endothelial dysfunction generally refers to a diminishing endothelium-dependent vasodilatation (34). In hypertension, endothelial dysfunction is caused by a combination of mechanical pressure-induced damage and augmented oxidative stress causing vascular endothelial inflammation. Increased production of reactive oxygen species (ROS) and decreased activity of antioxidants, such as the enzyme superoxide dismutase in endothelial cells, leads to accumulation of ROS (35). The ROS bind to NO and thereby reduce the availability of NO. NO promotes vascular relaxation, and decreased availability is a central factor in endothelial dysfunction and hypertension (36) (37).

The immune system might also play a central role in the pathophysiology of hypertension and this will be discussed further in the immune system section below.

1.3 The Lymphatic system

The first description of the lymphatic system is from the ancient Greek time, where Hippocrates refers to it as “white blood”, but it was not until the 17th century that the lymphatic vascular system was characterized. By the early 19th century the anatomy of the lymphatic system was almost fully characterized, but there were still new discoveries to be made. For a long time it was believed that there was no lymphatic drainage system in the central nervous system (CNS), but with the discovery of functional lymphatic vessels in the meninges (38) (39) and in the eyes (40) it appears that the lymphatic system also contributes to fluid homeostasis in the CNS. New and more specific markers like LYVE-1, podoplanin, and Prox-1 have given a better understanding of the function and organization of the lymphatic system (41).

The lymphatic system is a part of the vascular system and is a one-way transport. It is responsible for collecting excess fluid and proteins from the interstitial space and draining it back to the venous system, and therefore performs an important role in fluid homeostasis in the body. It is also an important route for transport of immune cells to the lymph nodes where immune responses are initiated. The

lymphatic system can be divided into two different tissue types, the lymphatic vasculature and lymph nodes. Lymph nodes are lymphoid tissue and will be discussed more in detail under the immune system section 1.5. below.

1.3.1 Lymphatic vasculature

The lymphatic vasculature is an open system and can be divided into four different types of lymphatic vessels; the lymphatic capillaries, pre-collecting vessels, collecting vessels and the bigger trunks and ducts (Figure 2).

Lymphatic capillaries are found in the interstitium and are the start of the lymphatic vasculature and they are therefore also referred to as initial lymphatics. These vessels are blind-ended and have a diameter between 10-60 μm (42). The branched organization of the lymphatic capillaries makes them able to cover a large surface area in the interstitium. The vessel wall is built up of a single layer of partly overlapping lymphatic endothelial cells (LECs) with an indistinct defined basement membrane (43). The organization and structure of the vessels leads to efficient absorption of fluid from the interstitium.

Fluid from the capillaries drain into the pre-collecting vessels and further to the collecting vessels. The collecting vessels are larger and are covered with a layer of circular smooth muscle. The lymphatic vascular endothelium has a continuous basement membrane and between the LECs there are zipper-like junctions that prevent leakage of lymph (44). Inside the vessels there are regularly distributed valves that avert retrograde flow and ensure unidirectional lymph flow from the periphery back to the venous circulation. These valves also form chambers inside the vessels, and together with the circular smooth musculature that surrounds the vessel, these chambers form a functional contractile unit called a lymphangion. Lymphangions can contract independently or in a coordinated contraction pattern with other lymphangions upstream and downstream (45). The coordinated contraction pattern facilitates effective transport of fluid toward the venous circulation against a pressure gradient caused by gravity. All collecting vessels pass through lymph nodes and are divided into prenodal and postnodal

collecting vessels. The prenodal or afferent vessels drain into lymph nodes, and multiple lymphatic vessels can drain into the same lymph node. The postnodal or efferent vessel exits the lymphatic node, and there is usually only one efferent vessel that exits the node. Lymph nodes and immune cell migration to the lymph nodes will be discussed further in the section 1.5. on the immune system below.

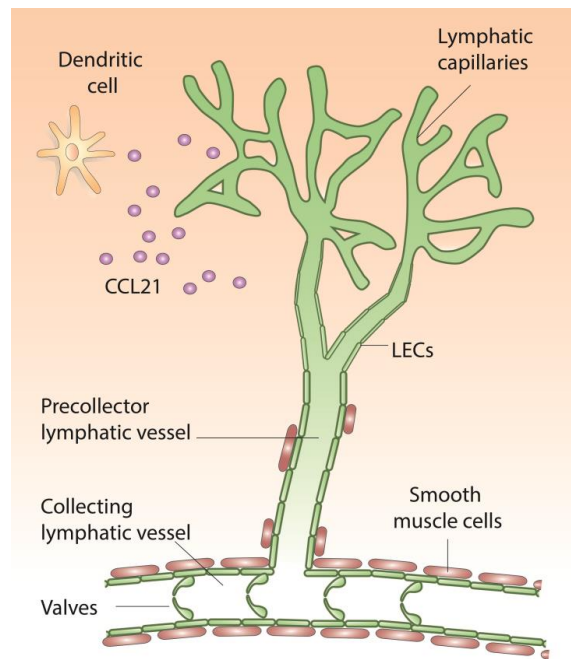


Figure 2. Lymphatic capillaries start as blind endings and are built up of partially overlapping LECs. Precollector lymphatic vessels are partially covered with smooth muscle cells, and LECs form zipper-like junctions to prevent leakage. Precollectors drains into collecting vessels that are covered with circular smooth muscle. Valves inside the vessels form chambers that to together with the circular smooth muscle form lymphangions. DCs migrate to lymphatic capillaries via a process driven by CCL21 chemokines.

The postnodal collecting vessels drain to trunks and ducts. These are larger vessels where the structure is similar to the collecting vessels. The trunks drain fluid from the most proximal lymph nodes into the thoracic duct and the right lymphatic duct. These ducts are the last vessels in the lymphatic vasculature before they drain into the venous circulation, respectively into the left subclavian vein and the right subclavian vein (46).

1.3.2 Lymph

The fluid transported by the lymphatic system is called lymph. Lymph is formed from interstitial fluid when it drains into the lymphatic capillaries. Interstitial fluid (IF) is the ultrafiltrate from blood capillaries in the microcirculation and is found in the interstitial space. IF plays an important role in transport of nutrients to and waste products from the cells, signalling molecules to and from the cells and of antigens and cytokines to the lymphatic vasculature (47). The hydrostatic pressure inside the capillaries and the osmotic pressure that occurs because of different composition of proteins and electrolytes in plasma and the interstitial fluid provide a low level of fluid filtration over the entire length of the capillaries toward the interstitial space (48, 49). This accumulation of IF will result in an increase in interstitial fluid pressure (P_{if}) that serves as driving force for fluid toward the initial lymphatics where lymph is produced. Initial lymph and IF is considered to have equal composition (47).

Lymph is the product of the ultrafiltrate of plasma and consists of various plasma proteins, cytokines, electrolytes, macromolecules, immune cells and antigens (50). The composition of lymph compared to plasma has been debated for decades. It was long thought that the protein composition would be similar with that of plasma, and that albumin and serum globulins made up most of the proteins in lymph. But lymph analysed with proteomics methods has indicated that there are differences in protein expression between lymph and plasma (51, 52). The major differences are the finding of proteins from the extracellular matrix in the lymph (e.g. glycoproteins, collagen, proteoglycans and laminins) and proteins that are specific to the parenchymal organ from which lymph drains (53, 54).

The concentration of electrolytes in lymph compared to plasma has also been discussed. There have been studies with conflicting results regarding the concentration of Na^+ , K^+ and Cl^- . Some studies have found no difference in the electrolyte composition of IF compared to plasma (55) and some a higher concentration of Na^+ and K^+ and a lower concentration of Cl^- (56). Technical

problems associated with the cannulation of the smaller lymphatic vessels as well as the small volume of lymph and IF collected that make the samples prone to evaporation, might be reasons for the conflicting results.

1.3.3 Lymph flow

The transport of lymph includes both its formation and flow in the initial lymphatic vasculature and the flow through the larger collecting lymphatic vessels. As mentioned earlier, the formation of lymph is a consequence of fluid in the interstitial space, whereby P_{if} is an important factor for filling the initial lymphatics (57). A rise in P_{if} has been shown to increase lymph flow, which in turn reduces P_{if} back towards to normal level (58). When the volume of newly formed lymph inside the initial lymphatic vessels rises, the lymph will flow downstream to the larger collecting vessels.

In the collecting vessel a combination of intrinsic and extrinsic factors regulate the lymph flow. The extrinsic factors are due to mechanical forces from the surrounding tissue acting on the lymphatic vasculature that thereby facilitate lymph flow. Skeletal muscle movement, negative pressure in the thoracic cavity during inspiration, vasomotion of blood vessel nearby and the suction effect from the blood flow in nearby large veins, are examples of such extrinsic mechanical forces (59).

The collecting vessels, as briefly described before, consist of lymphangions, which are contractile units with muscle on the outside and valves inside (45). Lymphangions are the intrinsic factor that regulates lymph flow in the collecting lymphatics. They propel lymph forward by contractions of the muscle surrounding the vessel, making each lymphangion act like a small heart. These contractions lead to a decrease in the diameter of the collecting vessel, which increases the pressure inside the vessel and thereby facilitates lymph flow downstream (60).

The regulation of the contractility of lymphangions is not well understood. Like the ventricles in the heart, lymphangions contract cyclically and the volume of

lymph pumped is dependent on preload, afterload, contractility and the frequency of the contractions (61). Lymphatic muscle cells (LMCs) surrounding the lymphatic vessels have similar characteristics to both cardiac and vascular muscle. LMCs have shown to express isoforms of actin and myosin filaments that contract coordinated and rhythmically. Electrophysiological experiments have shown that the contractions are preceded by action potentials generated by spontaneous depolarization that is created by electrical pacemaker activity (62, 63). This spontaneous pacemaker function can be modulated by different factors like temperature, shear stress and signal molecules and proteins. Additionally, interstitial osmolarity changes due to an increase or decrease in Na^+ and Cl^- have shown to affect the frequency of contraction of the lymphangions and thereby lymph flow (64).

1.3.4 Lymphangiogenesis

The term lymphangiogenesis is used to describe the growth of the initial lymphatic vasculature, the development of new lymphatic vessels from pre-existing lymphatic vasculature and the hyperplasia of existing vasculature.

At the beginning of the 20th-century the American anatomist Florence Sabin advocated that primitive lymphatic vessels originate from venous endothelial cells (65). Based on dye injection experiments, she showed that LECs originate from veins in embryonic pigs and later form patterns of dense lymphatic vasculature in tissue and organs. During the 20th-century it was debated whether LECs originated exclusively from veins or if there also were embryonic cells that could develop into LECs independently from veins. By the end of that same century it was postulated that lymphangioblasts were present in the embryonic mesenchyme (66), but it was not until 2015 that two independent research groups found the convincing evidence of a non-venous origin of LECs (67, 68). In adult tissue new lymphatic vasculature is generated from pre-existing lymphatic vessels and hyperplasia of existing vasculature. Inflammation is an important cause of lymphatic remodelling and lymphangiogenesis in adulthood (69).

Vascular endothelial growth factors (VEGFs) are signalling molecules that are important in the development and regulation of the lymphatic system, both in embryonic and adult tissue (70). VEGFs bind to vascular endothelial growth factor receptors (VEGFRs), and the VEGF/VEGFR signalling pathway has over the past decades emerged as the principal driver of angiogenesis, both for lymphatic vasculature and blood vessels. The VEGFs are a family consisting of five different molecules that includes VEGF-A, VEGF-B, VEGF-C, VEGF-D and placenta growth factor (PlGF). The VEGFR family consists of three different receptors: VEGFR-1, VEGFR-2 and VEGFR-3, each giving different outcomes when activated (71). VEGF-C-induced activation of VEGFR-3 is shown to be the prime signalling mechanism for lymphangiogenesis, both during embryonic development and in adult life (72) (73). A soluble form of VEGFR-3 (sVEGFR-3) that inactivates VEGF-C has been found, and experiments in genetically modified mice expressing sVEGFR-3 in the skin have shown inhibition of lymphatic vessel growth and development of lymphoedema in the skin (74). In mice overexpressing VEGF-C in the skin, the dermal lymphatic vascular network is enlarged (75).

In the embryonic stage VEGFR-3 is expressed in all vascular endothelial cells, but in adult life it is mainly expressed on the surface of LECs (76). Activated macrophages have also been found to express VEGFR-3 (77) which might play an important role in inflammation-induced lymphangiogenesis (78). Experiments have also shown that macrophages migrate to the skin of rodents after increased salt intake, indicating that they might be important for the regulation of sodium homeostasis in the skin (11). Macrophages may secrete VEGF-C and stimulate lymphangiogenesis in the skin. Depletion of the migrated macrophages in rats has been shown to reduce both the secretion of VEGF-C and lymphangiogenesis, leading to a change in sodium regulation in the skin and increased blood pressure (12).

1.4 Skin

Skin is the organ with the largest surface area in the body and it makes up around 15 % of the body weight (79). It is crucial for maintaining normal homeostasis in the body; e.g. preventing fluid loss, help regulating body temperature and is important for sensory inputs. The skin is also an important immune organ. It forms a physical barrier, and employs both biomolecules and immune and non-immune cells, to protect the rest of the body against microorganisms and other harmful substances (80). The skin is commonly divided in three layers; epidermis, dermis and hypodermis. (Figure 3).

The epidermis is the outmost layer of the skin and is a stratified structure of five different layers comprised primarily of keratinocytes. The stratum corneum is the outermost layer of epidermis and serves as a shielding overcoat due to keratinization and lipid content. The stratum lucidum consists of immortalized cells, which are only found in the skin of palms and soles. The stratum granulosum contains several cell layers and as the keratinocytes move outward in these layers, they begin to lose their nuclei. The stratum spinosum is the thickest layer in the epidermis and also consists of several cell layers. Here keratinocytes are connected by desmosomes, which allow them to be tightly bound to each other. The stratum basalis is the innermost layer and closest to the dermis. It consists of a single row of keratinocytes that evolve and mature as they migrate to the outer layers of the epidermis (81). The stratum basalis also contains stem cells and melanocytes, the latter producing melanin and thereby being responsible for our skin colour (82). There are also immune cells in epidermis, and these will be explored further in the section 1.5.1 entitled “Immune cells in the skin”.

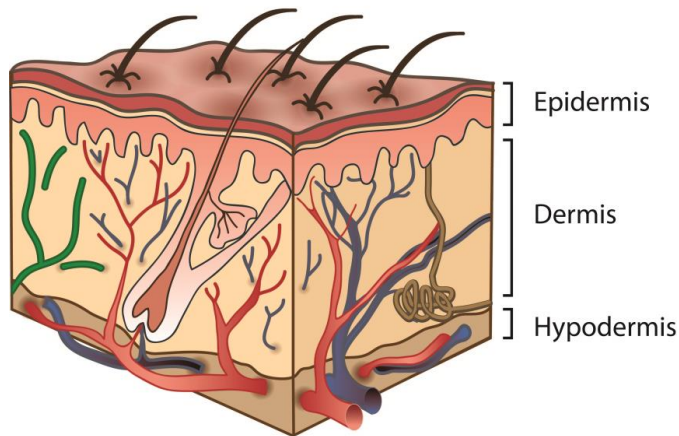


Figure 3. Cross section of the three layers of the skin; epidermis, dermis and hypodermis.

The dermis is the layer below the epidermis and the two layers are separated by a basement membrane. The basement membrane is comprised of extracellular matrix proteins that make a thin and tight sheet that regulate the migration of cells and the movement of proteins between the dermis and epidermis (83). The dermis is cell poor and is primarily made up of connective tissue that gives structure and elasticity to the skin. Fibroblasts are the primary cells found in the dermis, and they produce extracellular matrix elements such as collagen, elastin and glycosaminoglycans (GAGs). Histocytes, mast cells, macrophages and adipocytes are found in the dermis and they contribute in maintaining the function and structure of the dermis. Blood vessels, lymphatic vessels, nerve endings, glands and hair follicles are other structures important for the function of the dermis (84).

The hypodermis or subcutaneous tissue is the deepest layer of the skin. It is largely made up of adipose tissue and is connected to deep fascia (85).

1.4.1. The extracellular matrix of the skin

The interstitium is defined as the space between the vasculature and the cells (57). Its basic structure consists of a fibre framework of mainly collagen, a homogenous gel phase consisting of GAGs, different cells and a fluid phase derived from plasma containing plasma proteins and electrolytes (8) (Figure 4). The extracellular matrix (ECM) is the non-cellular component of the interstitium and is a well-organized network that provides physical support for tissues. The ECM is most prominent in the dermal layer of the skin where it is involved in the regulation of several cellular processes involving migration, growth, homeostasis and differentiation (86).

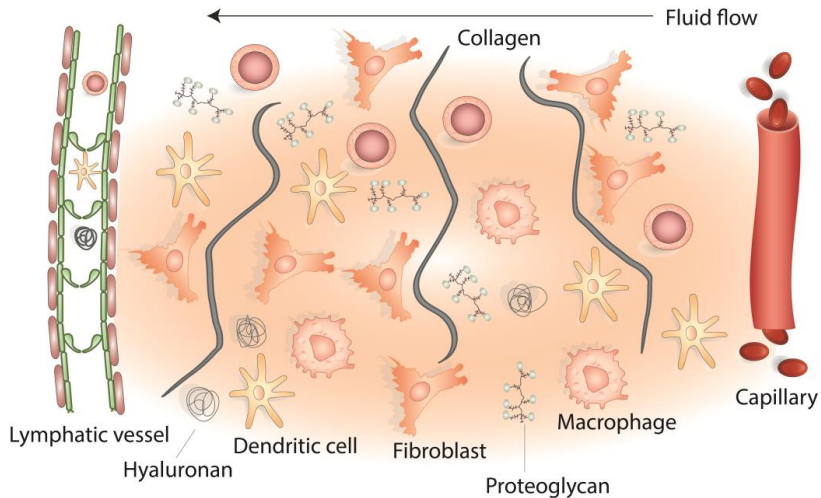


Figure 4. The basic structure of the interstitium showing different cells, proteins and fibre framework. Modified from Wiig ((87).

The fibre framework of the ECM is, as mentioned, mainly built up of collagen. Collagen is a large family of ECM proteins and account for 20-30% of total body proteins (88). Twenty-nine different types of collagen have been described and they are classified into different sub-types according to structural similarity and organization of macromolecules (89). In dried skin, collagen fibres account for almost 70% of the weight of the dermis. Other fibrous-forming proteins that also

make up the framework of the ECM are elastin, fibronectin and laminins. Elastin has more elastic properties than collagen and constitutes 2-4% of the dermis, where it contributes to the elasticity of the skin (90).

The other major structural constituents of the extracellular matrix are GAGs. GAGs are long linear polysaccharide molecules that are classified into six different types depending on the disaccharide molecule group (91). GAGs are negatively charged and therefore have a high water-holding capability. This water holding capability makes GAGs important for mechanical and space-filling functions and for the regulation of tissue water content in the skin (92). Hyaluronan (HA) is the most abundant GAG in the ECM of the skin and due to its coil structure it is able to hold about 1000-fold of its own molecular weight in water (93).

The ECM is a very dynamic structure that is constantly undergoing remodelling and repair, which is important to maintain a normal function and tissue homeostasis. Fibroblasts are crucial in this process with coordinated secretion of enzymatic and non-enzymatic regulators (94). Different proteases are involved in remodelling, but the major proteases are considered to be the matrix metalloproteinases (MMPs) (95). MMPs are primarily synthesized in fibroblasts and also immune cells such as monocytes and macrophages, but also endothelial cells have been observed to express genes for MMPs (96). Abnormal ECM remodelling occurs in different diseases and pathological processes like inflammation, leading to loss of structure and change in the composition of the ECM (97, 98). It has been suggested that negatively charged GAGs, which make up the gel phase of the extracellular matrix in the skin, might store sodium and hence be involved in the sodium homeostasis in the body (8, 11, 99).

1.5 Immune system

The traditional view of the immune system is that it provides protection from harmful invading microorganisms. The basic framework in this model is that antigen from invading microorganisms is taken up by immune cells that present

the antigen to other immune cells, which leads to an immune reaction against the harmful invaders (100). Over the last few decades it has also been revealed that the immune system has other fundamental roles beyond that of protection against invading microorganisms (100). It is an important part of physiological processes like wound healing and remodelling of organs during development and disease (101-104). It is also evident that the immune system and other physiological systems in the body such as metabolism, the central nervous and the cardiovascular system work closely together to maintain organ and body homeostasis (105-107). Further details about the immune system in the skin and the role of the immune system in hypertension will be discussed in the upcoming sections.

1.5.1 Immune cells in skin

A variety of different immune cells are localized in the various layers of the skin. In the epidermis are Langerhans cells (LCs), which are members of the dendritic cell family, the main antigen-presenting cells (APC). From the early development, the LCs form a dense network in the basal layer of the epidermis with dendritic processes that extends out to the other layers in the epidermis (108). During inflammation, LCs capture antigens and migrate through the basement membrane to the dermis before they enter the lymphatic vasculature and are transported to the nearest lymph node (109).

There are several types of immune cells found in the dermis, including mast cells, lymphocytes, neutrophils, macrophages, monocytes and dermal dendritic cells (dDC). Unlike the epidermis, the structure of the ECM permits free migration of immune cells within the dermis (82). Monocytes, macrophages and dDC are part of the mononuclear phagocyte system (MPS), a specialized family of phagocytes that are important for innate immunity and phagocytic processes (110). New research indicates that the MPS also play an important role in skin homeostasis like wound healing, tissue repair and stress response (111, 112). Depletion of macrophages during inflammatory processes has shown additional

consequences such as reduced vascularisation and reduced expression of growth factors like VEGF-A and VEGF-C (12, 113).

1.5.2 Lymph nodes

All lymph produced in the interstitial space is transported to regional lymph nodes before it is returned back into the venous circulation. Lymph nodes are small and bean-shaped organs enclosed by a capsule strategically located along the lymphatic vasculature (114). They are lymphoid organs that contain large amount of lymphocytes and APCs like macrophages and DCs. It is in the lymph node that the adaptive immune system is exposed to new antigens and the immune response towards antigens is initiated (115).

1.5.3 Immune cell migration from the skin to the lymph node

In addition to the transport of lymph, the lymphatic vasculature is also important for immune cell migration to lymph nodes. Of the MPS cells, it is the DCs that are specialized in migrating to lymph nodes, other MPS cells might also have migratory capabilities but they are generally regarded as non-migratory (116). DCs crawl through the interstitial space with help of fluid channels created by IF that is being pushed toward the lymphatic capillaries (117). Upon activation, the DCs upregulate the C-C chemokine receptor type 7 (CCR7), which helps guide the DCs towards the lymphatic capillaries by binding to the chemokine (C-C motif) ligand 21 (CCL21) that is expressed on the LECs (118) (Figure 2). CCL21 is stored in intracellular compartments in LECs and is under normal conditions released constitutively in low concentrations to maintain normal homeostasis in the skin (119). During inflammatory conditions or mechanical stimuli, such as an augmented lymph flow, the secretion of CCL21 is increased, which promotes DCs migration to the lymph node (120, 121). Mice lacking lymphatic vessels in the dermis have reduced DCs migration and an impaired immune response (122).

1.5.4 The immune system and hypertension

Accumulating evidence indicates that low-grade inflammation might play an important part in the development and maintenance of hypertension, however the mechanisms involved are unclear (123). Studies have shown that immune cells harvested from rats with hypertension after unilateral renal artery clipping and deoxycorticosterone (DOCA) combined with salt diet, induced hypertension when injected into normotensive rats (124, 125). It has also been shown that mice lacking B and T cells were protected against DOCA and salt induced hypertension, but restored sensitivity to the development of hypertension after replenishment of T-cells (126). The role of T-cells in hypertension is not clear. It has been reported that in hypertensive mouse models, T-cells infiltrated regions of the brain that control sympathetic outflow and that T-cell activation is enhanced (127, 128). T-cells are observed to be a contributor in endothelial dysfunction and microvascular remodelling and rarefaction (126, 129). In the kidneys, T-cell infiltration might alter function and thereby lead to increased retention of sodium and water (130).

As a part of the adaptive immune system, T-cells require antigens presented by APCs to be fully activated (131). Some of the most potent APCs are the DCs with their high expression of the molecule major histocompatibility complex class II (MHC II), which is important for the presentation of antigen to the T-cells (132). It is not clear what role DCs have in T-cell activation when it comes to the development of hypertension. In a hypertension model in mice involving angiotensin II infusion, the expression of the cell marker CD86, a costimulatory molecule needed for activation of lymphocytes, increased on dendritic cells (133). Mice with reduced capability to express CD86 had less activated T-cells and did not get the same increase in blood pressure as normal mice (133). The antigens that might be involved are not known. Hypertension models like DOCA and salt or angiotensin II infusion in rodents, leads to increased production of reactive oxygen species, which in turn lead to cell damage, lipid oxidation and

production of molecules that are suggested to act as antigens or neoantigens in the activation of T-cells by DCs (134-136).

It seems clear that no single immune cell type, pathway or mechanism mediate the immune reaction that leads to hypertension. It is more likely that different immune cells and pathways in different organs are activated and that each reaction communicates with its surroundings to activate additional immune responses or directly influence mechanisms that are important in blood pressure regulation.

1.6 Sodium

In an adult person water makes up 60% the total body weight and it is divided into two main compartments; two-thirds being intracellular and one-third being extracellular water (137). Body water contains different substances like electrolytes, metabolites and proteins. Of the electrolytes, sodium and potassium are the major cations and chloride the major anion. The composition of electrolytes is different between the intracellular and extracellular fluid. Sodium is the major cation in extracellular fluid whereas potassium has this role in intracellular fluid (138). Sodium is osmotically active, and the regulation of sodium is tightly linked to the water balance in the body and thereby the homeostasis of extracellular fluid volume. The normal range of sodium in the extracellular fluid is 135-145 mmol/L and the maintenance of a normal extracellular osmolality and fluid volume is critical for normal body homeostasis (139).

The kidneys are the main regulator of electrolytes and water in the body, and they are also important for the acid-base balance, the production of the hormone erythropoietin that facilitates the production of red blood cells and in the excretion of different metabolic waste products and toxins (140). Of the approximately 200-litres of fluid that is filtrated through the kidney per day, 99% is reabsorbed as the fluid passes along the tubules. Sodium is reabsorbed through the entire length of the tubule system in a very energy-consuming process and

the final concentration of sodium in the urine varies depending on water and salt intake (141).

1.6.1 Sodium and blood pressure

There are many studies linking a high dietary salt intake and hypertension, and reducing dietary salt intake has been shown to reduce blood pressure (142-144). Nevertheless, there is a substantial variation in blood pressure response between individuals after increased dietary salt intake, with some demonstrating an increase in blood pressure while others show no effect, a phenomenon referred to as salt sensitive and salt resistant individuals (145).

The factors that explain the association between increased dietary sodium intake and hypertension are not completely understood. More than 30 years ago Guyton and colleagues developed the “pressure natriuresis” model to demonstrate how dietary salt intake affects the blood pressure. This model suggested that the kidneys increase sodium excretion in response to increased blood pressure, thereby reducing the blood volume and returning blood pressure back to normal (146). If the capacity of the kidneys to excrete salt is reduced, the BP will increase over time to a new and higher level at which intake and output of salt will be in balance. This model places the kidneys at the very centre of how long-term sodium and water regulation lead to hypertension (7).

1.6.2 Sodium and the skin

New data from long-term observational studies in humans have shown that considerable amounts of sodium could be retained or removed from the subjects without commensurate water retention or loss (147-149). These data led to the proposal of an alternative model suggesting that osmotically inactive sodium could be stored somewhere in the body and that sodium concentration within the interstitial fluid does not necessarily equilibrate with the sodium concentration in the intravascular compartment (56, 150). By measuring sodium and water content in the skin of rats given a high salt diet, studies have revealed that the skin might serve as major reservoir and a buffer for excess sodium, and that the

skin microenvironment is hypertonic compared to plasma (9, 151, 152). Studies using $^{23}\text{Na}^+$ -magnetic resonance imaging (MRI) have suggested that sodium accumulation in the skin not only occurs in rodents, but also in humans (10, 153). When comparing normotensive and hypertensive patients there was a correlation between skin sodium and BP; patients with resistant hypertension had increased sodium accumulation in the skin compared to normotensive patients (153).

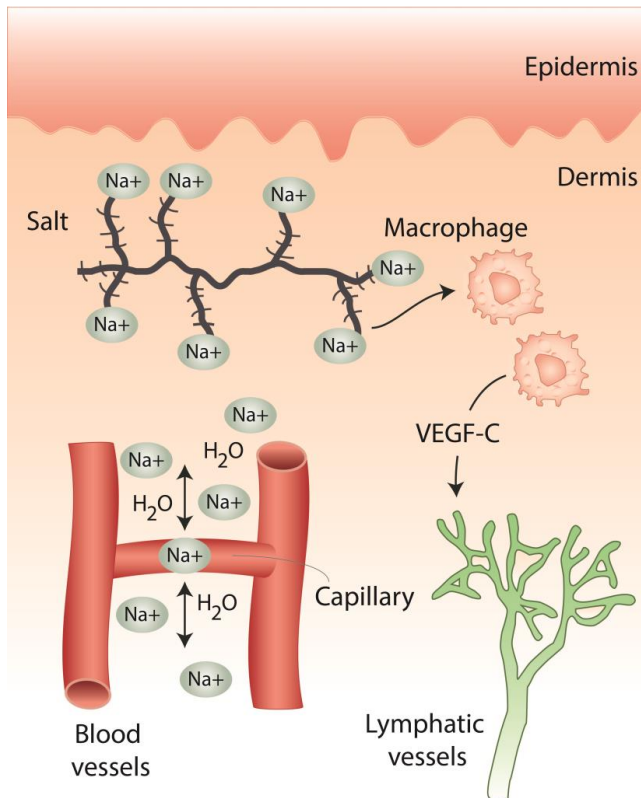


Figure 5. Skin sodium accumulation model suggested by Titze and colleagues. Modified from Coffman (15).

The hypertonic microenvironment caused by salt storage in the skin, is proposed to create osmotic stress that activates the transcription factor tonicity-responsive enhancer-binding protein (TonEBP) in MPS cells (11, 12). In vitro experiments have shown that a high concentration of extracellular sodium can be a chemoattractant for macrophages and that they migrate actively toward a salt-

induced hypertonic area (154). MPS cells infiltrate the hypertonic interstitium and induce TonEBP driven VEGF-C expression (11). VEGF-C induces lymphangiogenesis and restructures the lymphatic capillary network in the interstitium, which seems to be important for the regulation of tissue sodium and systemic blood pressure (Figure 5). Blocking VEGF-C signalling or depletion of macrophages has, in animal models, been shown to result in reduced density of the lymphatic vasculature and reduced accumulation of sodium in the skin, again resulting in an increased blood pressure after salt loading (11-13).

2. Aims

The kidneys are the main regulator of water and electrolytes in the body, but based on the new data presented above; additional local extrarenal regulation of electrolytes in skin might contribute to maintaining normal extracellular electrolyte homeostasis and blood pressure. There are several important questions that can be raised by this model and thus need to be pursued further. In particular the composition and remodelling of the interstitium and the functional consequences thereof are of interest. In this thesis I therefore had the following aims:

- To investigate whether hyperplastic and chronically expanded lymph vessels in the skin are functional (Paper I).
- To study whether lymph vessels formed after salt accumulation in the skin are functional and affect lymph flow (Paper II).
- To investigate how blood pressure regulation, lymphatic function and sodium accumulation are affected during salt loading in mice that either have a hypoplastic or hyperplastic lymphatic network in skin (Paper III).

3. Methods

In this section I will present the main methods used in paper I-III. For a more detailed description and protocols I refer to Materials and Methods in the respective papers. Methodological considerations will be addressed in the “Discussion” section.

3.1 Animal models

In this project, both rat and mouse models have been essential. All animals were exposed to light on a 12:12-h cycle in a humidity- and temperature- controlled environment. Only male rats and mice were used in this project.

NTac Sprague Dawley rats were purchased from Møllegaard Breeding Colony, Skensved, Denmark. (Paper II)

C57 BL/6 mice were purchased from Jackson Laboratories. (Paper II)

Chy mice on C3H background were obtained from MRC-Harwell Institute. These mice have a heterozygous mutation in the gene coding for the vascular endothelial growth factor receptor 3 (VEGFR-3), resulting in a phenotype with a hypoplastic lymphatic network in the dermis but not in the visceral organs (155). WT littermates were used as controls. (Paper III)

K14-VEGFR-3-Ig mice on C57BL/6 background were provided by Dr. Kari Alitalo, Helsinki, Finland. K14-VEGFR-3-Ig mice produce soluble VEGFR-3 in the skin under the keratin-14 promoter. Soluble VEGFR-3 binds and inactivates VEGF-C, resulting in a phenotype that lacks lymphatic vasculature in the dermis (156). WT littermates were used as controls. (Paper III).

K14-VEGF-C mice on FVB background were provided by Dr. Kari Alitalo, Helsinki, Finland. K14-VEGF-C mice express VEGF-C in the skin under the keratin-14 promoter, which gives a phenotype with hyperplastic lymph vessels in the skin (75). WT littermates were used as controls. (Paper I and III)

3.2 Inducing high blood pressure

Two different models were used to induce high blood pressure in the rodents; the High-Salt-Diet model (HSD) and the DOCA-Salt model.

High-Salt-Diet: Rats and mice received chow containing 8% and 4% NaCl, respectively, and 1% saline to drink for 2 weeks.

DOCA-Salt: A slow-release deoxycorticosterone acetate (DOCA) tablet (50 mg in mice and 100 mg in rats, Innovative Research of America) was implanted subcutaneously in the animal. Under isoflurane anaesthesia, a small surgical incision was made caudally on the cranial back skin region and with blunt dissection a subcutaneous tunnel was made to the cranial back skin region. The tablet was inserted through the tunnel in a plastic catheter to protect the tablet before it was lodged at the end of the tunnel. The animals were given 1% saline as drinking water and normal chow to eat for 2 weeks. Blood pressure was measured before the start and at termination of the experiment.

As a control we used a low salt diet (LSD) as well as regular chow considered as normal salt diet (NSD). Low salt chow contains less than 0.1% salt and regular chow 0.5% salt. Both control groups had normal tap water to drink.

3.3 Blood pressure measurements

We used two different methods to measure blood pressure in the animals. The measurements in rats were done with the tail-cuff method and in mice we used telemetric recording.

Tail-cuff

The CODA-6 tail-cuff system for rodents (Kent Scientific, Torrington, CT) was used for all blood pressure measurements in rats. The tail-cuff system detects volume changes in the tail due to changes in the blood flow with a volume-cuff after occlusion and gradual reduction of the pressure of the tail artery with an occlusion-cuff. Blood pressure was measured before the start and at the

termination of the experiment. The rats were preheated in an incubator at 34°C before measurements. The animals were awake and kept inside a restrainer during blood pressure measurements.

Telemetric recording

We used the PA-C10 telemetry implant from Data Sciences International (DSI) to measure blood pressure in mice. The implant consists of a transmitter with a catheter filled with gel. The transmitter converts pressure pulses from the catheter to radio waves that are detected by a receiver. A computer connected to the receiver transforms the radio waves to physiological data, such as blood pressure and heart rate (157). Before implantation the mice were anaesthetized with isoflurane. A midline incision on the ventral side of the neck was made and the left carotid artery was dissected free and ligated at the carotid bifurcation. The catheter of the transmitter was advanced towards the heart through a small incision in the wall of the carotid artery, so that the tip of the catheter was a few millimetres inside the aortic arch. The transmitter was placed subcutaneously on the left flank. Absorbable sutures were used to close the midline incision in the skin. The mice were given buprenorphine subcutaneously (0.1 mg/kg) for pain relief after the operation. After a minimum of 10 days recovery, baseline blood pressures were measured in freely moving mice.

3.4 Lymph flow in skin and muscle

Optical imaging was used to measure lymph flow in the skin of rats and mice. To measure lymph flow in the deeper positioned muscles in rats we used positron emission tomography – computer tomography (PET-CT).

Optical imaging

In the skin and skeletal muscle, large macromolecules will only be removed with the lymph (47). With optical imaging we measured the lymph flow indirectly by monitoring the clearance of intradermally injected albumin that was labelled with a near-infrared dye (158). With a Hamilton syringe (34G needle), 0.5 and 3

μ l Alexa 680-conjugated bovine serum albumin was injected into the skin of the hind paw of rats. At different time points, the skin was scanned using the Optic MX optical scanner, and the intensity of the fluorochrome was measured. The decrease in intensity over time, as albumin was washed out, was used to estimate the clearance of albumin, which is an indirect estimate of the lymph flow. During scanning the animals were anesthetized with 2% isoflurane. In the periods between scans the rats were awake and freely moving to facilitate lymph flow.

PET-CT

The principle for measuring lymph flow in muscle with PET is similar to optical imaging in skin. Instead of labelling the albumin with a near-infrared dye, we used the PET-emitter ^{124}I . The radionuclides are absorbed at a lower extent in tissues than fluorescent probes and can be used to estimate lymph flow in deeper positioned tissue. Albumin was conjugated with ^{124}I , which has a half-life of 4.18 days. The conjugated albumin was injected into thigh muscles and the rats were scanned in the PET-CT at different time points to measure the decrease in radioactivity. The rats were freely moving in between scans.

3.5 Flow cytometry

Flow cytometry is a laser-based analysis technique used for the characterization and detection of cells. We used the technique to quantify immune cell migration from skin to the draining lymph node in mice. Eighteen hours after their ears were painted with fluorescein isothiocyanate (FITC) solution (FITC 8mg/ ml in 1:1 acetone and dibutyl phthalate), the mice were sacrificed and the draining lymph nodes harvested. The lymph nodes were incubated with collagenase D and filtered through a 70 μ m cell strainer. The cell suspension was incubated with antibodies (CD45, CD11c and MHC II) and a live/dead marker (7AAD). The cell suspension was analysed using a BD LSR Fortessa Cytometer. Migrating dendritic cells were characterized as FITC⁺ CD11c⁺ MHC II⁺⁺ CD45⁺ positive cells from all living cells. Flow data were analysed using FlowJo.

3.6 Immunohistochemistry

Immunohistochemistry is a semi-quantitative method that we used to identify lymphatic and blood vessels, chemokines and immune cells in dermis. We prepared tissue samples for immunohistochemistry in three different ways:

Whole mount staining was used to quantify the amount of lymphatic and blood vessels and the chemokine CCL21 in ears. Freshly cut ears were harvested after the animals had been sacrificed. Hair was removed with depilatory cream and they were fixed overnight in 4% PFA at 4°C and thereafter washed and stored in PBS. The ears were split in half and the dorsal part was mounted with needles to a Sylgaard plate prepared with silicon in the bottom. The ears were then washed with 0.3% PBS-TritonX before adding blocking solution with 5% serum from the same species as the secondary antibodies were raised in to reduce unspecific binding and background fluorescence. A mixture of primary antibodies in the blocking solution was added and the ears were incubated for 3 days at 4°C. They were then washed with 0.3% PBS-TritonX overnight incubation with fluorescently labelled secondary antibodies at 4°C. After incubation with secondary antibodies, the ears were washed properly once again before being post-fixed with 4% PFA for 5 minutes followed by washing with PBS. The ears were then mounted to microscope slides and analysed with fluorescence microscopy. Quantification was performed using QuPath and/or ImageJ by selecting 3-5 different areas from each ear, which expressed suitable staining without signs of tissue damage after preparation.

Epidermal sheets staining was used to quantify the number of Langerhans cells in the epidermis of mice. Freshly cut ears from sacrificed mice were split in half after hair removal. The dorsal part of the ears, with the inner dermis side faced down, were placed in a well containing 0.5M ammonium thiocyanate for 40 minutes at 37°C. With fine forceps the epidermis was peeled off and fixed for 20 minutes in ice-cold acetone. After fixation, the sheets were repeatedly washed with PBS before being blocked with 5% serum from the same species as the secondary antibodies were raised in. The sheets were incubated for 2 hours with

the same blocking solution containing antibodies against Langerhans cells (CD207 and MHC II). After several washes with 0.3% PBS-TritonX, the sheets were incubated with fluorescent-labelled secondary antibodies for 1 hour. After washing the sheets, they were mounted on microscope slides and analysed with fluorescence microscopy. Quantification was performed using ImageJ by selecting 3-5 areas from each sheet, which expressed suitable staining without sign of tissue damage after preparation.

Serial section staining was performed to quantify the number of lymphatic vessels and immune cells in the dermis of rats and mice. Frozen 4% PFA fixed tissue sections and snap-frozen tissue samples were used to quantify lymphatic vessels in the dermis, while paraffin sections were used to quantify immune cells. The detailed protocol on how the different staining methods were performed on serial sections can be found in the individual papers.

3.7 Chemical analysis of tissue electrolytes

Two different methods were used to determine the concentration of different electrolytes in the tissue:

High performance liquid chromatography (HPLC) is a chromatographic technique used to identify, quantify or purify different molecules (i.e. protein, nucleic acids, electrolytes) of a mixture. A liquid mixture is run through a column that shows selective absorption for different solutes in the mixture. HPLC use high pressure to push the liquid through the column, which makes it much faster than ordinary column chromatography that uses gravity as driving force. By measuring the time that different molecules use to pass through the column to the detector, it is possible to determine the type and amount of molecules in the mixture. Samples from skin and muscle were collected upon termination of the experiment. Wet weight (WW) of the samples was measured before desiccation in a drying chamber. After 1 week of drying to obtain stable weight, the dry weight (DW) of the tissue samples was measured. Tissue water content was calculated as the difference between WW and DW. The dried

samples were eluted in ultrapure water (Milli-Q, Millipore Corporation) for 1 week, so that the added water would to equilibrate with the electrolyte concentration of the dried sample. After spinning the eluted sample, 50 μl of the eluate was analysed for sodium and potassium by HPLC-based ion chromatography.

Ashing is a method where dried tissue is ashed at 190°C and 450°C for 24 hours at each temperature level, and then at 600°C for 48 hours. Ashed tissue is then dissolved in 5% or 10% HNO_3 . We measured the concentration of electrolytes in such a solution by atomic absorption spectroscopy (Model 3100, Perkin Elmer).

4. Summary of the results

4.1 Paper 1: Lymphangiogenesis Facilitates Initial Lymph Formation and Enhances the Dendritic Cell Mobilizing Chemokine CCL21 Without Affecting Migration

In this paper we studied the functional consequences of an expanded lymphatic network in the skin. We showed that K14-VEGF-C mice that overexpress VEGF-C in skin have an expanded cutaneous lymphatic network with a changed morphology. Blood vessels appeared to have a normal morphology and the number of blood vessels was the same in both VEGF-C and WT littermate mice. The chemokine CCL21, which is expressed on lymphatic endothelial cells and acts as an attractant for dendritic cells, was overexpressed in VEGF-C mice. The dendritic cell numbers in the epidermis were similar in VEGF-C and WT mice. Despite the overexpression of CCL21 found in VEGF-C mice, dendritic cell migration from the skin to the draining lymph node was not enhanced. Total tissue water (TTW) and P_{if} in the skin were the same in both strains during control conditions, and there was also no difference in capillary permeability and lymph flow, indicating a normal capillary barrier. We observed an increase in TTW and P_{if} as well as reduced lymph flow after inducing chronic inflammation with topically applied oxazolone and acute inflammation with lipopolysaccharide injections. These findings were the same in VEGF-C and WT mice. The VEGF-C mice demonstrated enhanced lymph flow after local overhydration not induced by inflammation, suggesting that lymphangiogenesis may result in increased fluid clearance in a situation where there is increased fluid filtration.

4.2 Paper 2: High-Salt Diet Causes Expansion of the Lymphatic Network and Increased Lymph Flow in Skin and Muscle of Rats

Based on previous studies where salt accumulation in the skin has been shown to lead to VEGF-C secretion and lymphangiogenesis, we asked if this had any effect on lymphatic function. We found that rats in the HSD and DOCA group had an increased number of lymphatic vessels in the dermis of the ear. By using optical imaging to measure washout of fluorescently labelled albumin from the skin, we found a moderate increase in lymph flow in the HSD and DOCA group compared with LSD controls. The same results were also observed in skeletal muscle during HSD when recording lymph flow using PET-CT. HSD and DOCA did not affect transcapillary filtration, indicating that the capillary barrier was unaffected during salt loading. Lymph flow was significantly reduced after depletion of skin monocytes/ macrophages with clodronate in the skin, indicating that these cells might be involved in the lymph flow response observed in the HSD and DOCA groups. To further study whether a hyperosmotic environment has an effect on the function of lymphatic vessel pumping, we isolated skin lymphatic vessels and exposed these to a solution made hyperosmotic by adding Na^+ while measuring contractility. The lymphatic vessels increased their contraction frequency in response to an increased Na^+ concentration.

4.3 Paper 3: No evidence for a role of lymphatics in skin in electrolyte and blood pressure homeostasis in mice

To address the question of whether the lymphatic network in the skin has a functional role in electrolyte and blood pressure homeostasis, we exposed genetically engineered mice that either had a hypoplastic (Chy), hyperplastic (VEGF-C), or completely lacked (VEGFR3-Ig) lymphatic network in the dermis to salt loading. As controls we used WT littermates. The mice were given either HSD or DOCA, and blood pressure was measured with telemetric recording before, and at termination of the experiment. Skin was harvested to perform electrolyte concentration analysis with HPLC. For quantification of lymphangiogenesis, whole mount staining of lymphatic vessels in ears was performed. There were no differences in sodium content in the skin between the genetically engineered and control mice before start of the experiment, when the mice were fed NSD. Baseline blood pressure was the same in Chy and VEGF-C mice compared to WT controls, while VEGFR3-Ig had slightly lower blood pressure. HSD did not increase blood pressure in any of the mouse models, and there was no accumulation of Na^+ in the skin of Chy and WT controls after HSD. DOCA induced Na^+ accumulation in the skin and increased blood pressure in Chy and VEGFR3-Ig mice. However, no differences were found when compared to WT controls. VEGF-C and WT mice did not accumulate Na^+ after DOCA. We found no lymphangiogenesis in skin after DOCA or HSD compared to NSD and LSD controls. In WT (C3H) Na^+ accumulation led to increased migration of Langerhans cells from the skin. In genetically engineered and WT mice from all the three models, DOCA caused an increased Na^+ and a reduced K^+ concentration in skeletal muscle, compared to mice fed NSD and HSD. The total concentration of sodium and potassium in muscle was similar in all groups, indicating that DOCA generate a shift of sodium and potassium in muscle.

5. Discussion

The aim of this work was to study the role of the extracellular microenvironment and lymphatic vasculature in skin in electrolyte and blood pressure homeostasis. I will in this section first discuss some of the main methods and techniques used during the thesis and thereafter our main findings more in general.

5.1 Methodological considerations

5.1.1. Animal models of hypertension

Animal models have been essential for all the studies presented in this thesis. As described earlier, the pathophysiology of hypertension in humans is multifactorial and complex (4, 14), and no animal model alone can recapitulate all the features of the disease process. There are many advantages of using animal models; e.g. they are relatively cost effective, give a standardized study population, have fast recovery time after surgery, and provide research opportunities to study the effects of genetic modifications, that will not be possible in human studies. However, there are also many differences that are important to keep in mind when comparing hypertension in rodents and humans, e.g. that the hemodynamics, like heart rate, of rodents are fundamentally different compared to humans. The normal resting heart rate in a mouse is 500-700 beats per minute, which is approximately 10 times faster than in humans, resulting in a limited increase in cardiac output in mice by maximally 2-fold in comparison to a 10-fold increase in humans during stress (159). The fact that rodents walk on four feet might also influence the hemodynamic profile compared to humans that walk standing on two feet. The timeline for developing hypertension in the rodent models is very short compared to humans. It may take decades for a human to develop hypertension, as compared to animal models where the timeline is days to weeks. These aspects are important to be aware of when trying to translate results from animal studies to human models.

5.1.2. Inducing hypertension

Considering all the different factors that affect blood pressure, there is no ideal animal model that is the gold standard in hypertension research. Moreover, the reproducibility of hypertension models in animals has been a topic of discussion (160, 161). There are mainly three broad categories that animal models of hypertension can be divided into; spontaneous, surgically induced and pharmacologically or diet induced hypertension. Spontaneous hypertension models use animals that have a phenotype of developing hypertension spontaneously. These are primarily rat strains; most commonly the Dahl salt sensitive rats (DS) and Spontaneously Hypertensive rats (SHR). Surgical models involve the manipulation of renal blood flow, and this can be done by either constriction of one or both of the renal arteries, or by constriction of one renal artery with removal of the contralateral kidney. Our aim was to study the effect of salt on systemic blood pressure and the extracellular microenvironment in the skin, and we used a HSD model alone or in combination with a mineralcorticosteroid hormone that caused retention of sodium, the DOCA model.

The advantages of a HSD are that it is easy to administer and there is no use of invasive techniques. The increase in blood pressure caused by HSD alone is not always pronounced. There is also reported strain variation, some strains being more salt sensitive than others (162). The amount of salt consumed by rats and mice in this model is also quite high and the physiological relevance to eating chow containing, respectively 8% and 4% salt, and drink 1% saline might be questioned.

The DOCA model results in a more pronounced rise in blood pressure. DOCA affects renal sodium handling, leading to reabsorption of sodium in the kidney (163). This model is often combined with unilateral nephrectomy to increase the hypertension, but studies have shown that animals also develop hypertension without unilateral nephrectomy (164). We chose the latter model in order to reduce the amount of invasive procedures that the animals were exposed to. In

our experiments all animal groups exposed to DOCA got a pronounced increase in blood pressure. The DOCA-salt model creates an imbalance in the renin-angiotensin system and low-renin hypertension. Renin is also observed to be low in salt-sensitive persons, and it is advocated that the low renin phenomenon observed in the DOCA-salt model makes the model well suited to study salt-sensitive hypertension (165, 166). The disadvantage with the DOCA model is that surgery is needed to implant the slow release tablet. At the beginning of the project we observed that the tablets dissolved and irritated the surgical wound, resulting in premature termination of the experiments. Inserting the tablet through a subcutaneous tunnel with a plastic catheter solved this problem, and this procedure was applied throughout the project.

For the experiments involving rats given HSD or DOCA, we used LSD as a control group. The normal dietary salt requirement for rats has been a matter of discussion. It has been argued that normal commercial chow might contain sodium in excess of actual dietary needs and this might affect cardiovascular physiology (167). On the other hand, animals that receive LSD will have low levels of salt available in the chow. In earlier studies we have seen minimal differences between HSD and DOCA group sodium content, whereas LSD had significantly lower sodium content in skin (151). It is possible that these differences are not due to salt accumulation in the salt exposed groups but due to loss of salt from the skin in LSD groups. LSD is the most used control group in studies involving hypertension, although, from a physiological point of view it might be preferable to use NSD rather than LSD as a control group. We therefore used NSD as control group in some of the mouse experiments.

5.1.3. Measuring blood pressure in rodents

Four major techniques are used for measuring arterial blood pressure in rodents; the tail-cuff system, implanted fluid filled catheters, implanted telemetry systems and Millar tip pressure catheters (168). The first of these is a non-invasive method, whereas the three remaining are invasive. The implanted fluid catheters and Millar pressure catheters are not well suited for continuous blood pressure

recording over time and were therefore not ideal for use in our study, as we wanted to compare blood pressure before and after a diet that lasted for 2-3 weeks. The tail cuff and the implanted telemetric systems are the best suited methods to assess steady state blood pressure over time. These were the preferred methods in our studies and will be discussed further.

The tail-cuff system measures blood pressure by monitoring the volume of the tail as a measure of blood flow. The system consists of two rings, one for restriction and controlled re-initiation of blood flow in the tail (occlusion-cuff) and one for volume pressure recording (VPR-cuff). As the occlusion-cuff gradually releases pressure, blood flow into the tail will be restored and the volume of the tail will increase. When the blood flow in and out of the tail is equal there will be no changes in the volume of the tail. The timeline for these changes in the volume of the tail are recorded by the VPR-cuff. Systolic and diastolic pressures are determined by comparing the pressure in the occlusion-cuff with the time for changes in volume of the tail. The advantages of the tail cuff-system are that it is a non-invasive method that can be used in conscious animals for regular monitoring over time, it is cheap compared to other methods and simple to use. One disadvantage is that the animals must be restrained and will almost always experience some degree of stress during the inflation of the two balloons on the tail while blood pressure is measured. The blood flow in the tail is very sensitive to temperature changes and it is important that the animals are warm enough before starting the recording.

The implanted telemetry system is considered the gold standard for measuring blood pressure in intact and conscious mice. In this method a catheter attached to small a transmitter is inserted into the carotid artery so that the tip of the catheter lies inside the aortic arch, while the transmitter is placed subcutaneously on the left side of the abdomen of the mice. The catheter tip, that is pre-filled with gel, senses pressure waves that the transmitter converts into radio signals, which are transmitted wirelessly to a receiver outside the cage. The radio signal recorded by the receiver is translated into blood pressure by a computer. The

major advantage with the implanted telemetry system is the possibility to measure blood pressure over longer time in conscious animals moving freely in their natural living environment. The major disadvantage is the high cost of the system related to purchase as well as maintenance of the transmitters. Moreover, the operation itself and the post-operative recovery period make it a more time consuming method than e.g. the tail-cuff system. Additionally, the method requires good surgical skills that take time to learn. The insertion of the catheter and transmitter is a rather traumatic procedure for the mice, with a high mortality rate. Experienced users of the telemetry system have reported a success rate of 90% with carotid artery placement (169).

Studies comparing the flow-based tail-cuff system and implanted telemetry system have shown conflicting results. Whereas some find good, others find a poor correlation (170, 171). It seems that the tail-cuff system might be sufficient to measure blood pressure in rats, but given the variability found in mice, the American Heart Association recommend radiotelemetry for blood pressure measurements in mice in their latest statement regarding animal models of hypertension (161, 168, 170). Our experience was the same when measuring blood pressure in rats and mice with tail-cuff. Rats were calmer and easier to handle than mice. Mice appeared much more stressed with increased tail movement, as an indicator of stress (172), which was a constant source of error during inflation and deflation of the cuffs. Correct temperature of the tail was much harder to achieve in mice, which is crucial for blood flow in the tail. Hence, we concluded that telemetric recording was the preferred method for blood pressure measurements in mice.

5.1.4. Immunohistochemistry

Immunohistochemistry was chosen to quantify lymphatic and blood vessels, immune cells and chemokines. The advantage of immunohistochemistry is the low cost and the large numbers of easily accessible antibodies to detect specific proteins on cells and structures in the tissues. The possibility of using different chromogenic substrates or fluorescent markers makes it possible to stain for two

or more markers at the same time. If the same cell or structure expresses two different proteins, double staining with antigens for both proteins will make their identification and localization easier. Immunohistochemistry is a semiquantitative method, meaning that it is not quite precise. Mistakes in all parts of the assay performance may lead to variability and errors, e.g. handling and fixation of the tissue, sectioning, antigen retrieval, staining and quantification method (173).

Whole mount staining of the ear was used for quantification of lymphatic vessels in the dermis of mice. This staining technique provides a better total picture of the lymphatic vasculature than a series of thin sections through the ear. During the preparation of the ears for whole mount staining it is easy to disrupt the lymphatic vasculature, resulting in areas with poor staining that seem to lack lymphatic vasculature. This might be a source of error when analysing the ears, and to avoid this we selected areas where the lymphatic vasculature appeared intact with regular staining. Rat ears have a much thicker layer of connective tissue and when we performed whole mount staining on these, the lymphatic vasculature was much more disrupted and the staining became irregular after preparation. We therefore chose serial sections for quantification of lymphatic vessels in the skin of rats.

5.1.5. Flow cytometry

Flow cytometry is a laser/impedance-based technology with the ability to analyse thousands of particles rapidly. We used this method to study immune cell migration from skin to the draining lymph nodes. The principle behind the technology is the passage of cells in a single file in front of a laser. The cells are prepared in a suspension where fluorescent labelled antibodies, specific for the cells of interest to be examined, are added. The fluorochromes are excited by a laser and detection of the fluorescence is used to determine the cell type. By using fluorochromes with different absorption and emission spectra and lasers with different wavelengths, multiple antigens can be analysed at the same time to determine type and quantity of cells present in the suspension (174). Flow

cytometry is thus an ideal tool for the identification of small cell populations in more complex cell suspensions from e.g. a lymph node. There are limitations of this technique that are important to be aware of. Standardization of methods across laboratories is poor, and data interpretation is to some extent subjective. The use of multicolour flow cytometry increases the risk of physical overlap between the different fluorochromes emission spectra, termed spillover, meaning that a signal from one antibody can optically interfere with signals from others. To avoid spillover it is important to select fluorochromes where this effect is minimal. A process called compensation can correct for spillover. The goal of compensation is to neutralize the signals from an antibody from all other channels than its own. This is achieved by single-color controls and software that calculates spillover values, which are placed in a compensation matrix with the use of matrix algebra. For better identification between positive and negative populations, Fluorescence Minus One (FMO) controls can be used. These controls are cell samples from the experiment that are stained with all fluorochromes used except one. FMO controls help to better distinguish true positive staining of a cell population from spillover and background fluorescence and are thereby an important tool for a more precise analysis of flow cytometry data.

The migrated dendritic cell population in the lymph nodes after FITC painting that are detected with flow cytometry makes up a very small percentage of the total cell population, in most studies less than 1% (109). As negative control we used a lymph node draining an area from the skin where no FITC were applied. This negative control is equivalent to a FMO sample, and when compared to the FITC positive lymph node we clearly found a distinct FITC⁺ MHC II⁺⁺ population of migrating cells. As FITC positive cell make up a small percentage of the total number of cells in a lymph node, a small increase in migrating cells might be difficult to detect when analysing the data.

5.1.6. Lymph flow

As previously discussed, studies have shown that salt loading might lead to accumulation of salt in the skin, resulting in activation of immune cells and lymphangiogenesis (11, 13). To address the question if this might lead to enhanced lymph flow we indirectly measured lymph flow as clearance of injected Alexa-680-labelled albumin from the skin with an optical imager (158). Albumin has a molecular weight of approximately 67 kDa, which is within the optimal range for tissue washout through the lymph only (47). The volume of injected albumin is low to reduce the likelihood of an increase in P_{if} , which might contribute to an increase in the filling pressure of the lymphatic vasculature and thereby falsely increase lymph flow. The labelled albumin is stable and the injected solution is without any free dye to avoid unspecific binding to other extracellular proteins in the interstitium and clearance of free dye. For other methods used to measure lymph flow, such as clearance of Evans blue dye, this might be a problem as the dye binds to extracellular matrix proteins and free dye may be absorbed by the venous system (175). Because lymph flow is dependent on movement of the extremities, the animals were awake and freely moving during the experiment, except for the brief period during scanning. P_{if} was measured with micropipettes which is a practically atraumatic method and does not influence the fluid balance in the tissue (176).

A limitation of optical scanning is that it can only be applied in superficial tissues, like the skin. To assess the lymph flow in muscle we needed a method that was able to detect tracer molecules in deeper structures. We developed a PET/CT method where we injected the PET-emitter ^{124}I into a thigh muscle and determined clearance of the tracer with PET/CT at different time intervals. This method presents a new alternative for the determination of lymph flow, but is expensive and requires staff trained in the use of PET/CT and radioactive tracers.

5.2 General discussion

5.2.1 Lymphangiogenesis and function

Formation of new lymph vessels due to VEGF-C secretion from immune cells is suggested to be important for electrolyte homeostasis, and thereby blood pressure regulation (11, 15). The knowledge on the functional consequences of lymphangiogenesis is scarce. We therefore aimed to study the lymphatic function in a situation with a chronically expanded lymphatic network. We verified that the transgenic K14-VEGF-C mice have a hyperplastic lymphatic network and thereby should be a good animal model to study potential functional consequences of VEGF-C overexpression in skin (**paper I**). Results from previous studies of the lymphatic function in models of lymphangiogenesis are diverging, showing both increased, similar or reduced lymph flow during inflammation (69, 177-180). In our models, we found reduced lymph flow to the same extent in both VEGF-C and WT after inducing acute and chronic inflammation (**paper I**). The reduction in lymph flow occurred even though tissue water and P_{if} were increased, which in a situation without inflammation would be a driving force for lymph formation (57). Despite increased P_{if} due to enhanced capillary fluid filtration in inflammation, inflammatory mediators like NO have been shown to reduce the contractility strength and frequency in collecting lymph vessels, resulting in impaired lymph flow (181). The finding of similar reduction in lymph flow in VEGF-C and control mice during inflammation is contrasting to other studies in similar models of lymphangiogenesis (174). Our method of measuring clearance of labelled albumin with optical imaging should be better suited to determine lymph flow compared to clearance of Evans blue, as discussed previously, and could be an important factor to explain differences between our results and previous findings. To study lymph flow capacity during local overhydration we injected fluid intradermally. This injection led to local increase in tissue fluid and P_{if} in both genotypes, however, to a higher increase in lymph flow in the transgenic mice compared to WT mice. We concluded that resistance to filling of the

lymphatics was reduced in the VEGF-C overexpressing mice, suggesting that a hyperplastic lymphatic network is capable of an enhanced transport of fluid driven by increased P_{if} (**paper I**).

Migrating immune cells is an important component of lymph, and should be taken into account when evaluating lymphatic function. We addressed this question by using the FITC-painting to induce local inflammation on the ear and count the FITC positive cells in the draining lymph node after 18 hours. Although transgenic mice express nearly twice as much of the immune cell attractant CCL21 in the skin, FITC painting stimulated dendritic cell migration to the same extent in both WT and transgenic mice (**paper I**). This could be explained by suppression of CCL21 receptors on migrating dendritic cells in VEGF-C overexpressing mice (182) and an increased gradient of CCL21 is therefore not sufficient to induce increased migration of dendritic cells to lymph nodes.

Our results indicate that the assumption of a connection between an increased lymphatic network and increased function is necessarily not correct. It should be noticed, however, that our conclusion is based on the finding in a model where chronic overexpression of VEGF-C induces lymphangiogenesis, and that the situation might be different when the lymphangiogenesis is induced by Na^+ accumulation.

In **paper II**, we addressed how accumulation of Na^+ in the skin affects lymphatic vasculature and function. Rats in the HSD and DOCA group increased the number of lymph capillaries in the skin. A tendency of increased lymph flow compared to the control group was found in HSD and DOCA. However, when we included overnight measurement period there was a significantly increased lymph flow in high salt conditions. Even if the effect appears modest, it is important to keep in mind that a small increase in lymph flow will, over a longer period, increase the transport of fluid and electrolytes correspondingly and thereby significantly.

It has been reported an increase in the number of lymph capillaries in skin increase in rats and mice after salt loading, with one study reporting a twofold increase in lymphatic vasculature in ear of mice fed HSD (11). In mice we were not able to verify increased lymphangiogenesis after Na⁺ accumulation in the skin (**paper III**). A reason for the substantial discrepancy between our and previous data might be the selection of area for quantification. Lymphatic vasculature is easily disrupted when preparing ears for whole-mount staining, appearing as areas with irregular or no lymphatic vasculature. We therefore selected 3-5 areas that appeared intact with a continuous lymphatic network for quantification. In rats we were able to verify lymphangiogenesis after salt loading by quantification of lymphatic vessels in serial sections (**paper II**). The discrepancy between mice and rats could be explained by the different methods used. Whole-mount might not be accurate enough to detect small changes, which is better demonstrated by the serial sections. However, our findings indicate that salt accumulation does not stimulate lymphangiogenesis to the same extent as previously reported.

5.2.2 Blood pressure and lymphatics in the skin

Immune cells have been proposed to play a central role in the new hypothesis on salt-sensitive hypertension by producing VEGF-C during hypertonic conditions (11, 13). Depletion of macrophages in the skin by clodronate resulted in significant reduction in lymph flow, supporting the assumption that this cell type might be involved in lymphangiogenesis and lymph flow response observed during salt loading (**paper II**). Blocking lymphangiogenesis has been reported to result in more salt-sensitive animals with higher blood pressure after salt loading (13). Oppositely, we wanted to explore if existing lymphatic vasculature in the skin might affect blood pressure homeostasis during salt loading. Baseline blood pressure was the same in genetically engineered mice with either hyperplastic or reduced lymphatic skin vasculature as in WT controls (**paper III**). DOCA induced increased blood pressure to the same extent in mice with reduced lymphatic network and WT control mice, while HSD was insufficient

to induce blood pressure rise in any of the mouse models. In contrast, previous studies have reported higher blood pressure after HSD in mice lacking lymphatic vasculature in skin compared to mice with normal lymphatics, using the same mouse model (13). In the latter study, mice were awake in a restrainer while blood pressure was measured with an arterial line in the carotid artery one hour after insertion. It is likely that this method induced stress and thereby that the procedure itself results in an increase in blood pressure. In a later study, it was acknowledged that this method was not suitable for measurement of steady state blood pressure, but rather provides a method to measure stress-induced hypertension (183).

Dendritic cells have been reported to be involved in development salt-sensitive hypertension (134, 184). Increased dendritic cell migration from skin to the draining lymph in mice after DOCA might support the hypothesis that salt loading induces an immune response in the skin (**paper III**). Apparently, a hyperplastic lymphatic network does not itself lead to increased cell migration (**paper I**), indicating that the increased migration is due to other factors. If salt creates an inflammation in the skin with increased number of activated immune cells that secrete inflammatory mediators like VEGF-C, the observed increase in lymphatic vessels (**paper II**) might be a result of such inflammation. The reduced lymph flow in the skin observed after depletion of macrophages indicate that immune cells might be involved in lymphatic function (**paper II**). However, our results indicate that lymphangiogenesis per se does not affect blood pressure homeostasis (**paper III**). An increase of macrophages and no difference in the density of lymphatic vessels has also been found in the skin of patients with hypertension when compared to a normotensive control group (185).

Overall, our results indicate that lymphatic vasculature in the skin does not affect blood pressure homeostasis in mice after salt loading. This statement is supported by a recent study where the conclusion was that salt-sensitive hypertension seen after the use of sunitinib, a vascular endothelial growth factor inhibitor, is not due to impairment of skin lymphangiogenesis (186).

5.2.3 Salt accumulation in tissue

We found that rats accumulate Na^+ in the skin after HSD and DOCA (**paper II**). In contrast there was no accumulation of Na^+ in skin of mice after HSD, only after DOCA. There was no difference in salt content in the skin between genetically engineered and control mice (**paper III**). In a preliminary study, however, we found that the sodium content was reduced in the skin of FVB WT and VEGF-C mice after 5 weeks LSD, indicating a wash out of Na^+ from the skin. Still, Na^+ was reduced to the same extent in both groups. Overall, these findings indicate that skin might serve as reservoir for Na^+ . The differences in Na^+ accumulation between rats and mice after HSD might indicate that there are differences between species in the capability to store Na^+ in the skin.

DOCA induced a shift in Na^+ and K^+ balance in skeletal muscle, with increased Na^+ concentration and reduced concentration of K^+ (**paper III**). The shift of Na^+ and K^+ in muscle was the same in WT and genetically engineered mice and in agreement with other studies using DOCA (187, 188). Relative to skin, muscle has a high cell mass relative to interstitial space, making it a large depot for transcellular exchange of Na^+ for K^+ . NaMRI studies in humans have indicated that Na^+ appears to accumulate in muscle (153) and the increased lymph flow observed in rat muscle might be a result of such accumulation (**paper II**). In another preliminary study we also found redistribution of Na^+ and K^+ in the myocardium after DOCA, although not so prominent as in skeletal muscle. The membrane potential is crucial for heart function, and the regulation of potassium and sodium through the sodium-potassium pump is much more effectively controlled in heart compared to skeletal muscle (189).

DOCA and aldosterone both bind to mineralocorticoid receptors (MRs) with similar high affinity (190). MRs are best known as regulators of sodium and potassium transport in epithelial cells in the kidney and colon, but they are also expressed widely at low levels in heart, skeletal and smooth muscle (191, 192).

The shift of Na⁺ and K⁺ found in skeletal and heart muscle might be due to activation of MRs (**paper III**). In agreement with previous studies (187) we found no shift in the Na⁺ and K⁺ balance in muscle on HSD alone. However, further studies to look for a potential effect of HSD on the Na⁺ and K⁺ concentration in muscle would be of interest, especially in rats where an increased lymph flow was observed after salt loading.

6. Conclusion

The overall aim of this thesis was to study the role of the extracellular microenvironment and lymphatics in electrolyte and blood pressure regulation. Based on our studies in different animal models, we may conclude the following:

- Augmented lymphatic vasculature in the skin reduces resistance to lymph formation and facilitates enhanced clearance of fluid in situations with increased fluid filtration. In inflammation, lymph flow is however reduced. A hyperplastic lymphatic network expresses more chemoattractants, but this does not increase immune cell migration from the skin to the draining lymph node.
- Rats accumulate Na^+ in the skin, which induces lymphangiogenesis and is associated with increased lymph flow in the skin. Salt loading in rats moreover affect lymph flow in muscle, suggesting that also muscle may contribute in electrolyte and blood pressure homeostasis.
- Lymphatic vasculature in the skin does not affect skin accumulation of Na^+ or blood pressure homeostasis in mice. Accumulation of Na^+ does not stimulate lymphangiogenesis in mice. However, Na^+ accumulation might stimulate a general increase in immune cell activity in skin. DOCA induces a shift of Na^+ and K^+ in muscle.

7. Future perspectives

Although the evidence for a role of skin lymphatics in salt-sensitive hypertension is scarce, it seems that this idea is becoming more and more established as a fact. Our data, as well as others (186), do not support the strong connection between lymphangiogenesis and electrolyte and blood pressure homeostasis as previously reported. It is important to continue the work on skin accumulation of Na^+ to achieve a better understanding of the potential functional consequences, both regarding physiological changes and immune responses.

Our finding of sodium accumulation in muscle after DOCA has not been well described before. In subjects with resistant hypertension (RHTN), which is defined as the use of three or more antihypertensive drugs to control blood pressure, studies have shown that MR inhibitors might be useful to lower blood pressure (193). RHTN and MR-associated hypertension are linked to obesity, diabetes mellitus, polycystic ovary syndrome and chronic kidney disease (194). Excess aldosterone is often present in obesity, and patients with obesity are more likely to be salt-sensitive (195). The observation of increased sodium in muscle in hypertensive patients with ^{23}Na -MRI and a reduction of blood pressure and sodium content in muscle after treatment with the MR antagonist spironolactone may indicate that sodium storage and MRs in the muscle may play a role in salt-sensitive hypertension (153). Our findings of increased lymph flow in muscle after salt loading and changes in the sodium and potassium balance in skeletal and heart muscle after DOCA should be further addressed and might give a better understanding of the pathogenesis of salt-sensitive hypertension.

8. References

1. A global brief on hypertension; silent killer, global public health crisis. World Health Day 2013. Geneva: World Health Organization Press; 2013.
2. Hay J. A British Medical Association Lecture on THE SIGNIFICANCE OF A RAISED BLOOD PRESSURE. *Br Med J*. 1931;2(3679):43-7.
3. Xie X, Atkins E, Lv J, Bennett A, Neal B, Ninomiya T, et al. Effects of intensive blood pressure lowering on cardiovascular and renal outcomes: updated systematic review and meta-analysis. *Lancet*. 2016;387(10017):435-43.
4. Carretero OA, Oparil S. Essential hypertension. Part I: definition and etiology. *Circulation*. 2000;101(3):329-35.
5. Aburto NJ, Ziolkovska A, Hooper L, Elliott P, Cappuccio FP, Meerpohl JJ. Effect of lower sodium intake on health: systematic review and meta-analyses. *BMJ*. 2013;346:f1326.
6. Hall JE. *Textbook of medical physiology*. Thirteenth ed: Elsevier; 2016.
7. Guyton AC, Coleman TG, Cowley AV, Jr., Scheel KW, Manning RD, Jr., Norman RA, Jr. Arterial pressure regulation. Overriding dominance of the kidneys in long-term regulation and in hypertension. *Am J Med*. 1972;52(5):584-94.
8. Wiig H, Luft FC, Titze JM. The interstitium conducts extrarenal storage of sodium and represents a third compartment essential for extracellular volume and blood pressure homeostasis. *Acta Physiol (Oxf)*. 2018;222(3).
9. Titze J, Lang R, Ilies C, Schwind KH, Kirsch KA, Dietsch P, et al. Osmotically inactive skin Na⁺ storage in rats. *Am J Physiol Renal Physiol*. 2003;285(6):F1108-17.
10. Linz P, Santoro D, Renz W, Rieger J, Ruehle A, Ruff J, et al. Skin sodium measured with ²³Na MRI at 7.0 T. *NMR Biomed*. 2015;28(1):54-62.
11. Machnik A, Neuhofer W, Jantsch J, Dahlmann A, Tammela T, Machura K, et al. Macrophages regulate salt-dependent volume and blood pressure by a vascular endothelial growth factor-C-dependent buffering mechanism. *Nat Med*. 2009;15(5):545-52.
12. Machnik A, Dahlmann A, Kopp C, Goss J, Wagner H, van Rooijen N, et al. Mononuclear phagocyte system depletion blocks interstitial tonicity-responsive enhancer binding protein/vascular endothelial growth factor C expression and induces salt-sensitive hypertension in rats. *Hypertension*. 2010;55(3):755-61.
13. Wiig H, Schroder A, Neuhofer W, Jantsch J, Kopp C, Karlsen TV, et al. Immune cells control skin lymphatic electrolyte homeostasis and blood pressure. *J Clin Invest*. 2013;123(7):2803-15.
14. Oparil S, Acelajado MC, Bakris GL, Berlowitz DR, Cifkova R, Dominiczak AF, et al. Hypertension. *Nat Rev Dis Primers*. 2018;4:18014.
15. Coffman TM. Under pressure: the search for the essential mechanisms of hypertension. *Nat Med*. 2011;17(11):1402-9.
16. Li XC, Zhang J, Zhuo JL. The vasoprotective axes of the renin-angiotensin system: Physiological relevance and therapeutic implications in cardiovascular, hypertensive and kidney diseases. *Pharmacol Res*. 2017;125(Pt A):21-38.
17. Joyner MJ, Charkoudian N, Wallin BG. Sympathetic nervous system and blood pressure in humans: individualized patterns of regulation and their implications. *Hypertension*. 2010;56(1):10-6.

18. Miller AJ, Arnold AC. The renin-angiotensin system in cardiovascular autonomic control: recent developments and clinical implications. *Clin Auton Res.* 2019;29(2):231-43.
19. Turner AJ, Hooper NM. The angiotensin-converting enzyme gene family: genomics and pharmacology. *Trends Pharmacol Sci.* 2002;23(4):177-83.
20. Mirabito Colafella KM, Bovee DM, Danser AHJ. The renin angiotensin aldosterone system and its therapeutic targets. *Exp Eye Res.* 2019.
21. Cannavo A, Bencivenga L, Liccardo D, Elia A, Marzano F, Gambino G, et al. Aldosterone and Mineralocorticoid Receptor System in Cardiovascular Physiology and Pathophysiology. *Oxid Med Cell Longev.* 2018;2018:1204598.
22. de Leeuw PW, Bisognano JD, Bakris GL, Nadim MK, Haller H, Kroon AA, et al. Sustained Reduction of Blood Pressure With Baroreceptor Activation Therapy: Results of the 6-Year Open Follow-Up. *Hypertension.* 2017;69(5):836-43.
23. Vanhoutte PM, Mombouli JV. Vascular endothelium: vasoactive mediators. *Prog Cardiovasc Dis.* 1996;39(3):229-38.
24. Vallance P, Collier J, Moncada S. Effects of endothelium-derived nitric oxide on peripheral arteriolar tone in man. *Lancet.* 1989;2(8670):997-1000.
25. Pittner J, Wolgast M, Casellas D, Persson AE. Increased shear stress-released NO and decreased endothelial calcium in rat isolated perfused juxtamedullary nephrons. *Kidney Int.* 2005;67(1):227-36.
26. Ali A, Abu Zar M, Kamal A, Faquih AE, Bhan C, Iftikhar W, et al. American Heart Association High Blood Pressure Protocol 2017: A Literature Review. *Cureus.* 2018;10(8):e3230.
27. Rimoldi SF, Scherrer U, Messerli FH. Secondary arterial hypertension: when, who, and how to screen? *Eur Heart J.* 2014;35(19):1245-54.
28. Matchar DB, McCrory DC, Orlando LA, Patel MR, Patel UD, Patwardhan MB, et al. Systematic review: comparative effectiveness of angiotensin-converting enzyme inhibitors and angiotensin II receptor blockers for treating essential hypertension. *Ann Intern Med.* 2008;148(1):16-29.
29. Dahl LK, Heine M, Thompson K. Genetic influence of the kidneys on blood pressure. Evidence from chronic renal homografts in rats with opposite predispositions to hypertension. *Circ Res.* 1974;34(1):94-101.
30. Esler M. The 2009 Carl Ludwig Lecture: Pathophysiology of the human sympathetic nervous system in cardiovascular diseases: the transition from mechanisms to medical management. *J Appl Physiol (1985).* 2010;108(2):227-37.
31. Vallbo AB, Hagbarth KE, Torebjork HE, Wallin BG. Somatosensory, proprioceptive, and sympathetic activity in human peripheral nerves. *Physiol Rev.* 1979;59(4):919-57.
32. Smith PA, Graham LN, Mackintosh AF, Stoker JB, Mary DA. Relationship between central sympathetic activity and stages of human hypertension. *Am J Hypertens.* 2004;17(3):217-22.
33. Goldstein DS. Plasma catecholamines and essential hypertension. An analytical review. *Hypertension.* 1983;5(1):86-99.
34. Konukoglu D, Uzun H. Endothelial Dysfunction and Hypertension. *Adv Exp Med Biol.* 2017;956:511-40.
35. Dharmashankar K, Widlansky ME. Vascular endothelial function and hypertension: insights and directions. *Curr Hypertens Rep.* 2010;12(6):448-55.

36. Shiekh GA, Ayub T, Khan SN, Dar R, Andrabi KI. Reduced nitrate level in individuals with hypertension and diabetes. *J Cardiovasc Dis Res.* 2011;2(3):172-6.
37. Panza JA, Casino PR, Kilcoyne CM, Quyyumi AA. Role of endothelium-derived nitric oxide in the abnormal endothelium-dependent vascular relaxation of patients with essential hypertension. *Circulation.* 1993;87(5):1468-74.
38. Louveau A, Smirnov I, Keyes TJ, Eccles JD, Rouhani SJ, Peske JD, et al. Structural and functional features of central nervous system lymphatic vessels. *Nature.* 2015;523(7560):337-41.
39. Aspelund A, Antila S, Proulx ST, Karlsen TV, Karaman S, Detmar M, et al. A dural lymphatic vascular system that drains brain interstitial fluid and macromolecules. *J Exp Med.* 2015;212(7):991-9.
40. Aspelund A, Tammela T, Antila S, Nurmi H, Leppanen VM, Zarkada G, et al. The Schlemm's canal is a VEGF-C/VEGFR-3-responsive lymphatic-like vessel. *J Clin Invest.* 2014;124(9):3975-86.
41. Makinen T, Alitalo K. Molecular mechanisms of lymphangiogenesis. *Cold Spring Harb Symp Quant Biol.* 2002;67:189-96.
42. Swartz MA. The physiology of the lymphatic system. *Adv Drug Deliv Rev.* 2001;50(1-2):3-20.
43. Hirakawa S, Detmar M, Karaman S. Lymphatics in nanophysiology. *Adv Drug Deliv Rev.* 2014;74:12-8.
44. Vittet D. Lymphatic collecting vessel maturation and valve morphogenesis. *Microvasc Res.* 2014;96:31-7.
45. Scallan JP, Zawieja SD, Castorena-Gonzalez JA, Davis MJ. Lymphatic pumping: mechanics, mechanisms and malfunction. *J Physiol.* 2016;594(20):5749-68.
46. Breslin JW, Yang Y, Scallan JP, Sweat RS, Adderley SP, Murfee WL. Lymphatic Vessel Network Structure and Physiology. *Compr Physiol.* 2018;9(1):207-99.
47. Wiig H, Swartz MA. Interstitial fluid and lymph formation and transport: physiological regulation and roles in inflammation and cancer. *Physiol Rev.* 2012;92(3):1005-60.
48. Jacob M, Chappell D. Reappraising Starling: the physiology of the microcirculation. *Curr Opin Crit Care.* 2013;19(4):282-9.
49. Levick JR, Michel CC. Microvascular fluid exchange and the revised Starling principle. *Cardiovasc Res.* 2010;87(2):198-210.
50. Clement CC, Aphkhasava D, Nieves E, Callaway M, Olszewski W, Rotzschke O, et al. Protein expression profiles of human lymph and plasma mapped by 2D-DIGE and 1D SDS-PAGE coupled with nanoLC-ESI-MS/MS bottom-up proteomics. *J Proteomics.* 2013;78:172-87.
51. Leak LV, Liotta LA, Krutzsch H, Jones M, Fusaro VA, Ross SJ, et al. Proteomic analysis of lymph. *Proteomics.* 2004;4(3):753-65.
52. Dzieciatkowska M, D'Alessandro A, Moore EE, Wohlauer M, Banerjee A, Silliman CC, et al. Lymph is not a plasma ultrafiltrate: a proteomic analysis of injured patients. *Shock.* 2014;42(6):485-98.
53. Clement CC, Santambrogio L. The lymph self-antigen repertoire. *Front Immunol.* 2013;4:424.

54. Santambrogio L, Rammensee HG. Contribution of the plasma and lymph Degradome and Peptidome to the MHC Ligandome. *Immunogenetics*. 2019;71(3):203-16.
55. Haljamae H, Linde A, Amundson B. Comparative analyses of capsular fluid and interstitial fluid. *Am J Physiol*. 1974;227(5):1199-205.
56. Szabo G, Magyar Z. Electrolyte concentrations in subcutaneous tissue fluid and lymph. *Lymphology*. 1982;15(4):174-7.
57. Aukland K, Reed RK. Interstitial-lymphatic mechanisms in the control of extracellular fluid volume. *Physiol Rev*. 1993;73(1):1-78.
58. Guyton AC, Taylor AE, Brace RA. A synthesis of interstitial fluid regulation and lymph formation. *Fed Proc*. 1976;35(8):1881-5.
59. von der Weid PY. Review article: lymphatic vessel pumping and inflammation--the role of spontaneous constrictions and underlying electrical pacemaker potentials. *Aliment Pharmacol Ther*. 2001;15(8):1115-29.
60. Benoit JN, Zawieja DC, Goodman AH, Granger HJ. Characterization of intact mesenteric lymphatic pump and its responsiveness to acute edemagenic stress. *Am J Physiol*. 1989;257(6 Pt 2):H2059-69.
61. Olszewski WL, Engeset A. Intrinsic contractility of prenodal lymph vessels and lymph flow in human leg. *Am J Physiol*. 1980;239(6):H775-83.
62. Van Helden DF. Pacemaker potentials in lymphatic smooth muscle of the guinea-pig mesentery. *J Physiol*. 1993;471:465-79.
63. von der Weid PY, Zawieja DC. Lymphatic smooth muscle: the motor unit of lymph drainage. *Int J Biochem Cell Biol*. 2004;36(7):1147-53.
64. Solari E, Marcozzi C, Negrini D, Moriondo A. Fluid Osmolarity Acutely and Differentially Modulates Lymphatic Vessels Intrinsic Contractions and Lymph Flow. *Front Physiol*. 2018;9:871.
65. Sabin FR. The Method of Growth of the Lymphatic System. *Science*. 1916;44(1127):145-58.
66. Schneider M, Othman-Hassan K, Christ B, Wilting J. Lymphangioblasts in the avian wing bud. *Dev Dyn*. 1999;216(4-5):311-9.
67. Martinez-Corral I, Ulvmar MH, Stanczuk L, Tatin F, Kizhatil K, John SW, et al. Nonvenous origin of dermal lymphatic vasculature. *Circ Res*. 2015;116(10):1649-54.
68. Klotz L, Norman S, Vieira JM, Masters M, Rohling M, Dube KN, et al. Cardiac lymphatics are heterogeneous in origin and respond to injury. *Nature*. 2015;522(7554):62-7.
69. Kim H, Kataru RP, Koh GY. Regulation and implications of inflammatory lymphangiogenesis. *Trends Immunol*. 2012;33(7):350-6.
70. Karaman S, Leppanen VM, Alitalo K. Vascular endothelial growth factor signaling in development and disease. *Development*. 2018;145(14).
71. Shibuya M. Vascular Endothelial Growth Factor (VEGF) and Its Receptor (VEGFR) Signaling in Angiogenesis: A Crucial Target for Anti- and Pro-Angiogenic Therapies. *Genes Cancer*. 2011;2(12):1097-105.
72. Karkkainen MJ, Haiko P, Sainio K, Partanen J, Taipale J, Petrova TV, et al. Vascular endothelial growth factor C is required for sprouting of the first lymphatic vessels from embryonic veins. *Nat Immunol*. 2004;5(1):74-80.
73. Takahashi H, Shibuya M. The vascular endothelial growth factor (VEGF)/VEGF receptor system and its role under physiological and pathological conditions. *Clin Sci (Lond)*. 2005;109(3):227-41.

74. Makinen T, Jussila L, Veikkola T, Karpanen T, Kettunen MI, Pulkkanen KJ, et al. Inhibition of lymphangiogenesis with resulting lymphedema in transgenic mice expressing soluble VEGF receptor-3. *Nat Med.* 2001;7(2):199-205.
75. Jeltsch M, Kaipainen A, Joukov V, Meng X, Lakso M, Rauvala H, et al. Hyperplasia of lymphatic vessels in VEGF-C transgenic mice. *Science.* 1997;276(5317):1423-5.
76. Kaipainen A, Korhonen J, Mustonen T, van Hinsbergh VW, Fang GH, Dumont D, et al. Expression of the fms-like tyrosine kinase 4 gene becomes restricted to lymphatic endothelium during development. *Proc Natl Acad Sci U S A.* 1995;92(8):3566-70.
77. Schoppmann SF, Birner P, Stockl J, Kalt R, Ullrich R, Caucig C, et al. Tumor-associated macrophages express lymphatic endothelial growth factors and are related to peritumoral lymphangiogenesis. *Am J Pathol.* 2002;161(3):947-56.
78. Ran S, Montgomery KE. Macrophage-mediated lymphangiogenesis: the emerging role of macrophages as lymphatic endothelial progenitors. *Cancers (Basel).* 2012;4(3):618-57.
79. Dabrowska AK, Spano F, Derler S, Adlhart C, Spencer ND, Rossi RM. The relationship between skin function, barrier properties, and body-dependent factors. *Skin Res Technol.* 2018;24(2):165-74.
80. Nguyen AV, Soulika AM. The Dynamics of the Skin's Immune System. *Int J Mol Sci.* 2019;20(8).
81. Agarwal S, Krishnamurthy K. *Histology, Skin.* StatPearls. Treasure Island (FL)2019.
82. Richmond JM, Harris JE. Immunology and skin in health and disease. *Cold Spring Harb Perspect Med.* 2014;4(12):a015339.
83. Has C, Nystrom A. Epidermal Basement Membrane in Health and Disease. *Curr Top Membr.* 2015;76:117-70.
84. Brown TM, Krishnamurthy K. *Histology, Dermis.* StatPearls. Treasure Island (FL)2019.
85. Arda O, Goksugur N, Tuzun Y. Basic histological structure and functions of facial skin. *Clin Dermatol.* 2014;32(1):3-13.
86. Theocharis AD, Skandalis SS, Gialeli C, Karamanos NK. Extracellular matrix structure. *Adv Drug Deliv Rev.* 2016;97:4-27.
87. Wiig H, Keskin D, Kalluri R. Interaction between the extracellular matrix and lymphatics: consequences for lymphangiogenesis and lymphatic function. *Matrix Biol.* 2010;29(8):645-56.
88. Domene C, Jorgensen C, Abbasi SW. A perspective on structural and computational work on collagen. *Phys Chem Chem Phys.* 2016;18(36):24802-11.
89. Arora H, Falto-Aizpurua L, Cortes-Fernandez A, Choudhary S, Romanelli P. Connective Tissue Nevi: A Review of the Literature. *Am J Dermatopathol.* 2017;39(5):325-41.
90. Frances C, Robert L. Elastin and elastic fibers in normal and pathologic skin. *Int J Dermatol.* 1984;23(3):166-79.
91. Lee DH, Oh JH, Chung JH. Glycosaminoglycan and proteoglycan in skin aging. *J Dermatol Sci.* 2016;83(3):174-81.
92. Oh JH, Kim YK, Jung JY, Shin JE, Kim KH, Cho KH, et al. Intrinsic aging- and photoaging-dependent level changes of glycosaminoglycans and their correlation with water content in human skin. *J Dermatol Sci.* 2011;62(3):192-201.

93. Anderegg U, Simon JC, Averbek M. More than just a filler - the role of hyaluronan for skin homeostasis. *Exp Dermatol*. 2014;23(5):295-303.
94. Karsdal MA, Nielsen MJ, Sand JM, Henriksen K, Genovese F, Bay-Jensen AC, et al. Extracellular matrix remodeling: the common denominator in connective tissue diseases. Possibilities for evaluation and current understanding of the matrix as more than a passive architecture, but a key player in tissue failure. *Assay Drug Dev Technol*. 2013;11(2):70-92.
95. Visse R, Nagase H. Matrix metalloproteinases and tissue inhibitors of metalloproteinases: structure, function, and biochemistry. *Circ Res*. 2003;92(8):827-39.
96. Jablonska-Trypuc A, Matejczyk M, Rosochacki S. Matrix metalloproteinases (MMPs), the main extracellular matrix (ECM) enzymes in collagen degradation, as a target for anticancer drugs. *J Enzyme Inhib Med Chem*. 2016;31(sup1):177-83.
97. Theocharis AD, Manou D, Karamanos NK. The extracellular matrix as a multitasking player in disease. *FEBS J*. 2019.
98. Karamanos NK, Theocharis AD, Neill T, Iozzo RV. Matrix modeling and remodeling: A biological interplay regulating tissue homeostasis and diseases. *Matrix Biol*. 2019;75-76:1-11.
99. Muller DN, Wilck N, Haase S, Kleinewietfeld M, Linker RA. Sodium in the microenvironment regulates immune responses and tissue homeostasis. *Nat Rev Immunol*. 2019;19(4):243-54.
100. Sattler S. The Role of the Immune System Beyond the Fight Against Infection. *Adv Exp Med Biol*. 2017;1003:3-14.
101. Mirza R, DiPietro LA, Koh TJ. Selective and specific macrophage ablation is detrimental to wound healing in mice. *Am J Pathol*. 2009;175(6):2454-62.
102. Sattler S, Rosenthal N. The neonate versus adult mammalian immune system in cardiac repair and regeneration. *Biochim Biophys Acta*. 2016;1863(7 Pt B):1813-21.
103. Lin SL, Li B, Rao S, Yeo EJ, Hudson TE, Nowlin BT, et al. Macrophage Wnt7b is critical for kidney repair and regeneration. *Proc Natl Acad Sci U S A*. 2010;107(9):4194-9.
104. Lobov IB, Rao S, Carroll TJ, Vallance JE, Ito M, Ondr JK, et al. WNT7b mediates macrophage-induced programmed cell death in patterning of the vasculature. *Nature*. 2005;437(7057):417-21.
105. Ganeshan K, Chawla A. Metabolic regulation of immune responses. *Annu Rev Immunol*. 2014;32:609-34.
106. Abboud FM, Singh MV. Autonomic regulation of the immune system in cardiovascular diseases. *Adv Physiol Educ*. 2017;41(4):578-93.
107. Galloway DA, Phillips AEM, Owen DRJ, Moore CS. Phagocytosis in the Brain: Homeostasis and Disease. *Front Immunol*. 2019;10:790.
108. Clayton K, Vallejo AF, Davies J, Sirvent S, Polak ME. Langerhans Cells- Programmed by the Epidermis. *Front Immunol*. 2017;8:1676.
109. Platt AM, Randolph GJ. Dendritic cell migration through the lymphatic vasculature to lymph nodes. *Adv Immunol*. 2013;120:51-68.
110. Hettlinger J, Richards DM, Hansson J, Barra MM, Joschko AC, Krijgsveld J, et al. Origin of monocytes and macrophages in a committed progenitor. *Nat Immunol*. 2013;14(8):821-30.

111. Yanez DA, Lacher RK, Vidyarthi A, Colegio OR. The role of macrophages in skin homeostasis. *Pflugers Arch*. 2017;469(3-4):455-63.
112. Minutti CM, Knipper JA, Allen JE, Zaiss DM. Tissue-specific contribution of macrophages to wound healing. *Semin Cell Dev Biol*. 2017;61:3-11.
113. Willenborg S, Lucas T, van Loo G, Knipper JA, Krieg T, Haase I, et al. CCR2 recruits an inflammatory macrophage subpopulation critical for angiogenesis in tissue repair. *Blood*. 2012;120(3):613-25.
114. Willard-Mack CL. Normal structure, function, and histology of lymph nodes. *Toxicol Pathol*. 2006;34(5):409-24.
115. von Andrian UH, Mempel TR. Homing and cellular traffic in lymph nodes. *Nat Rev Immunol*. 2003;3(11):867-78.
116. Worbs T, Hammerschmidt SI, Forster R. Dendritic cell migration in health and disease. *Nat Rev Immunol*. 2017;17(1):30-48.
117. Boardman KC, Swartz MA. Interstitial flow as a guide for lymphangiogenesis. *Circ Res*. 2003;92(7):801-8.
118. Weber M, Hauschild R, Schwarz J, Moussion C, de Vries I, Legler DF, et al. Interstitial dendritic cell guidance by haptotactic chemokine gradients. *Science*. 2013;339(6117):328-32.
119. Scheinecker C, McHugh R, Shevach EM, Germain RN. Constitutive presentation of a natural tissue autoantigen exclusively by dendritic cells in the draining lymph node. *J Exp Med*. 2002;196(8):1079-90.
120. Miteva DO, Rutkowski JM, Dixon JB, Kilarski W, Shields JD, Swartz MA. Transmural flow modulates cell and fluid transport functions of lymphatic endothelium. *Circ Res*. 2010;106(5):920-31.
121. Martin-Fontecha A, Sebastiani S, Hopken UE, Uguccioni M, Lipp M, Lanzavecchia A, et al. Regulation of dendritic cell migration to the draining lymph node: Impact on T lymphocyte traffic and priming. *Journal of Experimental Medicine*. 2003;198(4):615-21.
122. Thomas SN, Rutkowski JM, Pasquier M, Kuan EL, Alitalo K, Randolph GJ, et al. Impaired humoral immunity and tolerance in K14-VEGFR-3-Ig mice that lack dermal lymphatic drainage. *J Immunol*. 2012;189(5):2181-90.
123. Drummond GR, Vinh A, Guzik TJ, Sobey CG. Immune mechanisms of hypertension. *Nat Rev Immunol*. 2019.
124. Okuda T, Grollman A. Passive transfer of autoimmune induced hypertension in the rat by lymph node cells. *Tex Rep Biol Med*. 1967;25(2):257-64.
125. Olsen F. Transfer of arterial hypertension by splenic cells from DOCA-salt hypertensive and renal hypertensive rats to normotensive recipients. *Acta Pathol Microbiol Scand C*. 1980;88(1):1-5.
126. Guzik TJ, Hoch NE, Brown KA, McCann LA, Rahman A, Dikalov S, et al. Role of the T cell in the genesis of angiotensin II induced hypertension and vascular dysfunction. *J Exp Med*. 2007;204(10):2449-60.
127. Pollow DP, Uhrlaub J, Romero-Aleshire M, Sandberg K, Nikolich-Zugich J, Brooks HL, et al. Sex differences in T-lymphocyte tissue infiltration and development of angiotensin II hypertension. *Hypertension*. 2014;64(2):384-90.
128. Lob HE, Marvar PJ, Guzik TJ, Sharma S, McCann LA, Weyand C, et al. Induction of hypertension and peripheral inflammation by reduction of extracellular superoxide dismutase in the central nervous system. *Hypertension*. 2010;55(2):277-83, 6p following 83.

129. Trott DW, Harrison DG. The immune system in hypertension. *Adv Physiol Educ.* 2014;38(1):20-4.
130. Saleh MA, McMaster WG, Wu J, Norlander AE, Funt SA, Thabet SR, et al. Lymphocyte adaptor protein LNK deficiency exacerbates hypertension and end-organ inflammation. *J Clin Invest.* 2015;125(3):1189-202.
131. Ren J, Crowley SD. Role of T-cell activation in salt-sensitive hypertension. *Am J Physiol Heart Circ Physiol.* 2019;316(6):H1345-H53.
132. Ugur M, Mueller SN. T cell and dendritic cell interactions in lymphoid organs: More than just being in the right place at the right time. *Immunol Rev.* 2019;289(1):115-28.
133. Vinh A, Chen W, Blinder Y, Weiss D, Taylor WR, Goronzy JJ, et al. Inhibition and genetic ablation of the B7/CD28 T-cell costimulation axis prevents experimental hypertension. *Circulation.* 2010;122(24):2529-37.
134. Kirabo A, Fontana V, de Faria AP, Loperena R, Galindo CL, Wu J, et al. DC isoketal-modified proteins activate T cells and promote hypertension. *J Clin Invest.* 2014;124(10):4642-56.
135. Salomon RG, Bi W. Isolevuglandin adducts in disease. *Antioxid Redox Signal.* 2015;22(18):1703-18.
136. Pons H, Ferrebuz A, Quiroz Y, Romero-Vasquez F, Parra G, Johnson RJ, et al. Immune reactivity to heat shock protein 70 expressed in the kidney is cause of salt-sensitive hypertension. *Am J Physiol Renal Physiol.* 2013;304(3):F289-99.
137. Tobias A, Mohiuddin SS. *Physiology, Water Balance.* StatPearls. Treasure Island (FL)2019.
138. Shrimanker I, Bhattarai S. *Electrolytes.* StatPearls. Treasure Island (FL)2019.
139. Chen JS, Al Khalili Y. *Physiology, Osmoregulation and Excretion.* StatPearls. Treasure Island (FL)2019.
140. Ogobuiro I, Tuma F. *Physiology, Renal.* StatPearls. Treasure Island (FL)2019.
141. Palmer LG, Schnermann J. Integrated control of Na transport along the nephron. *Clin J Am Soc Nephrol.* 2015;10(4):676-87.
142. Cook NR, Cutler JA, Obarzanek E, Buring JE, Rexrode KM, Kumanyika SK, et al. Long term effects of dietary sodium reduction on cardiovascular disease outcomes: observational follow-up of the trials of hypertension prevention (TOHP). *BMJ.* 2007;334(7599):885-8.
143. He FJ, MacGregor GA. A comprehensive review on salt and health and current experience of worldwide salt reduction programmes. *J Hum Hypertens.* 2009;23(6):363-84.
144. Sacks FM, Svetkey LP, Vollmer WM, Appel LJ, Bray GA, Harsha D, et al. Effects on blood pressure of reduced dietary sodium and the Dietary Approaches to Stop Hypertension (DASH) diet. DASH-Sodium Collaborative Research Group. *N Engl J Med.* 2001;344(1):3-10.
145. Weinberger MH, Miller JZ, Luft FC, Grim CE, Fineberg NS. Definitions and characteristics of sodium sensitivity and blood pressure resistance. *Hypertension.* 1986;8(6 Pt 2):II127-34.
146. Guyton AC. Blood pressure control--special role of the kidneys and body fluids. *Science.* 1991;252(5014):1813-6.

147. Heer M, Baisch F, Kropp J, Gerzer R, Drummer C. High dietary sodium chloride consumption may not induce body fluid retention in humans. *Am J Physiol Renal Physiol.* 2000;278(4):F585-95.
148. Titze J, Maillet A, Lang R, Gunga HC, Johannes B, Gauquelin-Koch G, et al. Long-term sodium balance in humans in a terrestrial space station simulation study. *Am J Kidney Dis.* 2002;40(3):508-16.
149. Rakova N, Juttner K, Dahlmann A, Schroder A, Linz P, Kopp C, et al. Long-term space flight simulation reveals infradian rhythmicity in human Na(+) balance. *Cell Metab.* 2013;17(1):125-31.
150. Titze J. Water-free sodium accumulation. *Semin Dial.* 2009;22(3):253-5.
151. Nikpey E, Karlsen TV, Rakova N, Titze JM, Tenstad O, Wiig H. High-Salt Diet Causes Osmotic Gradients and Hyperosmolality in Skin Without Affecting Interstitial Fluid and Lymph. *Hypertension.* 2017;69(4):660-8.
152. Hofmeister LH, Perisic S, Titze J. Tissue sodium storage: evidence for kidney-like extrarenal countercurrent systems? *Pflugers Arch.* 2015;467(3):551-8.
153. Kopp C, Linz P, Dahlmann A, Hammon M, Jantsch J, Muller DN, et al. ²³Na magnetic resonance imaging-determined tissue sodium in healthy subjects and hypertensive patients. *Hypertension.* 2013;61(3):635-40.
154. Muller S, Quast T, Schroder A, Hucke S, Klotz L, Jantsch J, et al. Salt-dependent chemotaxis of macrophages. *PLoS One.* 2013;8(9):e73439.
155. Karkkainen MJ, Saaristo A, Jussila L, Karila KA, Lawrence EC, Pajusola K, et al. A model for gene therapy of human hereditary lymphedema. *Proc Natl Acad Sci U S A.* 2001;98(22):12677-82.
156. Makinen T, Veikkola T, Mustjoki S, Karpanen T, Catimel B, Nice EC, et al. Isolated lymphatic endothelial cells transduce growth, survival and migratory signals via the VEGF-C/D receptor VEGFR-3. *EMBO J.* 2001;20(17):4762-73.
157. Niemeyer JE. Telemetry for small animal physiology. *Lab Anim (NY).* 2016;45(7):255-7.
158. Karlsen TV, McCormack E, Mujic M, Tenstad O, Wiig H. Minimally invasive quantification of lymph flow in mice and rats by imaging depot clearance of near-infrared albumin. *Am J Physiol Heart Circ Physiol.* 2012;302(2):H391-401.
159. Janssen PM, Biesiadecki BJ, Ziolo MT, Davis JP. The Need for Speed: Mice, Men, and Myocardial Kinetic Reserve. *Circ Res.* 2016;119(3):418-21.
160. Reckelhoff JF, Alexander BT. Reproducibility in animal models of hypertension: a difficult problem. *Biol Sex Differ.* 2018;9(1):53.
161. Lerman LO, Kurtz TW, Touyz RM, Ellison DH, Chade AR, Crowley SD, et al. Animal Models of Hypertension: A Scientific Statement From the American Heart Association. *Hypertension.* 2019;73(6):e87-e120.
162. Hartner A, Cordasic N, Klanke B, Veelken R, Hilgers KF. Strain differences in the development of hypertension and glomerular lesions induced by deoxycorticosterone acetate salt in mice. *Nephrol Dial Transplant.* 2003;18(10):1999-2004.
163. Drenjancevic-Peric I, Jelakovic B, Lombard JH, Kunert MP, Kibel A, Gros M. High-salt diet and hypertension: focus on the renin-angiotensin system. *Kidney Blood Press Res.* 2011;34(1):1-11.
164. Kandlikar SS, Fink GD. Splanchnic sympathetic nerves in the development of mild DOCA-salt hypertension. *Am J Physiol Heart Circ Physiol.* 2011;301(5):H1965-73.

165. Lin HY, Lee YT, Chan YW, Tse G. Animal models for the study of primary and secondary hypertension in humans. *Biomed Rep.* 2016;5(6):653-9.
166. Basting T, Lazartigues E. DOCA-Salt Hypertension: an Update. *Curr Hypertens Rep.* 2017;19(4):32.
167. Martus W, Kim D, Garvin JL, Beierwaltes WH. Commercial rodent diets contain more sodium than rats need. *Am J Physiol Renal Physiol.* 2005;288(2):F428-31.
168. Zhao X, Ho D, Gao S, Hong C, Vatner DE, Vatner SF. Arterial Pressure Monitoring in Mice. *Curr Protoc Mouse Biol.* 2011;1:105-22.
169. Carlson SH, Wyss JM. Long-term telemetric recording of arterial pressure and heart rate in mice fed basal and high NaCl diets. *Hypertension.* 2000;35(2):E1-5.
170. Kurtz TW, Griffin KA, Bidani AK, Davisson RL, Hall JE, Subcommittee of P, et al. Recommendations for blood pressure measurement in humans and experimental animals. Part 2: Blood pressure measurement in experimental animals: a statement for professionals from the subcommittee of professional and public education of the American Heart Association council on high blood pressure research. *Hypertension.* 2005;45(2):299-310.
171. Wilde E, Aubdool AA, Thakore P, Baldissera L, Jr., Alawi KM, Keeble J, et al. Tail-Cuff Technique and Its Influence on Central Blood Pressure in the Mouse. *J Am Heart Assoc.* 2017;6(6).
172. Salay LD, Ishiko N, Huberman AD. A midline thalamic circuit determines reactions to visual threat. *Nature.* 2018;557(7704):183-9.
173. Taylor CR, Levenson RM. Quantification of immunohistochemistry--issues concerning methods, utility and semiquantitative assessment II. *Histopathology.* 2006;49(4):411-24.
174. Adan A, Alizada G, Kiraz Y, Baran Y, Nalbant A. Flow cytometry: basic principles and applications. *Crit Rev Biotechnol.* 2017;37(2):163-76.
175. Proulx ST, Ma Q, Andina D, Leroux JC, Detmar M. Quantitative measurement of lymphatic function in mice by noninvasive near-infrared imaging of a peripheral vein. *JCI Insight.* 2017;2(1):e90861.
176. Wiig H, Reed RK, Aukland K. Micropuncture measurement of interstitial fluid pressure in rat subcutis and skeletal muscle: comparison to wick-in-needle technique. *Microvasc Res.* 1981;21(3):308-19.
177. Huggenberger R, Siddiqui SS, Brander D, Ullmann S, Zimmermann K, Antsiferova M, et al. An important role of lymphatic vessel activation in limiting acute inflammation. *Blood.* 2011;117(17):4667-78.
178. Huggenberger R, Ullmann S, Proulx ST, Pytowski B, Alitalo K, Detmar M. Stimulation of lymphangiogenesis via VEGFR-3 inhibits chronic skin inflammation. *J Exp Med.* 2010;207(10):2255-69.
179. Kataru RP, Jung K, Jang C, Yang H, Schwendener RA, Baik JE, et al. Critical role of CD11b+ macrophages and VEGF in inflammatory lymphangiogenesis, antigen clearance, and inflammation resolution. *Blood.* 2009;113(22):5650-9.
180. Lachance PA, Hazen A, Sevick-Muraca EM. Lymphatic vascular response to acute inflammation. *PLoS One.* 2013;8(9):e76078.
181. Chakraborty S, Davis MJ, Muthuchamy M. Emerging trends in the pathophysiology of lymphatic contractile function. *Semin Cell Dev Biol.* 2015;38:55-66.

-
182. Christiansen AJ, Dieterich LC, Ohs I, Bachmann SB, Bianchi R, Proulx ST, et al. Lymphatic endothelial cells attenuate inflammation via suppression of dendritic cell maturation. *Oncotarget*. 2016;7(26):39421-35.
183. Kitada K, Daub S, Zhang Y, Klein JD, Nakano D, Pedchenko T, et al. High salt intake reprioritizes osmolyte and energy metabolism for body fluid conservation. *J Clin Invest*. 2017;127(5):1944-59.
184. Van Beusecum JP, Barbaro NR, McDowell Z, Aden LA, Xiao L, Pandey AK, et al. High Salt Activates CD11c(+) Antigen-Presenting Cells via SGK (Serum Glucocorticoid Kinase) 1 to Promote Renal Inflammation and Salt-Sensitive Hypertension. *Hypertension*. 2019;74(3):555-63.
185. Chachaj A, Pula B, Chabowski M, Grzegorzolka J, Szahidewicz-Krupska E, Karczewski M, et al. Role of the Lymphatic System in the Pathogenesis of Hypertension in Humans. *Lymphat Res Biol*. 2018;16(2):140-6.
186. Lankhorst S, Severs D, Marko L, Rakova N, Titze J, Muller DN, et al. Salt Sensitivity of Angiogenesis Inhibition-Induced Blood Pressure Rise: Role of Interstitial Sodium Accumulation? *Hypertension*. 2017;69(5):919-26.
187. Titze J, Bauer K, Schafflhuber M, Dietsch P, Lang R, Schwind KH, et al. Internal sodium balance in DOCA-salt rats: a body composition study. *Am J Physiol Renal Physiol*. 2005;289(4):F793-802.
188. Ziomber A, Machnik A, Dahlmann A, Dietsch P, Beck FX, Wagner H, et al. Sodium-, potassium-, chloride-, and bicarbonate-related effects on blood pressure and electrolyte homeostasis in deoxycorticosterone acetate-treated rats. *Am J Physiol Renal Physiol*. 2008;295(6):F1752-63.
189. Fuller W, Tulloch LB, Shattock MJ, Calaghan SC, Howie J, Wypijewski KJ. Regulation of the cardiac sodium pump. *Cell Mol Life Sci*. 2013;70(8):1357-80.
190. Doyle D, Smith R, Krozowski ZS, Funder JW. Mineralocorticoid specificity of renal type I receptors: binding and metabolism of corticosterone. *J Steroid Biochem*. 1989;33(2):165-70.
191. Tesch GH, Young MJ. Mineralocorticoid Receptor Signaling as a Therapeutic Target for Renal and Cardiac Fibrosis. *Front Pharmacol*. 2017;8:313.
192. Chadwick JA, Hauck JS, Gomez-Sanchez CE, Gomez-Sanchez EP, Rafael-Fortney JA. Gene expression effects of glucocorticoid and mineralocorticoid receptor agonists and antagonists on normal human skeletal muscle. *Physiol Genomics*. 2017;49(6):277-86.
193. Nishizaka MK, Zaman MA, Calhoun DA. Efficacy of low-dose spironolactone in subjects with resistant hypertension. *Am J Hypertens*. 2003;16(11 Pt 1):925-30.
194. Shibata H, Itoh H. Mineralocorticoid receptor-associated hypertension and its organ damage: clinical relevance for resistant hypertension. *Am J Hypertens*. 2012;25(5):514-23.
195. Rocchini AP, Key J, Bondie D, Chico R, Moorehead C, Katch V, et al. The effect of weight loss on the sensitivity of blood pressure to sodium in obese adolescents. *N Engl J Med*. 1989;321(9):580-5.

Paper I

Lymphangiogenesis facilitates initial lymph formation and enhances the dendritic cell mobilizing chemokine CCL21 without affecting migration

Tine V Karlsen^{1,*}, Tore Reikvam^{1*}, Anne Tofteberg¹, Elham Nikpey^{1,2}, Trude Skogstrand¹, Marek Wagner^{1,3}, Olav Tenstad¹ and Helge Wiig¹

*Equal contribution

¹Department of Biomedicine, University of Bergen, Norway

²Department of Medicine, Haukeland University Hospital, Bergen, Norway

³Department of Pathology, Haukeland University Hospital, Bergen, Norway

Running title: Functional effects of lymphangiogenesis

Corresponding authors:

Tine V Karlsen and Helge Wiig

Department of Biomedicine,

Jonas Lies vei 91,

N-5009 Bergen, Norway

Email: tine.karlsen@uib.no and

helge.wiig@uib.no

key words: lymphatics, extracellular fluid, extracellular volume regulation, immune cell migration

Abstract

Objective: Lymphatic vessels play an important role in body fluid as well as immune system homeostasis. Whereas the role of malfunctioning or missing lymphatics has been studied extensively, less is known on the functional consequences of a chronically expanded lymphatic network or lymphangiogenesis.

Approach and Results: To this end, we used K14-VEGF-C transgenic mice overexpressing the vascular endothelial growth factor C in skin, and investigated the responses to inflammatory and fluid volume challenges. We also recorded interstitial fluid pressure, a major determinant of lymph flow. Transgenic mice had a strongly enhanced lymph vessel area in skin. Acute inflammation induced by lipopolysaccharide and chronic inflammation by delayed-type hypersensitivity both resulted in increased interstitial fluid pressure and reduced lymph flow, both to the same extent in wild type and transgenic mice. Hyperplastic lymphatic vessels, however, demonstrated enhanced transport capacity after local fluid overload not induced by inflammation. In this situation, interstitial fluid pressure was increased to a similar extent in the two strains, thus suggesting that the enhanced lymph vessel area facilitated initial lymph formation. The increased lymph vessel area resulted in an enhanced production of the chemoattractant CCL21 that, however, did not result in augmented dendritic cell migration after induction of local skin inflammation by fluorescein isothiocyanate.

Conclusions: An expanded lymphatic network is capable of enhanced chemoattractant production, and lymphangiogenesis will facilitate initial lymph formation favoring increased clearance of fluid in situations of augmented fluid filtration.

Abbreviations

BSA; bovine serum albumin

FITC; fluorescein isothiocyanate

HSA; human serum albumin

K14; keratin-14

LPS; lipopolysaccharide

Lyve-1; lymph vessel endothelial hyaluronan receptor-1

P_{if} ; interstitial fluid pressure

TTW; total tissue water

VEGF-C; vascular endothelial growth factor-C

Introduction

Lymphatic vessels play an important role in body fluid as well as immune system homeostasis. To maintain fluid homeostasis, the filtration of fluid and plasma proteins must be balanced by the formation of lymph that is transported into initial lymphatics and eventually returned to the general circulation. Lymph vessels are also the major transporters of soluble antigens and antigen-presenting cells from peripheral tissues to lymph nodes where they mount an immune response(196). The discovery of lymph vessel growth factors and molecular markers two decades ago enabled us to ask new and targeted questions and has led to a dramatic increase in available knowledge in this field.

Malfunctioning or missing lymphatics may result in tissue fluid accumulation and lymphedema that has been studied extensively in experimental models as well as clinically (for review see(196, 197)). Less is known, however, on the functional consequences of a chronically expanded lymphatic network. It is well established that many inflammatory conditions result in an expansion of initial lymphatics and lymphatic remodeling(198, 199), and that the lymphangiogenic factor Vascular Endothelial Growth Factor (VEGF)-C plays a central role in these processes. In skin, it has been shown that stimulation of lymphangiogenesis by VEGFR-3 or its ligand VEGF-C reduces acute and chronic inflammation, most likely mediated by a stimulation of lymph drainage from the inflamed tissue(178, 200, 201). In contrast, in models known to stimulate lymphangiogenesis, other groups have shown either no change in clearance(179), or a reduced lymphatic pumping activity indicating a reduced clearance in acute inflammation(180, 202).

Previous data on the function of an expanded lymphatic network are therefore conflicting. In this context, it is pertinent to remember that both components of lymph, fluid and cells, should be taken into account when evaluating lymphatic function. Moreover, interstitial fluid pressure (P_{if}) is a major determinant of lymph flow(47), transcapillary fluid balance and interstitial fluid volume, and this parameter has not been evaluated in a situation with an expanded lymphatic network.

In the present study, we therefore aimed to resolve questions related to the function of an expanded lymphatic network discussed above, or to state it differently, what lymphangiogenesis achieves(203). To this end we applied a transgenic mouse model stably overexpressing human VEGF-C in the skin under the control of the keratin-14 (K14) promoter(75). This model could be used to ask questions of lymphatic function related to inherent or induced lymphangiogenesis by applying a recently developed optical imaging method to record lymph flow. We found that VEGF-C overexpression did not affect tissue hydration and P_{if} in control situation. Moreover, these parameters were not differently influenced in the two strains in acute and chronic inflammation. Hyperplastic lymphatic vessels, however, had increased transport capacity in a situation involving fluid overload not induced by inflammation. These findings imply that the hyperplastic vessels facilitate initial lymph formation and thus increase transport rate provided the absence of inflammatory mediators. Nevertheless, the hyperplastic vessels were not capable of inducing increased immune cell migration in spite of an enhanced production of immune cell chemoattractants.

Materials and Methods

Materials and Methods are available in the online-only Data Supplement.

Results

Lymphatic vessel area in the skin is substantially enlarged in K14-VEGF-C mice

Our major aim was to resolve questions related to the function of an expanded lymphatic network, and thereby what is achieved by lymphangiogenesis(203). To this end we chose an established transgenic model overexpressing VEGF-C in skin(75). To confirm that K14-VEGF-C overexpression led to increased lymphangiogenesis we performed whole mount staining on WT and K14-VEGF-C ears, co-staining with the lymphatic specific marker LYVE-1 and

the blood vessel marker CD31. In line with previous studies on K14-VEGF-C mice, we found a much denser ear lymphatic network in K14-VEGF-C than in WT mice (Fig 1A) with a $\approx 100\%$ increase in LYVE-1⁺ area (Fig. 1B). On the other hand, the blood vessel network as stained with CD31 in K14-VEGF-C mice appeared normal (Fig. 1A), and the blood vessel area was not different in the two strains (Fig 1B). We also assessed the lymph vessels in other regions to study whether the phenotype applied to all skin areas. Serial sections of paw and back skin confirmed a significant increase in LYVE-1⁺ lymphatic vessel area in K14-VEGF-C mice (Fig. 1 C), and thereby that this model was suitable for functional studies of lymphangiogenesis.

Lymphatic drainage and fluid balance parameters are similar to WT in K14-VEGF-C mice in control situation and during inflammation

To assess whether the expanded lymphatic network influenced lymphatic drainage from the skin, we injected 0.5 μ l Alexa680-labelled bovine serum albumin into the dermis of the hind paw and followed the washout of tracer by optical imaging over the course of 6 hours. The removal of albumin is restricted exclusively to lymphatics due to its size, and will thus reflect lymph flow from the injected area. To facilitate lymph flow, the mice were freely moving in their cage in between the hourly imaging sessions. Despite having more lymphatic vessels than WT mice, washout of tracer and thereby lymph flow in K14-VEGF-C mice was similar to WT (Fig. 2A). The equal lymph flow suggested a similar lymph production and protein extravasation. We therefore assessed the extravasation of radioactively labelled albumin, and found the protein extravasation to be not different in the two strains in the unperturbed control situation (Fig. 2B). The similar lymph flow and protein extravasation suggest that the lymph production, i.e. transcapillary fluid filtration, is equal in the two strains.

The fluid volume parameters and potential drivers of lymph flow, total tissue water (TTW) and interstitial fluid pressure (P_{if}), were also found to be not different from WT in K14-VEGF-C mice hind paw (Fig. 3A,C) and ear (Fig. 3B,D) in control situation. These findings were also reflected in back skin (data not shown). Moreover, systolic as well as mean arterial blood pressures were similar, averaging 113 ± 5 mm Hg (systolic) and 92 ± 3 mmHg (mean) in WT (n=11) with corresponding pressures of 114 ± 4 mmHg and 92 ± 4 mmHg in K14-VEGF-C mice (n=10).

We hypothesized that a potential difference in transport capacity of the two strains would manifest in skin inflammation known to induce an increase in capillary filtration. To induce inflammation, we used two models, one acute based on injection of lipopolysaccharide (LPS) and one chronic based on topical application of oxazolone that will induce delayed-type hypersensitivity. Seven days after the initial sensitization with 2% oxazolone, and 2 days after challenge (1% oxazolone) we measured lymph flow, P_{if} and TTW. The delayed-type hypersensitivity response resulted in significantly increased TTW in paw skin (Fig. 3A) and ear (Fig. 3B) as well as P_{if} in corresponding sites (Fig. 3C,D) reflecting accumulation of fluid, but to the same extent in both strains.

The observed increase in P_{if} , again a consequence of increased fluid accumulation during inflammation, will represent an increased driving force for filling of initial lymphatics that might promote lymph drainage(47). We observed, however, that lymph transport was significantly halted in oxazolone-induced

inflammation, resulting in an equally reduced washout rate of $\approx 15\%$ in both strains when compared with the control situation (Fig. 2C).

We also induced an acute inflammation by local injection of LPS. LPS actually resulted in an increase in TTW and P_{if} that was even more pronounced than the corresponding responses observed after oxazolone treatment in paw skin (Fig 3A,C) as well as ear (Fig. 3B,D). Surprisingly, more fluid accumulated in the ear in K14-VEGF-C than in WT (Fig. 3B), an effect that was not seen in the paw (Fig. 3A). In spite of an even stronger stimulus for lymph vessel filling, the reduction in lymphatic tracer washout was even more reduced than in oxazolone-induced inflammation, amounting to 43% in K14-VEGF-C and 38% in WT when compared with respective controls (Fig 2C). Moreover, this impeded lymph flow effect was long-lasting, as shown by the observation of close to twice the amount of tracer retained in skin 24 h after LPS injection in both strains (Fig 2D).

Interstitial fluid volume overload increases lymph flow to a greater extent in K14-VEGF-C mice

As described above we observed no effect of an increased lymph vessel area after induction of lymphangiogenesis after acute as well as chronic inflammation. Inflammation may, however, result in the release of numerous mediators, notably NO, that can interfere with lymphatic endothelial function and result in lymphatic contractile dysfunction(45), and thus counteract the stimulus effect of increased capillary filtration and interstitial fluid volume on lymphatic flow. To separate these effects, we investigated whether there were functional consequences of an expanded lymphatic network in a situation where solely the interstitial volume was increased by assessing lymph flow in the two strains after local overhydration. To this end, we injected 30 μ l isotonic saline into the dermis of the hind paw with an insulin syringe after an initial control washout period lasting for 120 min (Fig 4A). In response to the fluid volume overload at 180 min, the K14-VEGF-C mice experienced a faster washout of tracer for the following period up to 300 min compared to WT (Fig. 4A), quantified as an increase (more negative) in average rate constant k of 25% in K14-VEGF-C compared with WT mice (Fig 4B).

To investigate the local driving pressure for lymph formation we also assessed P_{if} in the overhydrated skin area. We found that the local P_{if} increased dramatically, from average values of -1 mm Hg in control situation before injection to 7-8 mm Hg immediately after injection (Fig. 4C). Although P_{if} in the K14-VEGF-C in the first period after injection (denoted "0" in Fig. 4C) tended to be lower than in WT, this difference was not significant ($P=0.12$). The pressure subsided gradually, but was still higher than control pressure 120 min after saline injection in both strains. The observed increased lymph transport capacity in K14-VEGF-C in spite of a similar (or slightly lower) pressure gradient for lymph vessel filling suggests that the enhanced lymph vessel area in this strain facilitates initial lymph formation compared with WT.

Reduced effect of local interstitial fluid overload on lymph flow in Chy mice

To study the effect of lymphatic hypoplasia on local overhydration we injected 30 μ l isotonic saline into hindlimb skin of Chy mice missing initial lymphatic vessels in dermis resulting in lymphedema(155). In agreement with previous studies(158), Chy mice had visible hindlimb edema, lower washout rate,

and thus lymph formation and flow, than WT mice in control situation before local saline injection (Fig 5A). This occurred in spite of an increased P_{if} and thus driving pressure for lymph formation (Fig. 5C), suggesting the initial lymph formation was impeded even in control situation. Intradermal injection of 30 μ l isotonic saline into the same hind paw resulted in an apparent immediate, but not significant, increase in washout in the Chy mice (Fig. 5A). As described above, there was, however, an increase in washout in WT mice after this local volume stimulus, maintaining the difference in rate constants (k) between the strains compared with the control situation (Fig 5B). Apparently, the increased driving pressure for lymph formation, P_{if} , in control situation (Fig 5C) could not counteract the reduction in control lymph flow in Chy. Surprisingly, there was a more pronounced increase in P_{if} in WT than in Chy after local overhydration (Fig 5C), but this is likely a result of a faster local fluid volume and pressure dissipation in the Chy hindlimb, because of a strongly increased hydraulic conductivity in edema(204). The observed reduced lymph transport capacity in Chy in spite of an increased pressure gradient for lymph vessel filling in control situation, and a similar gradient >60 min after local overhydration, suggests that the reduced lymph vessel area in Chy results in an increased impediment of initial lymph formation compared with WT.

Synthesis of CCL21 and migration of immune cells from skin enhanced in K14-VEGF-C mice

Lymphatic vasculature has been shown to be highly dynamic, and lymphatic endothelial cells are producers of chemokines and adhesion molecules that play active roles in inflammatory and immune processes(198). We asked whether the enhanced area of LYVE-1⁺ lymphatics shown in K14-VEGF-C mice resulted in an increased content of the chemokine CCL21, known as one of the most central immune cell, notably dendritic cell, attractants in skin(116). By whole mount staining, we showed the presence of CCL21 in LYVE-1⁺ initial lymphatics in skin (Fig. 6A). Interestingly, when CCL21 expression was calculated as % area per field of view, the expression in the transgenic mice was almost twice that of WT mice (Fig. 6B), suggesting a higher content of this chemokine in the transgenic mice. The positive staining per lymph vessel area, however, did not differ in K14-VEGF-C and WT mice (Fig 6C).

We then tested whether the increased content of CCL21 affected migration of immune cells from skin. First, we assessed the number of dendritic cells determined as CD207⁺/MHC⁺ cells in ear skin from epidermal sheets, and found no difference between the strains during control conditions (Fig. 7A,B). We then induced local inflammation by painting with fluoroisothiocyanate (FITC), and recorded the cell uptake in draining lymph nodes by flow cytometry. There was no increased migration of FITC positive MHCII⁺CD11c⁺ cells neither at 12 h (data not shown) or at 18 h after painting (Fig. 7C), suggesting that even though there was an enhanced lymph vessel area producing the dendritic cell mobilizing chemokine CCL21 in K14-VEGF-C mice, this had no effect on dendritic cell migration to the draining lymph node.

Discussion

Whether the formation of new lymphatics, i.e. lymphangiogenesis, has functional consequences for lymphatic transport is a controversial issue that was

addressed in the present study. To this end, we used a transgenic mouse model expressing VEGF-C in keratinocytes, producing a hyperplastic lymphatic network in skin. Transgenic mice had normal water content, P_{if} , capillary permeability and lymph flow during control conditions suggesting a normal capillary barrier. Induction of acute as well as chronic inflammation reduced lymph flow to an equal extent in transgenic and WT mice. Interestingly, local infusion of fluid in skin stimulated fluid removal more forcefully in the transgenic mice. Such an expanded lymphatic network is capable of enhanced clearance of fluid, possibly because of an increased area that will offer less resistance to fluid uptake and thus facilitate initial lymph formation. In spite of an increased production of the DC mobilizing chemokine CCL21, however, immune cell migration from skin was unchanged. Our data suggest that an expanded lymphatic network is capable of enhanced clearance of fluid provided that there is an increased interstitial fluid driving pressure for filling of initial lymphatics, and that the downstream pumping capacity is not compromised by, e.g., an acute inflammation.

Evaluation of methods

When attempting to understand diverging results derived from various studies on the functional role of lymphatics, a closer analysis of the methods used is pertinent since methodological aspects may explain at least some of this variation. Here we chose an extensively evaluated near infrared imaging method to assess lymph flow. This method is based on washout of Alexa-680-labelled albumin with a molecular weight of ≈ 67 kDa and thus within the optimal range for tissue clearance through lymph(158). Moreover, with this technique, the injection volume is low, that will reduce the possibility of an increase in local P_{if} that *per se* will contribute to an increased filling pressure of lymphatics and thereby artificially enhanced lymph flow. The imaging probe is also very stable and without any free dye. Thereby unspecific binding to proteins in the tissue as well as clearance of free dye to plasma is not a problem, as might be expected with e.g. Evans blue and Indocyanin green(205, 206). Although well suited for paw and back skin, we experienced problems with exact positioning and tissue photon absorption when imaging the ear, resulting in variable count recovery and non-linear washout curves. Although the ear is a frequently used site for studies of skin fluid homeostasis, we therefore chose paw skin as our preferential area of study. We also chose the micropipette method for measurement of P_{if} that is practically atraumatic and does not add to or remove fluid from the tissue to minimize trauma and fluid volume artifacts.

Comparison to previous studies

The conspicuous change in lymphatic vessel area in the K14-VEGF-C mouse model had no obvious transcapillary fluid exchange phenotype in control situation; the protein extravasation, P_{if} , and tissue water content was not different from that in WT mice. Since these parameters were not different, it is to be expected that the lymph flow is not different, as actually observed. In contrast, Huggenberger et al(200) found an increased skin lymph flow in the K14-VEGF-C model based on clearance of Evans blue, a tracer that is not well suited for quantification of lymph flow as discussed above. Moreover, an increase was also found in a recent study based on tissue clearance of near infrared tracer(182).

In light of several previous observations of an increased clearance of tissue fluid in closely related models(178, 179, 200, 201), it was surprising that we actually found a similarly reduced lymph flow in K14-VEGF-C and WT mice in two different models of skin inflammation, i.e. that there was no lymph flow effect of enhanced lymphangiogenesis. This occurred in spite of an increased amount of tissue water and a higher P_{if} that should both act as a driving force for increased lymph formation and flow(47, 57). Still, a reduced lymph pumping has been shown in many types of inflammation as recently summarized by Scallan et al(45), notably in acute inflammation induced by LPS(207) as well as in delayed-type hypersensitivity induced by oxazolone(202), as used here. Release of NO will inhibit lymphatic tone and spontaneous contractions(45), and it is likely that iNOS, shown to be released by immune cells locally in inflamed tissue(202), contributed to the reduced lymph flow seen in both our inflammation models. There are several factors that may explain discrepancies between our and previous data. One of these is variation of iNOS-expression between mouse strains(45), and other factors are the methods used to assess lymph flow as discussed above.

Because initial lymphatics also take up and transport immune cells to draining lymph nodes where they influence the immune response, we also assessed dendritic cells in skin and their ability to migrate to draining lymph nodes after stimulation with FITC. The DC numbers as well as their migration was unaffected by strain, in spite of a markedly increased level of the lymphoid homing cytokine CCL21 in the K14-VEGF-C mice. Apparently, the increased lymphatic vessel area is capable of augmenting the production and thereby the gradient of chemoattractants, but this is not sufficient to mobilize tissue resident immune cells to initial lymphatics. The reason might be downregulation of the CC chemokine receptor 7 (CCR-7) for which CCL21 serves as a ligand on DCs that may occur in VEGF-C overexpressing mice(182). It should be noted, though, that our findings are a result of VEGF-C overexpression only, and that the situation may be different in more complex models where the lymphangiogenesis is induced by inflammation(199)

Mechanism for lymph formation

To our knowledge, all previous studies on the K14-VEGF-C model have used interventions involving inflammation. As discussed above, inflammatory reactions will result in capillary hyperfiltration, fluid extravasation and thereby increased tissue fluid content. Accumulated fluid will result in an increased P_{if} , and together these parameters will stimulate filling of the initial lymphatics and fluid transport. In inflammation, this picture is complicated by the fact that several inflammatory mediators, notably NO, have an inhibitory effect on collecting vessel pumping, thereby counteracting the effect of increased volume and pressure. The tipping of the balance in one or the other direction may explain the diverging results discussed above. To avoid the influence of inflammation we injected fluid directly intradermally, and could thereby show that the expanded lymphatic network was actually capable of an enhanced lymphatic fluid transport that was driven by a local increase in volume and P_{if} . Clearly, the hyperplastic network of initial lymphatics deriving from overexpression of VEGF-C resulted in a strongly enhanced lymphatic vessel area, that will enhance the fluid uptake and accordingly lymph transport in response to pressure gradients. Lymph flow might

have been influenced by a difference in structure and thus resistance in downstream lymph nodes, but that is not likely because of our finding of similar structure and area of lymph node sinusoids in K14-VEGF-C and WT mice(208). The fact that the lymph flow was higher in transgenic than in WT mice for the same P_{if} gradient suggests that lymphangiogenesis results in reduced resistance against lymph formation.

VEGF-C gene therapy – clinical implications

The present study shows the importance of a functional evaluation of a morphological phenotype resulting from genetic modifications, and may have implications for therapy of lymphatic disorders. The lack of effects when inducing inflammation likely reflects that lymph drainage can be modulated downstream of the initial lymphatics, as discussed above. Additional knowledge on such downstream mechanisms is needed when considering the potential benefits of VEGF-C induced lymphangiogenesis in humans. Our findings of facilitated initial lymph formation and enhanced chemokine production after lymphangiogenesis may explain the previously observed favorable effects of VEGF-C in inflammatory edema and lymphedema therapy. Karkkainen et.al. used adenovirus-mediated VEGF-C gene therapy, and could generate functional lymphatic vessels that reduced swelling in a mouse model of primary lymphedema(155). Transgenic overexpression of VEGF-C moreover inhibited chronic skin inflammation and reduced edema in a mouse model(178), and attenuated joint tissue damage(209). In addition, VEGF-C treatment has been shown to be important in forming both afferent and efferent connections with the preexisting lymphatic vessel network, and to result in improved postoperative lymph drainage and enhanced survival and functionality of transferred lymph nodes, suggesting that VEGF-C therapy may be beneficial to counteract postoperative lymphedema(210). It has been suggested that VEGF-C might act as an endogenous counter-regulatory mechanism for limiting edema formation and inflammation(178), but facilitated initial lymph formation and enhanced chemoattractant production by lymphatics as shown here is a potential common explanation for the therapeutic effect.

Acknowledgements

a) Acknowledgements: None.

b) Sources of funding: Financial support from the Research Council of Norway (project # 262079) and from The Western Norway Regional Health Authority (project # 911888 and 912168) is gratefully acknowledged. TR is a recipient of a PhD scholarship from The Norwegian Association on Cardiovascular Diseases.

c) Disclosures: None.

References

1. Alitalo K. The lymphatic vasculature in disease. *Nat Med.* 2011;17:1371-1380.
2. Aspelund A, Robciuc MR, Karaman S, Makinen T, Alitalo K. Lymphatic System in Cardiovascular Medicine. *Circ Res.* 2016;118:515-530.
3. Aebischer D, Iolyeva M, Halin C. The inflammatory response of lymphatic endothelium. *Angiogenesis.* 2014;17:383-393.
4. Kim H, Kataru RP, Koh GY. Inflammation-associated lymphangiogenesis: a double-edged sword? *J Clin Invest.* 2014;124:936-942.
5. Huggenberger R, Siddiqui SS, Brander D, Ullmann S, Zimmermann K, Antsiferova M, Werner S, Alitalo K, Detmar M. An important role of lymphatic vessel activation in limiting acute inflammation. *Blood.* 2011;117:4667-4678.
6. Huggenberger R, Ullmann S, Proulx ST, Pytowski B, Alitalo K, Detmar M. Stimulation of lymphangiogenesis via VEGFR-3 inhibits chronic skin inflammation. *J Exp Med.* 2010;207:2255-2269.
7. Kajiya K, Sawane M, Huggenberger R, Detmar M. Activation of the VEGFR-3 pathway by VEGF-C attenuates UVB-induced edema formation and skin inflammation by promoting lymphangiogenesis. *J Invest Dermatol.* 2009;129:1292-1298.
8. Kataru RP, Jung K, Jang C, Yang H, Schwendener RA, Baik JE, Han SH, Alitalo K, Koh GY. Critical role of CD11b+ macrophages and VEGF in inflammatory lymphangiogenesis, antigen clearance, and inflammation resolution. *Blood.* 2009;113:5650-5659.
9. Lachance PA, Hazen A, Seveck-Muraca EM. Lymphatic vascular response to acute inflammation. *PLoS One.* 2013;8:e76078.
10. Liao S, Cheng G, Conner DA, Huang Y, Kucherlapati RS, Munn LL, Ruddle NH, Jain RK, Fukumura D, Padera TP. Impaired lymphatic contraction associated with immunosuppression. *Proc Natl Acad Sci U S A.* 2011;108:18784-18789.
11. Wiig H, Swartz MA. Interstitial fluid and lymph formation and transport: physiological regulation and roles in inflammation and cancer. *Physiol Rev.* 2012;92:1005-1060.
12. Randolph GJ, Ivanov S, Zinselmeyer BH, Scallan JP. The Lymphatic System: Integral Roles in Immunity. *Annu Rev Immunol.* 2016.
13. Jeltsch M, Kaipainen A, Joukov V, Meng X, Lakso M, Rauvala H, Swartz M, Fukumura D, Jain RK, Alitalo K. Hyperplasia of lymphatic vessels in VEGF-C transgenic mice. *Science.* 1997;276:1423-1425.
14. Scallan JP, Zawieja SD, Castorena-Gonzalez JA, Davis MJ. Lymphatic pumping: mechanics, mechanisms and malfunction. *J Physiol.* 2016;594:5749-5768.
15. Karkkainen MJ, Saaristo A, Jussila L, Karila KA, Lawrence EC, Pajusola K, Bueler H, Eichmann A, Kauppinen R, Kettunen MI, Yla-Herttuala S, Finegold DN, Ferrell RE, Alitalo K. A model for gene therapy of human hereditary lymphedema. *Proc Natl Acad Sci U S A.* 2001;98:12677-12682.
16. Karlsen TV, McCormack E, Mujic M, Tenstad O, Wiig H. Minimally invasive quantification of lymph flow in mice and rats by imaging depot clearance of near-infrared albumin. *Am J Physiol Heart Circ Physiol.* 2012;302:H391-401.

17. Guyton AC, Scheel K, Murphree D. Interstitial fluid pressure. 3. Its effect on resistance to tissue fluid mobility. *Circ Res*. 1966;19:412-419.
18. Worbs T, Hammerschmidt SI, Forster R. Dendritic cell migration in health and disease. *Nat Rev Immunol*. 2017;17:30-48.
19. Bates DO, Lodwick D, Williams B. Vascular endothelial growth factor and microvascular permeability. *Microcirculation*. 1999;6:83-96.
20. Modi S, Stanton AW, Mortimer PS, Levick JR. Clinical assessment of human lymph flow using removal rate constants of interstitial macromolecules: a critical review of lymphoscintigraphy. *Lymphat Res Biol*. 2007;5:183-202.
21. Christiansen AJ, Dieterich LC, Ohs I, Bachmann SB, Bianchi R, Proulx ST, Hollmen M, Aebischer D, Detmar M. Lymphatic endothelial cells attenuate inflammation via suppression of dendritic cell maturation. *Oncotarget*. 2016;7:39421-39435.
22. Aukland K, Reed RK. Interstitial-lymphatic mechanisms in the control of extracellular fluid volume. *Physiol Rev*. 1993;73:1-78.
23. Aldrich MB, Sevick-Muraca EM. Cytokines are systemic effectors of lymphatic function in acute inflammation. *Cytokine*. 2013;64:362-369.
24. Papadakou P, Bletsas A, Yassin MA, Karlsen TV, Wiig H, Berggreen E. Role of Hyperplasia of Gingival Lymphatics in Periodontal Inflammation. *J Dent Res*. 2017;96:467-476.
25. Zhou Q, Guo R, Wood R, Boyce BF, Liang Q, Wang YJ, Schwarz EM, Xing L. Vascular endothelial growth factor C attenuates joint damage in chronic inflammatory arthritis by accelerating local lymphatic drainage in mice. *Arthritis Rheum*. 2011;63:2318-2328.
26. Lahteenvuo M, Honkonen K, Tervala T, Tammela T, Suominen E, Lahteenvuo J, Kholova I, Alitalo K, Yla-Herttuala S, Saaristo A. Growth factor therapy and autologous lymph node transfer in lymphedema. *Circulation*. 2011;123:613-620.

Highlights

- Studies on the functional consequences of a chronically expanded lymphatic network or lymphangiogenesis are few and the results are diverging
- We used K14-VEGF-C transgenic mice overexpressing the vascular endothelial growth factor C in skin, and investigated the responses to inflammatory and fluid volume challenges
- Acute and chronic inflammation resulted in increased interstitial fluid pressure and reduced lymph flow, both to the same extent in wild type and transgenic mice.
- Hyperplastic lymphatic vessels demonstrated enhanced transport capacity after local fluid overload not induced by inflammation
- Lymphangiogenesis may facilitate initial lymph formation favoring increased clearance of fluid in situations of augmented fluid filtration

Figures

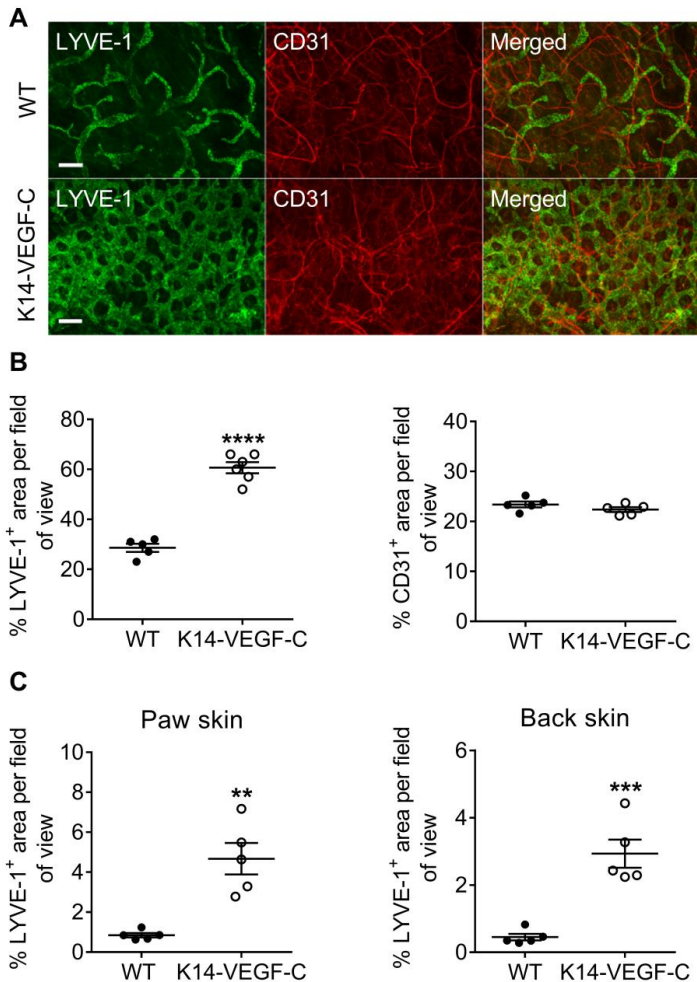


Figure 1. The lymphatic network is enlarged in K14-VEGF-C mice. (A) Representative whole-mount staining of LYVE-1⁺ lymphatic capillaries and CD31⁺ blood vessels in ears from WT and K14-VEGF-C mice. Scale bar = 200 μ m. (B) Quantification of lymphatic (left) and blood vessel (right) area in ear skin of WT and K14-VEGF-C mice. Four areas from each ear whole-mount preparation were counted per mouse. The LYVE-1⁺ lymphatics and CD31⁺ blood vessels were manually encircled and area calculated in ImageJ. (C) Serial sections (10 μ m) from intact paw (left) and back skin (right) of WT and K14-VEGF-C stained for LYVE-1. LYVE-1⁺ lymphatic vessels were manually encircled in three sections from each mouse and total area per mm dermis calculated. Mean \pm SEM, n=5-6. **P<0.01, *** P<0.001, **** P<0.0001.

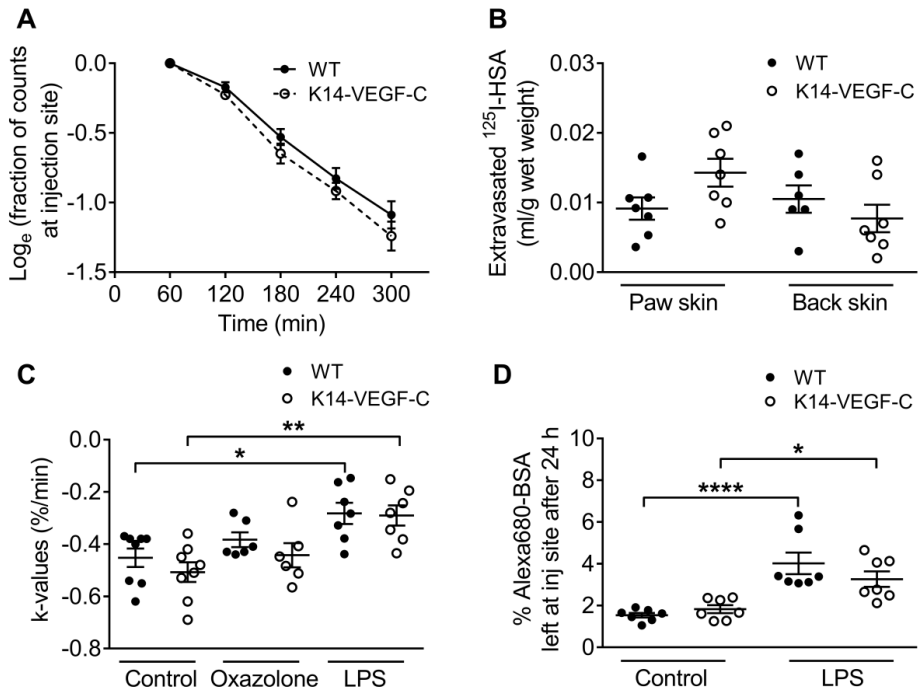


Figure 2. Lymph flow is impeded to a similar extent in WT and K14-VEGF-C mice in response to inflammation. (A) Average Log_e fraction of counts remaining in the intradermally injected depot of the fluorescent macromolecular tracer Alexa-680 BSA in hind paw of WT and K14-VEGF-C mice during basal conditions. (B) Extravasation of the radioactive macromolecular tracer ¹²⁵I-HSA (human serum albumin) from the vasculature into paw and back skin of WT and K14-VEGF-C mice after 30 min during basal conditions. Five min extravasation of ¹²⁵I-HSA was subtracted from these values to correct for any ¹²⁵I-HSA present in the vasculature of the excised tissue at 30 min. (C) Rate constants (*k*) calculated by determining the slope of the individual wash-out curves for WT and K14-VEGF-C mice during basal conditions, after oxazolone-induced hypersensitivity response (day 7) or after intradermal injection of 2 μl LPS (4 μg/μl). (D) Fraction of counts remaining in the intradermal depot in hind paw of WT and K14-VEGF-C mice 24 hours after injection of a mixture of either 2 μl isotonic saline (control group) or 2 μl LPS (4 μg/μl) both in combination with 1 μl Alexa680-BSA. Mean ± SEM, n=6-8. **p*<0.05, ***p*<0.01, *****p*<0.0001.

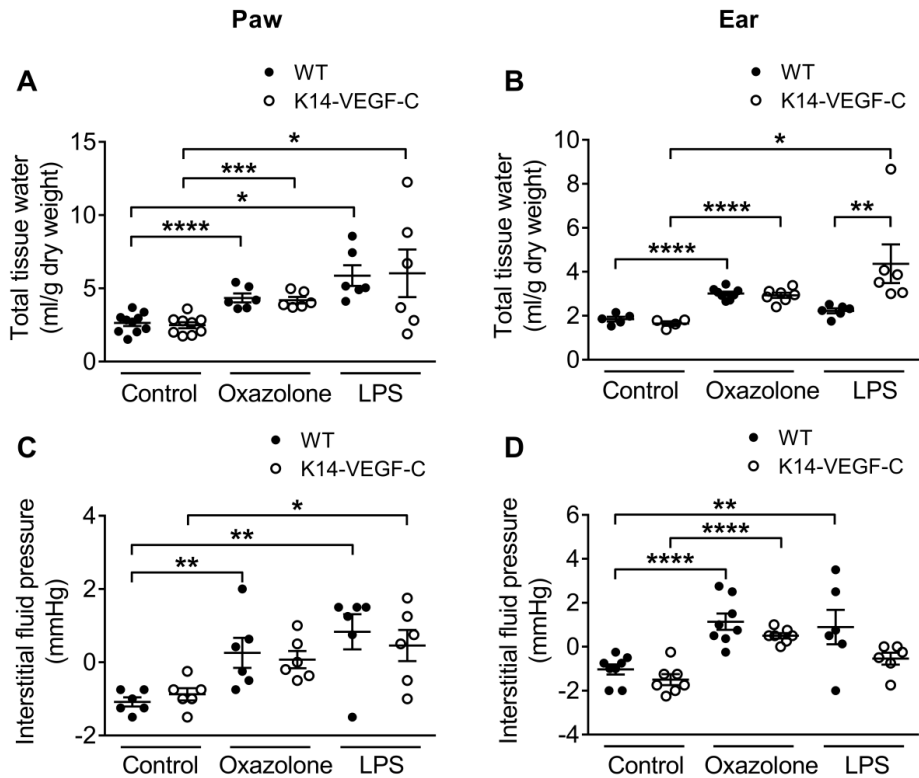


Figure 3. Interstitial driving forces for lymph formation are enhanced to a similar extent in WT and K14-VEGF-C in response to inflammation. Total tissue water in hind paw skin (A) and ear (B) of WT and K14-VEGF-C mice in response to oxazolone-induced hypersensitivity response or to acute inflammation induced by intradermal injection of LPS ($4 \mu\text{g}/\mu\text{l}$). Interstitial fluid pressure in hind paw skin (C) or ear (D) of WT and K14-VEGF-C mice in response to oxazolone-induced hypersensitivity response or to acute inflammation induced by intradermal injection of LPS ($4 \mu\text{g}/\mu\text{l}$). Mean \pm SEM, $n=4-10$. * $p < 0.05$, ** $p < 0.01$, *** $p < 0.001$, **** $p < 0.0001$.

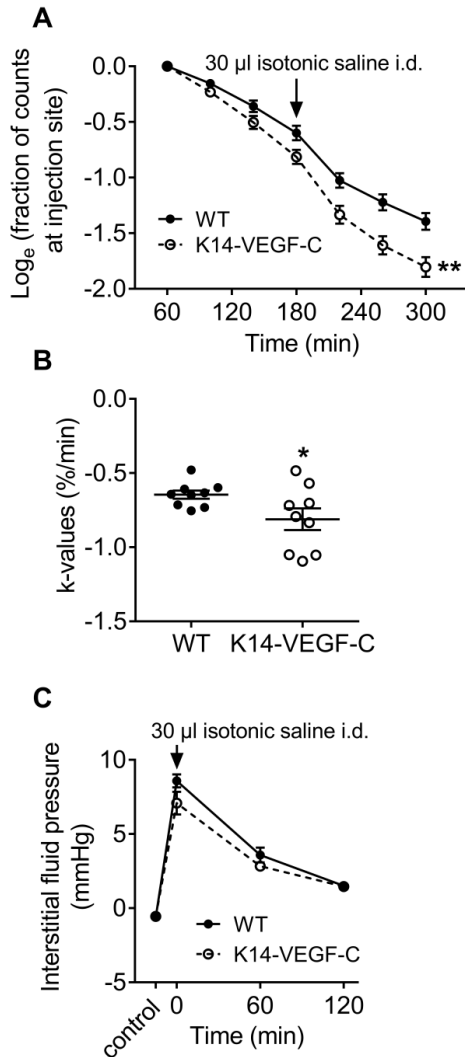


Figure 4. Intradermal overhydration enhances lymph formation to a greater extent in K14-VEGF-C mice. (A) Average Log_e fraction of counts remaining in the intradermally injected depot of 0.5 μ l Alexa680-BSA in hind paw of WT and K14-VEGF-C mice during a control period (60-180 min) and after an intradermal injection of 30 μ l isotonic saline into the same hind paw (180-300 min). (B) Rate constants (k) calculated by determining the slope of the individual wash-out curves for the time period after intradermal saline injection (180-300 min) by linear regression analysis. (C) Interstitial fluid pressure measured in hind paw skin of WT ($n=6$) and K14-VEGF-C ($n=7$) mice in control situation and at different time points after an intradermal injection of 30 μ l isotonic saline (arrow). Mean \pm SEM, $n=6-9$. * $p<0.05$, ** $p<0.01$.

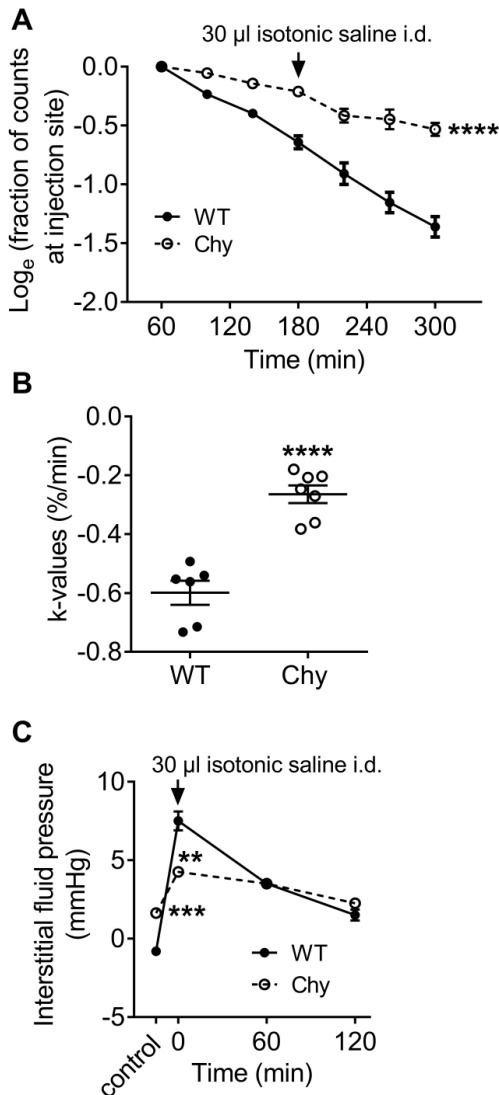


Figure 5. Reduced lymph formation in *vegfr3* mutant Chy mice with skin lymphatic vessel hypoplasia. (A) Average Log_e fraction of counts remaining in the intradermally injected depot of 0.5 μ l Alexa680-BSA in hind paw of WT and Chy mice during a control period (60-180 min) and after an intradermal injection of 30 μ l isotonic saline into the same hind paw (180-300 min). (B) Rate constants (*k*) calculated by determining the slope of the individual wash-out curves for the time period after intradermal saline injection (180-300 min) by linear regression analysis. (C) Interstitial fluid pressure measured in hind paw skin of WT (n=4) and Chy (n=4) mice in control situation and at different time points after an intradermal injection of 30 μ l isotonic saline (arrow). Mean \pm SEM, n=4-6. ***p*<0.01, ****p*<0.001, *****p*<0.0001.

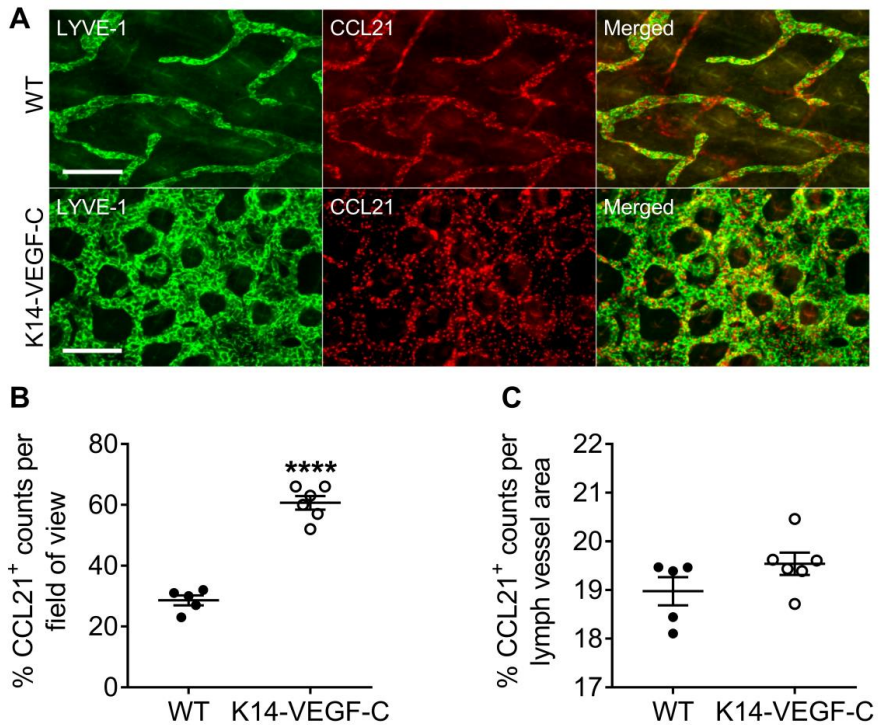


Figure 6. Increased amount of the immune cell attractant CCL21 in K14-VEGF-C mice (A) Representative whole-mount co-staining of LYVE-1⁺ lymphatic capillaries and CCL21 in ears from WT and K14-VEGF-C mice. Scale bar = 200 μ m. (B) Quantification of total CCL21 counts per field of view. (C) Proportions of CCL21 counts per LYVE-1⁺ lymphatic vessel area. The LYVE-1⁺ lymphatics were encircled and area calculated while lymphatic CCL21 staining was counted manually in ImageJ. Mean \pm SEM, n=5-6. **** p <0.0001.

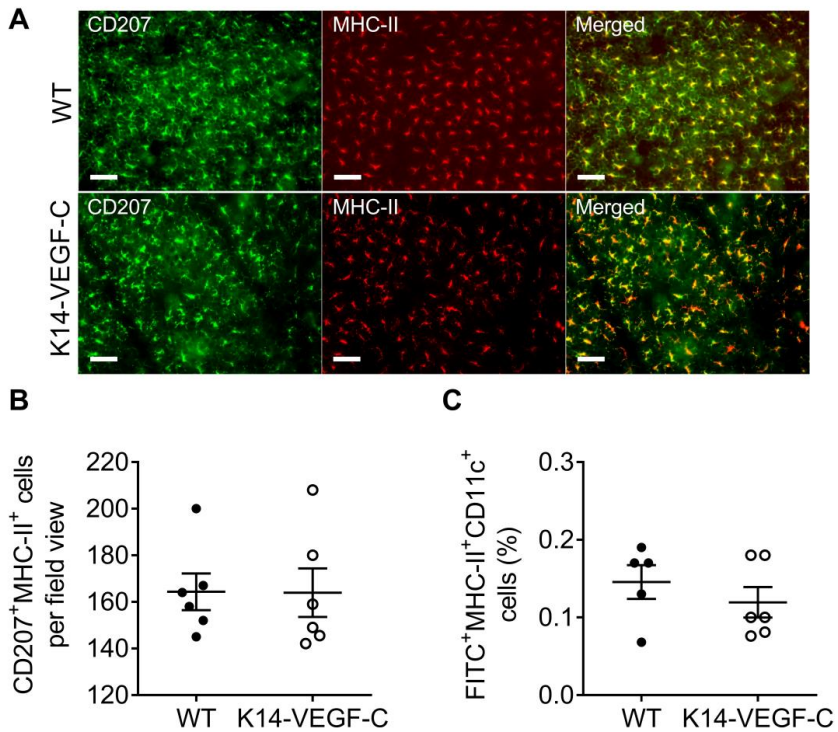


Figure 7. Unaltered dendritic cell mobilization from skin to lymph nodes in K14-VEGF-C mice in response to FITC painting. (A) Representative epidermal sheets double-stained for the Langerhans cell marker CD207 and MHC-II. Scale bar = 50 μ m. (B) Quantification of CD207⁺MHC-II⁺ Langerhans cells in epidermal sheets of WT and K14-VEGF-C mice. (C) Proportions of FITC⁺MHC-II⁺CD11c⁺ dendritic cells in lymph nodes of WT and K14-VEGF-C mice 18 h after FITC painting. Mean \pm SEM, n=6. ** p <0.01, *** p <0.001, **** p <0.0001.

Paper II

High salt diet causes expansion of the lymphatic network and increased lymph flow in skin and muscle of rats

Tine V. Karlsen¹, Elham Nikpey^{1,2}, Jianhua Han¹, Tore Reikvam¹, Natalia Rakova³, Jorge A. Castorena-Gonzalez⁴, Michael J Davis⁴, Jens M Titze^{5,6,7}, Olav Tenstad¹, Helge Wiig¹

¹Department of Biomedicine, University of Bergen, Norway

²Department of Medicine, Haukeland University Hospital, Bergen, Norway

³Experimental and Clinical Research Center, Charité Medical Facility and the Max-Delbrueck Center for Molecular Medicine, Berlin, Germany

⁴Department of Medical Pharmacology and Physiology, University of Missouri, Columbia, MO, USA

⁵Junior Research Group 2, Interdisciplinary Center for Clinical Research, University Clinic Erlangen, Erlangen, Germany

⁶Division of Clinical Pharmacology, Vanderbilt University Medical Center, Nashville, USA

⁷Cardiovascular and Metabolic Disorders program, Duke-NUS Medical School, Singapore

Short title: Lymph flow during salt storage in skin and muscle

Correspondence to:

Helge Wiig, Department of Biomedicine, Jonas Lies vei 91, N-5009 Bergen, Norway

Phone: +47 55 58 63 87, fax +47 55 58 63 60

Email: helge.wiig@uib.no

Word count: 7621, Figures: 6, Tables: 0

Abstract

Objective: A commonly accepted pivotal mechanism in fluid volume and blood pressure regulation is the parallel relationship between body Na⁺ and extracellular fluid content. Several recent studies have, however, shown that a considerable amount of Na⁺ can be retained in skin without commensurate water retention. Here we asked whether a salt accumulation shown to result in VEGF-C secretion and lymphangiogenesis had any influence on lymphatic function.

Approach and Results: By optical imaging of macromolecular tracer washout in skin we found that salt accumulation resulted in an increase in lymph flow of 26% that was noticeable only after including an overnight recording period. Surprisingly, lymph flow in skeletal muscle recorded with a new PET/CT method was also increased after salt exposure. The transcapillary filtration was unaffected by the high salt diet and deoxycorticosterone-salt treatment, suggesting that the capillary barrier was not influenced by the salt accumulation. A significant reduction in lymph flow after depletion of macrophages/monocytes by clodronate suggests these cells are involved in the observed lymph flow response, together with collecting vessels shown here to enhance their contraction frequency as a response to extracellular Na⁺.

Conclusions: The observed changes in lymph flow suggest that the lymphatics may influence long term regulation of tissue fluid balance during salt accumulation by contributing to fluid homeostasis in skin and muscle. Our studies identify lymph clearance as a potential disease modifying factor that might be targeted in conditions characterized by salt accumulation like chronic kidney disease and salt-sensitive hypertension.

Key words: blood pressure; hypertension; body water; extracellular fluid; extracellular matrix; lymph flow, sodium.

Abbreviations

DOCA; deoxycorticosterone, HSD; high salt diet, HPLC; high performance liquid chromatography, HSA; human serum albumin, LSD; low salt diet, LYVE-1; lymphatic vessel endothelial hyaluronan receptor 1, MPS; mononuclear phagocyte system, PET/CT; positron emission tomography-computed tomography,

Introduction

A commonly accepted pivotal mechanism in fluid volume and blood pressure regulation is the parallel relationship between body Na⁺ and extracellular fluid content(211). To maintain blood pressure homeostasis, body fluid volume, and thereby body Na⁺ content, has to be maintained within very narrow limits. Several recent studies in humans have, however, shown that a considerable amount of Na⁺ is retained or removed from the subjects' bodies without a corresponding water retention or loss(147-149, 212) that would have been predicted if the extracellular fluid volume was determined by the amount of body Na⁺ only. These observations suggest that Na⁺ could be stored somewhere in the body without commensurate water retention, and thereby be inactive from a fluid balance viewpoint, e.g.(9), also implying that unidentified extrarenal, tissue-specific regulatory mechanisms might control the release and storage of Na⁺ from a kidney-independent reservoir. Later studies have indicated that skin might serve as a major Na⁺ reservoir, e.g.(12, 213-215), again suggesting that there might not be strict isotonicity of all body fluids, and that skin electrolyte concentrations do not necessarily equilibrate with blood electrolytes. One consequence of such electrolyte accumulation in excess of water would be that it might cause local hypertonicity. Indeed, using vapor

pressure osmometry we recently demonstrated that Na^+ accumulation in skin as a consequence of feeding rats a high-salt diet (HSD) results in a tissue that is hyperosmotic relative to plasma(13).

Because of the demonstration of its role in salt storage and buffering discussed above, the skin is a potential actor in blood pressure regulation. Mice and rats fed HSD develop hypertension and have a hyperplastic lymphatic capillary network in the skin induced by VEGF-C secreted by mononuclear phagocyte system (MPS) cells(11, 13). Blocking the ability for lymphangiogenesis results in an increased blood pressure response to salt loading(13). An unresolved and central question is whether such HSD-induced lymphangiogenesis results in increased lymph flow, i.e. whether the vessels are functional. We therefore asked if the Na^+ concentration dependent lymph vessel hyperplasia has functional importance. To this end we decided to assess the importance of lymphatic vessel phenotype for fluid drainage, and whether lymph flow is actually increased in rats with hypertension induced by HSD or deoxycorticosterone (DOCA) treatment using a recently developed optical imaging technique(158). We also assessed how skin lymphatic collectors, studied *ex vivo*, would respond to elevated Na^+ . Moreover, since Na^+ also appear to accumulate in skeletal muscle in hypertensive patients(153), we asked if such accumulation also influenced fluid drainage in muscle, and developed a positron emission tomography-computed tomography (PET/CT) method to be able to assess lymph flow in deeper structures.

Collectively, the present results indicate that the newly formed lymphatics induced by salt accumulation either by HSD or DOCA are functional. Moreover, our data suggest that existing and newly formed lymph vessels contribute to blood pressure control and to the previously observed attenuation of the rise in blood pressure in models of salt sensitive hypertension.

Materials and Methods

The data that support the findings of this study are available from the corresponding author upon reasonable request.

Ethical approval. All animal experiments were conducted in accordance with the regulations of the Norwegian State Commission for Laboratory Animals, harmonized to be in accordance with the European Convention for the Protection of Vertebrate Animals used for Experimental and Other Scientific Purposes and Council of Europe (ETS 123), and with approval from the AAALAC International Accredited Animal Care and Use Program at University of Bergen. All mouse protocols were approved by the University of Missouri Animal Care and Use Committee and conformed to the US Public Health Service policy for the humane care and use of laboratory animals (PHS Policy, 1996).

Animals. We used mice and rats. The animals were of male sex only because background data for the hypothesis to be tested were derived from this sex only. Mice (C57Bl/6), weighing between 18 and 22 g, were obtained from Jackson Laboratories (JAX, USA) and used for isolation of skin lymphatic collecting vessels (please see the Major Resources Table in the Supplemental Material). NTac Sprague Dawley rats were from Møllegaard Breeding Colony, Skensved, Denmark, weighing between 150-200 g at the start of the experiment. The rats were randomly assigned into three groups with different diet regimes; group low salt diet (LSD) received low salt chow (< 0.1% NaCl) and tap water; group HSD received high salt chow (8% NaCl) and 1 % saline drinking water; group DOCA received low salt chow and 1% saline drinking water after subcutaneous implantation of

a deoxycorticosterone acetate (DOCA) tablet (100 mg/pellet, Innovative Research of America) in the neck region. In a separate set of experiments the three different diet groups were treated with intraperitoneal injections of 1 ml clodronate liposomes (5 mg/ml Clodrosome, Encapsula Nanosciences) every 4th day, at day 0, 4, 8 and 12.

After 2 weeks on diet blood pressure was measured in all groups with a non-invasive tail cuff system (CODA-6, Kent Scientific, Torrington, CT) and further experiments conducted as described below.

During experiments the rats were either anesthetized with 3% isoflurane (DOCA pellet implantation, optical imaging and extravasation) or 2% sevoflurane (PET/CT) both in 100% O₂. The body temperature was maintained at 37°C while under anesthesia. The experiments were terminated by excising the heart while under deep anesthesia.

Mice were anesthetized with an intraperitoneal injection of sodium pentobarbital (60 mg/kg). After anesthesia, an incision was made near the midline of the lower back and the skin covering the left rear flank was retracted to the side. A segment of the afferent lymphatic draining the skin and feeding into the inguinal lymph node fat pad was cleared of loose connective tissue, and excised.

Preparation of radiolabeled probes. Human serum albumin (HSA) (Albunorm, Octopharma, 200 mg/ml) was labeled with ¹²⁵I and ¹³¹I (for extravasation studies) or ¹²⁴I (for PET/CT) by Iodo-Gen as described in detail previously(216).

Albumin extravasation. Blood-to-tissue clearance of albumin in hind paw skin and thigh muscle was determined as the difference between the 35 and 5 min plasma equivalent space of ¹²⁵I-HSA and ¹³¹I-HSA, respectively, as described in detail elsewhere(217).

Optical imaging. To assess lymph flow in skin we monitored the depot clearance of an intradermally injected near-infrared macromolecular tracer with time by optical imaging as described in detail previously(158).

PET/CT scanning. To assess lymph flow in muscle we developed a PET/CT method. ¹²⁴I-HSA (3 µl) was injected into thigh muscle with a graded Hamilton syringe. PET and CT scans (small-animal PET/CT, NanoScan PC PET/CT; Mediso Ltd, Budapest, Hungary) were performed 1, 3, 5, 7 and 22 hours post-injection to determine the clearance of macromolecular tracer from the injected area. The rats were awake and freely moving in between scans to facilitate lymph flow. First, a CT scan was performed to obtain anatomical information and for attenuation correction, with the following acquisition parameters: Helical scan, 70 kVp, 300 ms, Projections: 360 and reconstructed using Shepp Logan filter. Directly thereafter a 10 min per bed position PET scan was performed with acquisitions parameters as follows: field of view (FOV) 9.6 cm in the axial direction and 10 cm in the transaxial direction, 1:5 coincidence mode and normal count rate mode. The body temperature was maintained at 37 degrees throughout the whole procedure. Reconstruction of the PET data was performed with 3D OSEM and 1:3 coincidence mode, no filtering, attenuation correction, decay correction and normalization of detectors. The images were analyzed using Interview fusion software (version 2.02.029.2010 BETA) and number of photon counts calculated for each region of interest. For the determination of removal rate constants (k), the natural logarithm of the fractional amount of counts remaining at the injection site was plotted against time. The resultant monoexponential curves were fitted with linear regression. The k values were found as the slope of the

curve for each animal. The rate constant for each animal was calculated as the slope of the curve, as previously described(158).

Chemical analysis of tissue electrolytes and water content. Chemical analysis of tissue electrolytes and water content was performed as described in detail previously(13).

Immunohistochemistry frozen sections. Frozen sections from 4% PFA fixed and sucrose dehydrated ears were incubated in 0.3% H₂O₂ in methanol, before blocking in goat serum, both for 30 min (please see the Major Resources Table in the Supplemental Material). Rabbit anti-mouse/rat lymphatic vessel endothelial hyaluronan receptor 1 (LYVE-1) primary antibody (1:100, Novus Biologicals) in blocking serum was added for an overnight incubation at 4°C. Thereafter, secondary antibody (goat anti-rabbit; 1:200, Vector Laboratories Inc.) in blocking serum was added for 30 min before incubating with avidin-biotin complex (Vectastain ABC kit – peroxidase Rabbit IgG PK4001, Vector Laboratories Inc.). Bound antigen was visualized using 3,3'-diaminobenzidine (Sigma Aldrich) in combination with nickel. To validate antibody specificity staining was compared to negative controls run with rabbit IgG (Merckmillipore) replacing the primary antibody. The quantification was performed blindly, counting LYVE-1+ vessels from 5-6 consecutive fields of view (20 x magnification, 3 rats per group).

Immunohistochemistry paraffin sections. Ears were fixed overnight in 4% PFA before paraffin embedding and sectioning. After deparaffinization, antigen retrieval was performed in Dako Target Retrieval solution pH 9 for 30 min at 98°C. Sections were blocked in horse serum and bovine serum albumin for 30 min, before overnight incubation at 4°C with mouse anti-rat CD68 primary antibody (1:100, Abcam) in blocking solution (please see the Major Resources Table in the Supplemental Material). After incubation in 0.3% H₂O₂ for 30 min, secondary antibody (horse anti-mouse; 1:200, Vector Laboratories Inc.) in blocking solution was added for another 30 min. The sections were reacted with avidin-biotin complex (Vectastain ABC kit, Vector Laboratories Inc.) for 30 min and bound antigen visualized using diaminobenzidine substrate kit (Abcam). To validate antibody specificity staining was compared to negative controls run with mouse IgG (Merckmillipore) replacing the primary antibody. The quantification was performed blindly, counting CD68+ cells from 4 consecutive fields of view (60 x magnification, 4 rats per group).

Contractility of isolated mouse afferent skin lymphatics. The excised segment of afferent lymphatic was placed in 145 Na⁺ Krebs solution + 0.5% bovine serum albumin, cleaned of fat and connective tissue and cannulated at each end with a micropipette as described previously(218) (for composition of solutions used in contractility experiments please see the Major Resources Table in the Supplemental Material). Pipettes contained 145 Na⁺ Krebs + 0.5% bovine serum albumin. The vessel, bath chamber and pipette holders were mounted onto the stage of an inverted microscope and connected to independent pressure controllers (219). The vessel equilibrated at 37°C for 60-90 minutes, at 3 cmH₂O, with the bath was exchanged with 145 Na⁺ Krebs solution (0.5ml/min). Video and data acquisition were the same as described previously(219).

Protocols used in contractility assessment. Spontaneous contractions typically began within 15 minutes. Pressure was stepped through a physiological range of pressures, 0.5 to 10 cmH₂O in a sequence of 3, 2, 1, 0.5, 1, 2, 3, 5, 8, 10 cmH₂O, with contractions recorded

for 2-3 minutes at each pressure. Input and output pressures were equal at all times so that there was no net gradient for flow that might influence the contraction pattern due to production of endothelial nitric oxide(220). The bath was exchanged with 165 or 185 Na⁺ Krebs solution or 40 or 80 mosm urea solution and allowed to equilibrate for 60 minutes after which another set of pressure steps was imposed. Afterwards the bath was exchanged with Ca²⁺ free Krebs solution for 20 minutes and the passive diameter of the vessel was recorded at each of the different pressures used.

After the experiment, end systolic and diastolic diameters (ESD and EDD, respectively) were determined for each individual spontaneous contraction at each pressure level. Contraction frequency (FREQ) was computed on a contraction-by-contraction basis and the following contraction parameters were calculated:

$$\text{Amplitude} = \text{EDD} - \text{ESD} \quad (1)$$

$$\text{Tone (\%)} = [(\text{MaxD} - \text{EDD})/\text{MaxD}] * 100 \quad (2)$$

$$\text{Ejection Fraction} = (\text{EDD2} - \text{ESD2})/\text{EDD2} \quad (3)$$

$$\text{Fractional Pump Flow} = \text{FREQ} * \text{EF} \quad (4)$$

MaxD was the maximum passive diameter obtained in Ca²⁺-free Krebs solution at each respective pressure. The average of each of the parameters was determined over each 2-3-minute interval at each pressure and the values were tabulated in Excel to produce the summary graphs.

Data analysis and statistics. Data and statistical analysis was performed using GraphPad PRISM Version 7.0. All data passed normality and equal variance tests, therefore parametric two-tailed t-tests were chosen to compare two groups while differences between multiple groups were assessed by analysis of variance (ANOVA) followed by Dunnett's or Bonferroni's multiple comparisons test as specified in the figure legends. Values are given as mean \pm SD, and $p < 0,05$ % was considered statistically significant.

Results

Establishment of models of salt sensitive hypertension

Here we applied the same models as those used in a recent study by us(151) and previously by Titze and collaborators to induce skin salt accumulation and that have been shown to be accompanied by lymphangiogenesis in skin, i.e. feeding a high salt diet (HSD)(11) and the DOCA-salt model without uni-nephrectomy(12).

Blood pressure as measured with the tail cuff method at the initiation of HSD or DOCA treatment (day 0), was not different between rats assigned to LSD, HSD and DOCA-salt groups (data not shown). Figure 1A shows collected mean arterial pressures for all the rats included in the study, and we observed that HSD as well as DOCA-salt induced an increase in mean blood pressure averaging 18 and 51 mm Hg compared with LSD, respectively. This corresponds well with our own recently published data(151) and with previous reports employing the same models but where blood pressure was measured with a catheter in awake animals(11, 12).

In a subset of rats, we investigated whether the HSD and DOCA-salt treatment resulted in salt and fluid accumulation in skin. Skin water content assessed by drying until the weight stabilized tended to be increased in HSD compared with LSD, but the increase was statistically significant only in DOCA-salt rats, averaging 19% (Fig 1B). There was, however, a significant increase in Na⁺ content relative to water (Fig. 1C) as well as Na⁺ content relative to dry weight (Fig. 1D) in HSD and DOCA-salt treatment compared with the LSD group, in line with corresponding data in own(151) as well as previous experiments with these models(11, 12).

To investigate whether our high salt models also led to an increased lymphangiogenesis we stained for LYVE-1 in skin (Fig 1E). As shown in Fig 1F, the lymph vessel number was increased in HSD and DOCA-salt fed rats in agreement with previous studies(11).

Salt accumulation induces increased lymph flow in skin

To assess whether the lymphangiogenesis in skin induced by HSD and DOCA-salt treatment had an influence on lymph flow we used an optical imaging method based on washout of the near infrared probe Alexa680 bound to albumin(158). With this method, the rate constant of the washout will reflect lymph flow. Washout curves for LSD, HSD and DOCA-salt are shown in Fig 2A and the corresponding rate constants for the washout in Fig 2B. The slopes of HSD and DOCA-salt washout curves were significantly different from that of LSD, suggesting an increased lymph flow under high salt conditions (Fig 2A). Although the average washout of tracer was faster and thus the rate constants for HSD and DOCA-salt were 27 and 33% higher (more negative value), and might indicate a higher lymph flow, particularly for the DOCA-salt group as shown by the $p=0.058$ when compared with LSD, these rate constants were not significantly different (Fig. 2B).

To increase the sensitivity of the analysis, and also include the night time in the washout period when the rat is more active, we recorded the tracer remaining in the depot 22 h after injection (Fig. 2C). In this analysis, we included all animals that were employed in the study, also those from subgroups that were used as controls in the clodronate experiments (see below). Whereas on average 24% of the tracer remained in the LSD group, the corresponding fraction averaged 19% in the HSD as well as the DOCA group, both significantly lower than in the LSD group ($p<0.01$ for both comparisons) (Fig. 2C). This shows that with increased resolution of the tracer washout, we were able to demonstrate an increased lymph flow in both of the groups that accumulated salt.

Lymph flow in muscle increased as recorded with PET

Recent studies have indicated that Na^+ appears to accumulate in both skin and skeletal muscle in hypertensive patients(153). We therefore asked whether such accumulation also influenced lymph drainage in muscle. Since photons emitted by fluorescent probes are absorbed in tissues to a higher extent than radionuclides, we decided to develop a PET-CT method to be able to assess lymph flow in the deeper positioned muscle. By labeling human serum albumin with ^{124}I we could, as for optical imaging, record washout of radioactive tracer and thereby lymph flow in muscle.

As shown by HPLC, we made a macromolecular probe that after labeling was inseparable from the native substance and without any free tracer that might have been taken up by the capillaries and thus led to an overestimation of the tracer washout rate (Fig 3A). An example of original recordings of tracer washout in one rat at different time points is shown in Figure 3B, and a summary of tracer washout for LSD and HSD in Fig. 3C. The rate constants (k -values) for muscle were not different between the LSD and HSD (Fig. 3D) when recorded in intermittent sessions during day-time. As for skin, we also recorded the tracer remaining 22h after injection in muscle. Interestingly, we found a subtle, but statistically significant difference between LSD and HSD, inasmuch as 15 and 12% of the tracer ($p<0.05$) remained in skeletal muscle 22 h post injection (Fig 3E), suggesting that the high-salt diet increases lymph flow in muscle as well as in skin.

Extravasation of ^{125}I -human serum albumin

In a steady-state situation with no fluid accumulation, the net amount of fluid filtered across the capillaries will be taken up and removed by lymphatics. Because we found that the lymph flow was increased in skin and muscle, we estimated the fluid extravasation in paw skin and thigh muscle using the double isotope tracer technique for all groups in skin and for LSD and HSD in muscle. As can be seen from Figure 4, there was no difference in extravasation in either tissue (Figure 4 A,B). A similar protein extravasation in HSD and LSD indicates that the endothelial barrier is intact in the HSD situation, and that the increase in lymph flow in high salt conditions is not a result of an influence of salt on the endothelial barrier.

Effect of blocking MPS-cells by clodronate

Previous studies have shown that depletion of MPS-cells with clodronate prevents the lymphangiogenesis induced by salt accumulation and increases the blood pressure(11, 12). To confirm that skin MPS cells were depleted in response to clodronate in our experiment we stained with the MPS cell marker CD68 in skin sections from LSD, HSD and DOCA-salt rats with or without such treatment (Fig 5A). CD68+ MPS cells increased significantly in skin after HSD, but not after DOCA-salt diet, while clodronate treatment reduced the number of CD68+ cells below basal levels in all the three diet groups (Fig. 5B). To assess whether such MPS-cell blockage also influenced the drainage of fluid from the tissue, we measured clearance of tracer with optical imaging in skin following clodronate administration in all group of rats (Fig 5C). Although the average rate constant, k , after clodronate treatment was slightly higher in HSD and DOCA-salt rats indicating a reduced lymph flow, this difference was statistically significant in the DOCA group only (Fig. 5C).

We then measured the amount of tracer remaining of the injected depot after 22 h i.e. including an overnight washout period, and found that more tended to remain in the HSD and DOCA-salt rats after clodronate treatment when compared with the corresponding control fraction. The remaining fractions after clodronate were significantly different from their respective controls for HSD and DOCA-salt, whereas clodronate treatment had no effect in the LSD group. This finding suggests that the depletion of MPS cells resulted in a dysfunction of the lymphatics under high salt conditions and a reduced clearance function (Fig 5D).

Increased contraction of lymphatics in high salt environment

Based on our finding of an increase in lymph flow in rats with salt accumulation in skin interstitium we asked whether this affected the contraction properties of the small lymph collecting vessels. To this end we isolated and cannulated afferent lymph vessels from normal mouse skin (Fig 6A), and examined these under conditions where the external salt concentration was enhanced but where the intravascular buffer was isosmotic with plasma. Example recordings showing the pattern of spontaneous lymphatic contractions at each level of pressure (0.5 to 10 cmH₂O) in 145 mM Na⁺ Krebs solution and 185 mM Na⁺ Krebs solution are shown in Fig. 6B,C. Each downward deflection represents a single contraction lasting 3-5 sec. Pin and Pout are the pressures set by the input and output cannulas, respectively, and were equal throughout the pressure step protocol. Lowering pressure in steps from 3 to 0.5 cmH₂O resulted in a slowing of spontaneous contraction frequency and an increase in contraction amplitude at 1 and 2 cmH₂O but a decrease in amplitude at 0.5 cmH₂O; raising pressure from 0.5 to 10 cmH₂O resulted in an increase in frequency and decrease in amplitude such that only weak contractions were observed at pressures higher than 5 cmH₂O. These patterns are

consistent with those reported previously for lymphatic collectors from both rat mesentery and other peripheral regions of the mouse(219, 220). Exposure of the vessel to 185 mM Na⁺ Krebs solution produced increases in frequency and slight decreases in amplitude at all pressures (Fig 6C).

Results from 5 vessels exposed to both 145, 165 and 185 mM Na⁺ Krebs solutions have been summarized in Fig. 6D,E and Supplemental Fig. I. For contraction frequency and fractional pump flow there was a dose-dependent effect of Na⁺ in the Krebs buffer solution surrounding the vessel (Fig. 6D,E), whereas for amplitude, ejection fraction and vessel tone there was no difference between the groups. Replacing the additional Na⁺ with urea to obtain a similar osmolality had no effect on any of the recorded parameters (Fig. 6D,E and Supplemental Fig. II). Therefore, exposure of the adventitia of the collecting vessel to a hypertonic solution that has a tonicity in the upper range of what might be expected after HSD and DOCA-salt treatment resulted in increased contraction frequency that was most pronounced at high pressures as well as pump flow at low pressures. An increased pumping may thus be part of the explanation for the observed rise lymph flow.

Discussion

The major question asked in the present study was whether the salt accumulation shown to result in macrophage accumulation and lymphangiogenesis had any influence on lymphatic function. Here we found that high salt conditions resulted in an increase in lymph flow that was detectable only after including an overnight recording period. We moreover developed a PET-CT method to assess lymph flow in skeletal muscle, and observed that lymph flow was increased after salt exposure in muscle too. Ex vivo studies of isolated afferent collecting vessels suggested that a high interstitial concentration of Na⁺ gave more frequent contractions, without a significant compromise in contraction amplitude, that might contribute to the observed flow increase. The transcapillary extravasation of albumin was unaffected by the HSD treatment, indicating that the capillary barrier was not influenced by the salt accumulation. A significant reduction in lymph flow after depletion of macrophages by clodronate indicates that these cells are involved in the observed lymph flow response. The enhanced tissue fluid clearance suggests that the lymphatics may contribute to long term regulation of tissue fluid balance during salt accumulation by contributing to electrolyte and fluid homeostasis in skin and muscle.

Evaluation of methods and limitations

To assess lymph flow in skin we used a sensitive and minimally invasive optical imaging method that we have validated in a recent paper(158). One limitation regarding optical imaging is photon absorption in the tissue. This stimulated us to develop a PET-CT based method that is not limited by tissue depth(221) to be able to record reliably from the deeper structures like muscle that, similarly to skin, has been shown to accumulate Na⁺ in hypertensive patients(153).

To our knowledge, PET-CT has not been used to monitor lymph flow previously, but has been applied to visualize inflammation and tumor-induced lymph node lymphangiogenesis by i.v. injection of a PET-probe targeting lymphatic-specific epitopes(222). Clearly, PET-CT is an expensive and labor-intensive method, but we present a new and valuable alternative for recording of lymph flow that can be used in several species, including mice, when recordings from deeper structures are required.

Our use of mouse afferent lymphatics from skin to determine contraction properties of the vessels in a hyperosmotic environment might be considered as a

limitation of the relevance to all the other data obtained from rats. It should be noted though, that mouse and rat lymphatics have been found to respond similarly in comparable experiments *ex vivo*(219, 220) and *in vivo*(223). Importantly, in a recent comprehensive study, it was concluded that peripheral lymph vessels, as studied by us, from mice and rats respond similarly to contraction stimuli(224). Moreover, in preliminary experiments we have results indicating that peripheral rat vessels respond similarly as mouse vessels when exposed to high salt conditions. Together, these studies suggest that the present contraction data obtained from mouse vessels are relevant also for rats. Moreover, these lymph vessel contraction data are also relevant because much of the work having shown a role of skin lymphatics in blood pressure regulation originate from mice(11, 13).

Comparison to previous studies

In a recent study, Kwon et al(223) have tried to assess lymphatic contractile function in rats and mice after induction of hypertension with HSD. By using indocyanine green, they were able to show dilated vessels having an increased contractility in the HSD animals, a contractility response pointing in the same direction as our *ex vivo* results. Their contraction frequency response was however quite dramatic, amounting to $\approx 200\%$ after 14 days of HSD in both species. Such an increment is surprising considering the modest augmentation needed to provide for the subtle change in lymph flow found in the present study. It is possible that the rather large volume of indocyanine green needed for the imaging of the hindlimb (10 and 50 μl , the amount not specified in the various experiments), volumes shown by us to increase lymph flow(217), might have influenced these results.

The present models for hypertension, HSD and DOCA-salt feeding, are characterized by generation of VEGF-C, which also has a potential effect on contractility of lymphatic collectors. Breslin et al(225) superfused rat mesentery lymphatics with VEGF-C and found an increased lymphatic pumping mediated through VEGFR-3. Although the dose they chose was based on data from humans, it apparently was sufficient to augment the capillary permeability in the mesenteric circulation. Since the albumin extravasation in skin and muscle was unaltered in high salt conditions in our experiments, it seems unlikely that VEGF-C contributed to the lymph flow effect that we observed.

Implications of findings

Ever since the demonstration that HSD induces mononuclear phagocyte system (MPS) cell accumulation, VEGF-C secretion and subsequent lymphangiogenesis(11), a crucial question has been what the functional consequence of such lymphangiogenesis are, adding to the more general question of "what lymphangiogenesis achieves"(203). Apparently, both blocking of the MPS-cell accumulation by clodronate during salt loading and inhibiting the lymphatic hyperplasia(11, 12), as well as curbing the ability for lymphangiogenesis by the use of a VEGF-C receptor trap mouse model(13) or an angiogenesis inhibitor(186), have resulted in hypertension. These studies suggest that lymphangiogenesis has a role in blood pressure control in high salt conditions. The question then is whether the lymph capillary network has an integral role in the maintenance of interstitial electrolyte and volume homeostasis as recently proposed(11).

With regard to electrolyte homeostasis, if the lymphatics were to contribute one might think that the concentration of electrolytes and other osmolytes would be higher in lymph draining skin that is hyperosmotic due to salt accumulation. In HSD and DOCA-salt treated rats, however, the osmolality and electrolyte concentration were equal to those of

control LSD rats(151), showing that there is no gradient between interstitium and lymph. Still, given the same electrolyte concentration in lymph in LSD on one hand and HSD and DOCA-salt on the other, an increased lymph flow in the high salt groups would transport more electrolytes from the tissue and thus contribute to clearance of osmolytes and electrolytes from tissues with accumulated salt. This mechanism, possibly assisted by increased lymphatic pumping due to a hyperosmotic interstitium as indicated by our experiments, may contribute to the maintenance of electrolyte homeostasis. Our finding of a subtle increase in lymph flow that was first recognized after long-term observation in a period where the rats are more active thereby suggests that an enhanced clearance of fluid from the tissue is an integrated element of this homeostasis.

There are, indeed, clinical data that support the hypothesis that the lymphatics are influencing disease development. In end stage renal disease patients undergoing hemodialysis, Dahlmann et al(226) measured Na^+ in skin and muscle and observed an increase content with age. Interestingly, there was a reduction in VEGF-C with age, and thus an inverse relation to Na^+ in skin and VEGF-C in plasma. They proposed that the lower VEGF-C levels could reduce the Na^+ clearance and lead to Na^+ accumulation in the skin. Even though we do not know whether the reduced VEGF-C results in reduced pumping efficiency, insufficient lymphangiogenesis or reduced lymph flow, these data clearly point to lymphatic function as an important factor in Na^+ homeostasis and a disease modulating factor. This factor might be targeted in other conditions characterized by salt accumulation such as chronic kidney disease and hypertension(153, 226).

In spite of significant salt accumulation, the water accumulation was modest. It is therefore likely that the interstitial fluid volume was in steady state at the time of study. The extravasation experiments suggest that the capillary permeability and thereby the integrity of vessel wall was not changed by the high salt intake that has been proposed to induce an inflammatory reaction(227). With an intact vessel barrier and no (HSD) or limited fluid accumulation (DOCA), we may assume a transcapillary filtration equal to that of lymph flow, and thus a higher filtration when recorded over a longer period involving the night.

To summarize, here we have been able to address the question “what lymphangiogenesis achieves”(203) in a situation where salt accumulation results in a hyperosmotic interstitium with macrophage accumulation, VEGF-C production and ensuing lymphangiogenesis. Accumulation of salt resulted in an increase in lymph flow of 26 and 20% from skin and muscle, respectively, and was first recognized after long-term observation. Such increase is likely the result of a corresponding enhanced filtration of fluid in combination with an increased contraction frequency of lymphatic collectors. Although this increase in flow might appear modest, we must remember that the transport of Na^+ (and other ions) from these tissues back to the general circulation will increase correspondingly, and suggests that an enhanced clearance of fluid from the tissue is an integrated element of electrolyte homeostasis and a regulatory mechanism working over long time. These studies point to the importance of lymph flow as a potential disease modifying factor that might be targeted in other conditions characterized by salt accumulation like chronic kidney disease and hypertension.

Sources of funding

Financial support from the Research Council of Norway (Project #262079) and from The Western Norway Regional Health Authority (Project # 912168) to HW is gratefully acknowledged.

Conflicts of interest/Disclosures

None

References

1. A global brief on hypertension; silent killer, global public health crisis. World Health Day 2013. Geneva: World Health Organization Press; 2013.
2. Hay J. A British Medical Association Lecture on THE SIGNIFICANCE OF A RAISED BLOOD PRESSURE. *Br Med J.* 1931;2(3679):43-7.
3. Xie X, Atkins E, Lv J, Bennett A, Neal B, Ninomiya T, et al. Effects of intensive blood pressure lowering on cardiovascular and renal outcomes: updated systematic review and meta-analysis. *Lancet.* 2016;387(10017):435-43.
4. Carretero OA, Oparil S. Essential hypertension. Part I: definition and etiology. *Circulation.* 2000;101(3):329-35.
5. Aburto NJ, Ziolkovska A, Hooper L, Elliott P, Cappuccio FP, Meerpohl JJ. Effect of lower sodium intake on health: systematic review and meta-analyses. *BMJ.* 2013;346:f1326.
6. Hall JE. *Textbook of medical physiology.* Thirteenth ed: Elsevier; 2016.
7. Guyton AC, Coleman TG, Cowley AV, Jr., Scheel KW, Manning RD, Jr., Norman RA, Jr. Arterial pressure regulation. Overriding dominance of the kidneys in long-term regulation and in hypertension. *Am J Med.* 1972;52(5):584-94.
8. Wiig H, Luft FC, Titze JM. The interstitium conducts extrarenal storage of sodium and represents a third compartment essential for extracellular volume and blood pressure homeostasis. *Acta Physiol (Oxf).* 2018;222(3).
9. Titze J, Lang R, Iliès C, Schwind KH, Kirsch KA, Dietsch P, et al. Osmotically inactive skin Na⁺ storage in rats. *Am J Physiol Renal Physiol.* 2003;285(6):F1108-17.
10. Linz P, Santoro D, Renz W, Rieger J, Ruehle A, Ruff J, et al. Skin sodium measured with ²³Na MRI at 7.0 T. *NMR Biomed.* 2015;28(1):54-62.
11. Machnik A, Neuhofer W, Jantsch J, Dahlmann A, Tammela T, Machura K, et al. Macrophages regulate salt-dependent volume and blood pressure by a vascular endothelial growth factor-C-dependent buffering mechanism. *Nat Med.* 2009;15(5):545-52.
12. Machnik A, Dahlmann A, Kopp C, Goss J, Wagner H, van Rooijen N, et al. Mononuclear phagocyte system depletion blocks interstitial tonicity-responsive enhancer binding protein/vascular endothelial growth factor C expression and induces salt-sensitive hypertension in rats. *Hypertension.* 2010;55(3):755-61.
13. Wiig H, Schroder A, Neuhofer W, Jantsch J, Kopp C, Karlsen TV, et al. Immune cells control skin lymphatic electrolyte homeostasis and blood pressure. *J Clin Invest.* 2013;123(7):2803-15.
14. Oparil S, Acelajado MC, Bakris GL, Berlowitz DR, Cifkova R, Dominiczak AF, et al. Hypertension. *Nat Rev Dis Primers.* 2018;4:18014.
15. Coffman TM. Under pressure: the search for the essential mechanisms of hypertension. *Nat Med.* 2011;17(11):1402-9.
16. Li XC, Zhang J, Zhuo JL. The vasoprotective axes of the renin-angiotensin system: Physiological relevance and therapeutic implications in cardiovascular, hypertensive and kidney diseases. *Pharmacol Res.* 2017;125(Pt A):21-38.
17. Joyner MJ, Charkoudian N, Wallin BG. Sympathetic nervous system and blood pressure in humans: individualized patterns of regulation and their implications. *Hypertension.* 2010;56(1):10-6.
18. Miller AJ, Arnold AC. The renin-angiotensin system in cardiovascular autonomic control: recent developments and clinical implications. *Clin Auton Res.* 2019;29(2):231-43.

19. Turner AJ, Hooper NM. The angiotensin-converting enzyme gene family: genomics and pharmacology. *Trends Pharmacol Sci.* 2002;23(4):177-83.
20. Mirabito Colafella KM, Bovee DM, Danser AHJ. The renin angiotensin aldosterone system and its therapeutic targets. *Exp Eye Res.* 2019.
21. Cannavo A, Bencivenga L, Liccardo D, Elia A, Marzano F, Gambino G, et al. Aldosterone and Mineralocorticoid Receptor System in Cardiovascular Physiology and Pathophysiology. *Oxid Med Cell Longev.* 2018;2018:1204598.
22. de Leeuw PW, Bisognano JD, Bakris GL, Nadim MK, Haller H, Kroon AA, et al. Sustained Reduction of Blood Pressure With Baroreceptor Activation Therapy: Results of the 6-Year Open Follow-Up. *Hypertension.* 2017;69(5):836-43.
23. Vanhoutte PM, Mombouli JV. Vascular endothelium: vasoactive mediators. *Prog Cardiovasc Dis.* 1996;39(3):229-38.
24. Vallance P, Collier J, Moncada S. Effects of endothelium-derived nitric oxide on peripheral arteriolar tone in man. *Lancet.* 1989;2(8670):997-1000.
25. Pittner J, Wolgast M, Casellas D, Persson AE. Increased shear stress-released NO and decreased endothelial calcium in rat isolated perfused juxtamedullary nephrons. *Kidney Int.* 2005;67(1):227-36.
26. Ali A, Abu Zar M, Kamal A, Faquih AE, Bhan C, Iftikhar W, et al. American Heart Association High Blood Pressure Protocol 2017: A Literature Review. *Cureus.* 2018;10(8):e3230.
27. Rimoldi SF, Scherrer U, Messerli FH. Secondary arterial hypertension: when, who, and how to screen? *Eur Heart J.* 2014;35(19):1245-54.
28. Matchar DB, McCrory DC, Orlando LA, Patel MR, Patel UD, Patwardhan MB, et al. Systematic review: comparative effectiveness of angiotensin-converting enzyme inhibitors and angiotensin II receptor blockers for treating essential hypertension. *Ann Intern Med.* 2008;148(1):16-29.
29. Dahl LK, Heine M, Thompson K. Genetic influence of the kidneys on blood pressure. Evidence from chronic renal homografts in rats with opposite predispositions to hypertension. *Circ Res.* 1974;34(1):94-101.
30. Esler M. The 2009 Carl Ludwig Lecture: Pathophysiology of the human sympathetic nervous system in cardiovascular diseases: the transition from mechanisms to medical management. *J Appl Physiol* (1985). 2010;108(2):227-37.
31. Vallbo AB, Hagbarth KE, Torebjork HE, Wallin BG. Somatosensory, proprioceptive, and sympathetic activity in human peripheral nerves. *Physiol Rev.* 1979;59(4):919-57.
32. Smith PA, Graham LN, Mackintosh AF, Stoker JB, Mary DA. Relationship between central sympathetic activity and stages of human hypertension. *Am J Hypertens.* 2004;17(3):217-22.
33. Goldstein DS. Plasma catecholamines and essential hypertension. An analytical review. *Hypertension.* 1983;5(1):86-99.
34. Konukoglu D, Uzun H. Endothelial Dysfunction and Hypertension. *Adv Exp Med Biol.* 2017;956:511-40.
35. Dharmashankar K, Widlansky ME. Vascular endothelial function and hypertension: insights and directions. *Curr Hypertens Rep.* 2010;12(6):448-55.
36. Shiekh GA, Ayub T, Khan SN, Dar R, Andrabi KI. Reduced nitrate level in individuals with hypertension and diabetes. *J Cardiovasc Dis Res.* 2011;2(3):172-6.
37. Panza JA, Casino PR, Kilcoyne CM, Quyyumi AA. Role of endothelium-derived nitric oxide in the abnormal endothelium-dependent vascular relaxation of patients with essential hypertension. *Circulation.* 1993;87(5):1468-74.

38. Louveau A, Smirnov I, Keyes TJ, Eccles JD, Rouhani SJ, Peske JD, et al. Structural and functional features of central nervous system lymphatic vessels. *Nature*. 2015;523(7560):337-41.
39. Aspelund A, Antila S, Proulx ST, Karlsten TV, Karaman S, Detmar M, et al. A dural lymphatic vascular system that drains brain interstitial fluid and macromolecules. *J Exp Med*. 2015;212(7):991-9.
40. Aspelund A, Tammela T, Antila S, Nurmi H, Leppanen VM, Zarkada G, et al. The Schlemm's canal is a VEGF-C/VEGFR-3-responsive lymphatic-like vessel. *J Clin Invest*. 2014;124(9):3975-86.
41. Makinen T, Alitalo K. Molecular mechanisms of lymphangiogenesis. *Cold Spring Harb Symp Quant Biol*. 2002;67:189-96.
42. Swartz MA. The physiology of the lymphatic system. *Adv Drug Deliv Rev*. 2001;50(1-2):3-20.
43. Hirakawa S, Detmar M, Karaman S. Lymphatics in nanophysiology. *Adv Drug Deliv Rev*. 2014;74:12-8.
44. Vittet D. Lymphatic collecting vessel maturation and valve morphogenesis. *Microvasc Res*. 2014;96:31-7.
45. Scallan JP, Zawieja SD, Castorena-Gonzalez JA, Davis MJ. Lymphatic pumping: mechanics, mechanisms and malfunction. *J Physiol*. 2016;594(20):5749-68.
46. Breslin JW, Yang Y, Scallan JP, Sweat RS, Adderley SP, Murfee WL. Lymphatic Vessel Network Structure and Physiology. *Compr Physiol*. 2018;9(1):207-99.
47. Wiig H, Swartz MA. Interstitial fluid and lymph formation and transport: physiological regulation and roles in inflammation and cancer. *Physiol Rev*. 2012;92(3):1005-60.
48. Jacob M, Chappell D. Reappraising Starling: the physiology of the microcirculation. *Curr Opin Crit Care*. 2013;19(4):282-9.
49. Levick JR, Michel CC. Microvascular fluid exchange and the revised Starling principle. *Cardiovasc Res*. 2010;87(2):198-210.
50. Clement CC, Aphkhasava D, Nieves E, Callaway M, Olszewski W, Rotzschke O, et al. Protein expression profiles of human lymph and plasma mapped by 2D-DIGE and 1D SDS-PAGE coupled with nanoLC-ESI-MS/MS bottom-up proteomics. *J Proteomics*. 2013;78:172-87.
51. Leak LV, Liotta LA, Krutzsch H, Jones M, Fusaro VA, Ross SJ, et al. Proteomic analysis of lymph. *Proteomics*. 2004;4(3):753-65.
52. Dzieciatkowska M, D'Alessandro A, Moore EE, Wohlauer M, Banerjee A, Silliman CC, et al. Lymph is not a plasma ultrafiltrate: a proteomic analysis of injured patients. *Shock*. 2014;42(6):485-98.
53. Clement CC, Santambrogio L. The lymph self-antigen repertoire. *Front Immunol*. 2013;4:424.
54. Santambrogio L, Rammensee HG. Contribution of the plasma and lymph Degradome and Peptidome to the MHC Ligandome. *Immunogenetics*. 2019;71(3):203-16.
55. Haljamae H, Linde A, Amundson B. Comparative analyses of capsular fluid and interstitial fluid. *Am J Physiol*. 1974;227(5):1199-205.
56. Szabo G, Magyar Z. Electrolyte concentrations in subcutaneous tissue fluid and lymph. *Lymphology*. 1982;15(4):174-7.
57. Aukland K, Reed RK. Interstitial-lymphatic mechanisms in the control of extracellular fluid volume. *Physiol Rev*. 1993;73(1):1-78.

58. Guyton AC, Taylor AE, Brace RA. A synthesis of interstitial fluid regulation and lymph formation. *Fed Proc.* 1976;35(8):1881-5.
59. von der Weid PY. Review article: lymphatic vessel pumping and inflammation--the role of spontaneous constrictions and underlying electrical pacemaker potentials. *Aliment Pharmacol Ther.* 2001;15(8):1115-29.
60. Benoit JN, Zawieja DC, Goodman AH, Granger HJ. Characterization of intact mesenteric lymphatic pump and its responsiveness to acute edemagenic stress. *Am J Physiol.* 1989;257(6 Pt 2):H2059-69.
61. Olszewski WL, Engeset A. Intrinsic contractility of prenodal lymph vessels and lymph flow in human leg. *Am J Physiol.* 1980;239(6):H775-83.
62. Van Helden DF. Pacemaker potentials in lymphatic smooth muscle of the guinea-pig mesentery. *J Physiol.* 1993;471:465-79.
63. von der Weid PY, Zawieja DC. Lymphatic smooth muscle: the motor unit of lymph drainage. *Int J Biochem Cell Biol.* 2004;36(7):1147-53.
64. Solari E, Marcozzi C, Negrini D, Moriondo A. Fluid Osmolarity Acutely and Differentially Modulates Lymphatic Vessels Intrinsic Contractions and Lymph Flow. *Front Physiol.* 2018;9:871.
65. Sabin FR. The Method of Growth of the Lymphatic System. *Science.* 1916;44(1127):145-58.
66. Schneider M, Othman-Hassan K, Christ B, Wilting J. Lymphangioblasts in the avian wing bud. *Dev Dyn.* 1999;216(4-5):311-9.
67. Martinez-Corral I, Ulvmar MH, Stanczuk L, Tatin F, Kizhatil K, John SW, et al. Nonvenous origin of dermal lymphatic vasculature. *Circ Res.* 2015;116(10):1649-54.
68. Klotz L, Norman S, Vieira JM, Masters M, Rohling M, Dube KN, et al. Cardiac lymphatics are heterogeneous in origin and respond to injury. *Nature.* 2015;522(7554):62-7.
69. Kim H, Kataru RP, Koh GY. Regulation and implications of inflammatory lymphangiogenesis. *Trends Immunol.* 2012;33(7):350-6.
70. Karaman S, Leppanen VM, Alitalo K. Vascular endothelial growth factor signaling in development and disease. *Development.* 2018;145(14).
71. Shibuya M. Vascular Endothelial Growth Factor (VEGF) and Its Receptor (VEGFR) Signaling in Angiogenesis: A Crucial Target for Anti- and Pro-Angiogenic Therapies. *Genes Cancer.* 2011;2(12):1097-105.
72. Karkkainen MJ, Haiko P, Sainio K, Partanen J, Taipale J, Petrova TV, et al. Vascular endothelial growth factor C is required for sprouting of the first lymphatic vessels from embryonic veins. *Nat Immunol.* 2004;5(1):74-80.
73. Takahashi H, Shibuya M. The vascular endothelial growth factor (VEGF)/VEGF receptor system and its role under physiological and pathological conditions. *Clin Sci (Lond).* 2005;109(3):227-41.
74. Makinen T, Jussila L, Veikkola T, Karpanen T, Kettunen MI, Pulkkanen KJ, et al. Inhibition of lymphangiogenesis with resulting lymphedema in transgenic mice expressing soluble VEGF receptor-3. *Nat Med.* 2001;7(2):199-205.
75. Jeltsch M, Kaipainen A, Joukov V, Meng X, Lakso M, Rauvala H, et al. Hyperplasia of lymphatic vessels in VEGF-C transgenic mice. *Science.* 1997;276(5317):1423-5.
76. Kaipainen A, Korhonen J, Mustonen T, van Hinsbergh VW, Fang GH, Dumont D, et al. Expression of the *fms*-like tyrosine kinase 4 gene becomes restricted to lymphatic endothelium during development. *Proc Natl Acad Sci U S A.* 1995;92(8):3566-70.

77. Schoppmann SF, Birner P, Stockl J, Kalt R, Ullrich R, Caucig C, et al. Tumor-associated macrophages express lymphatic endothelial growth factors and are related to peritumoral lymphangiogenesis. *Am J Pathol.* 2002;161(3):947-56.
78. Ran S, Montgomery KE. Macrophage-mediated lymphangiogenesis: the emerging role of macrophages as lymphatic endothelial progenitors. *Cancers (Basel).* 2012;4(3):618-57.
79. Dabrowska AK, Spano F, Derler S, Adlhart C, Spencer ND, Rossi RM. The relationship between skin function, barrier properties, and body-dependent factors. *Skin Res Technol.* 2018;24(2):165-74.
80. Nguyen AV, Soulika AM. The Dynamics of the Skin's Immune System. *Int J Mol Sci.* 2019;20(8).
81. Agarwal S, Krishnamurthy K. *Histology, Skin.* StatPearls. Treasure Island (FL)2019.
82. Richmond JM, Harris JE. Immunology and skin in health and disease. *Cold Spring Harb Perspect Med.* 2014;4(12):a015339.
83. Has C, Nystrom A. Epidermal Basement Membrane in Health and Disease. *Curr Top Membr.* 2015;76:117-70.
84. Brown TM, Krishnamurthy K. *Histology, Dermis.* StatPearls. Treasure Island (FL)2019.
85. Arda O, Goksugur N, Tuzun Y. Basic histological structure and functions of facial skin. *Clin Dermatol.* 2014;32(1):3-13.
86. Theocharis AD, Skandalis SS, Gialeli C, Karamanos NK. Extracellular matrix structure. *Adv Drug Deliv Rev.* 2016;97:4-27.
87. Wiig H, Keskin D, Kalluri R. Interaction between the extracellular matrix and lymphatics: consequences for lymphangiogenesis and lymphatic function. *Matrix Biol.* 2010;29(8):645-56.
88. Domene C, Jorgensen C, Abbasi SW. A perspective on structural and computational work on collagen. *Phys Chem Chem Phys.* 2016;18(36):24802-11.
89. Arora H, Falto-Aizpurua L, Cortes-Fernandez A, Choudhary S, Romanelli P. Connective Tissue Nevi: A Review of the Literature. *Am J Dermatopathol.* 2017;39(5):325-41.
90. Frances C, Robert L. Elastin and elastic fibers in normal and pathologic skin. *Int J Dermatol.* 1984;23(3):166-79.
91. Lee DH, Oh JH, Chung JH. Glycosaminoglycan and proteoglycan in skin aging. *J Dermatol Sci.* 2016;83(3):174-81.
92. Oh JH, Kim YK, Jung JY, Shin JE, Kim KH, Cho KH, et al. Intrinsic aging- and photoaging-dependent level changes of glycosaminoglycans and their correlation with water content in human skin. *J Dermatol Sci.* 2011;62(3):192-201.
93. Anderegg U, Simon JC, Averbek M. More than just a filler - the role of hyaluronan for skin homeostasis. *Exp Dermatol.* 2014;23(5):295-303.
94. Karsdal MA, Nielsen MJ, Sand JM, Henriksen K, Genovese F, Bay-Jensen AC, et al. Extracellular matrix remodeling: the common denominator in connective tissue diseases. Possibilities for evaluation and current understanding of the matrix as more than a passive architecture, but a key player in tissue failure. *Assay Drug Dev Technol.* 2013;11(2):70-92.
95. Visse R, Nagase H. Matrix metalloproteinases and tissue inhibitors of metalloproteinases: structure, function, and biochemistry. *Circ Res.* 2003;92(8):827-39.

96. Jablonska-Trypuc A, Matejczyk M, Rosochacki S. Matrix metalloproteinases (MMPs), the main extracellular matrix (ECM) enzymes in collagen degradation, as a target for anticancer drugs. *J Enzyme Inhib Med Chem.* 2016;31(sup1):177-83.
97. Theocharis AD, Manou D, Karamanos NK. The extracellular matrix as a multitasking player in disease. *FEBS J.* 2019.
98. Karamanos NK, Theocharis AD, Neill T, Iozzo RV. Matrix modeling and remodeling: A biological interplay regulating tissue homeostasis and diseases. *Matrix Biol.* 2019;75-76:1-11.
99. Muller DN, Wilck N, Haase S, Kleinewietfeld M, Linker RA. Sodium in the microenvironment regulates immune responses and tissue homeostasis. *Nat Rev Immunol.* 2019;19(4):243-54.
100. Sattler S. The Role of the Immune System Beyond the Fight Against Infection. *Adv Exp Med Biol.* 2017;1003:3-14.
101. Mirza R, DiPietro LA, Koh TJ. Selective and specific macrophage ablation is detrimental to wound healing in mice. *Am J Pathol.* 2009;175(6):2454-62.
102. Sattler S, Rosenthal N. The neonate versus adult mammalian immune system in cardiac repair and regeneration. *Biochim Biophys Acta.* 2016;1863(7 Pt B):1813-21.
103. Lin SL, Li B, Rao S, Yeo EJ, Hudson TE, Nowlin BT, et al. Macrophage Wnt7b is critical for kidney repair and regeneration. *Proc Natl Acad Sci U S A.* 2010;107(9):4194-9.
104. Lobov IB, Rao S, Carroll TJ, Vallance JE, Ito M, Ondr JK, et al. WNT7b mediates macrophage-induced programmed cell death in patterning of the vasculature. *Nature.* 2005;437(7057):417-21.
105. Ganeshan K, Chawla A. Metabolic regulation of immune responses. *Annu Rev Immunol.* 2014;32:609-34.
106. Abboud FM, Singh MV. Autonomic regulation of the immune system in cardiovascular diseases. *Adv Physiol Educ.* 2017;41(4):578-93.
107. Galloway DA, Phillips AEM, Owen DRJ, Moore CS. Phagocytosis in the Brain: Homeostasis and Disease. *Front Immunol.* 2019;10:790.
108. Clayton K, Vallejo AF, Davies J, Sirvent S, Polak ME. Langerhans Cells- Programmed by the Epidermis. *Front Immunol.* 2017;8:1676.
109. Platt AM, Randolph GJ. Dendritic cell migration through the lymphatic vasculature to lymph nodes. *Adv Immunol.* 2013;120:51-68.
110. Hettinger J, Richards DM, Hansson J, Barra MM, Joschko AC, Krijgsveld J, et al. Origin of monocytes and macrophages in a committed progenitor. *Nat Immunol.* 2013;14(8):821-30.
111. Yanez DA, Lacher RK, Vidyarthi A, Colegio OR. The role of macrophages in skin homeostasis. *Pflugers Arch.* 2017;469(3-4):455-63.
112. Minutti CM, Knipper JA, Allen JE, Zaiss DM. Tissue-specific contribution of macrophages to wound healing. *Semin Cell Dev Biol.* 2017;61:3-11.
113. Willenborg S, Lucas T, van Loo G, Knipper JA, Krieg T, Haase I, et al. CCR2 recruits an inflammatory macrophage subpopulation critical for angiogenesis in tissue repair. *Blood.* 2012;120(3):613-25.
114. Willard-Mack CL. Normal structure, function, and histology of lymph nodes. *Toxicol Pathol.* 2006;34(5):409-24.
115. von Andrian UH, Mempel TR. Homing and cellular traffic in lymph nodes. *Nat Rev Immunol.* 2003;3(11):867-78.
116. Worbs T, Hammerschmidt SI, Forster R. Dendritic cell migration in health and disease. *Nat Rev Immunol.* 2017;17(1):30-48.

117. Boardman KC, Swartz MA. Interstitial flow as a guide for lymphangiogenesis. *Circ Res.* 2003;92(7):801-8.
118. Weber M, Hauschild R, Schwarz J, Moussion C, de Vries I, Legler DF, et al. Interstitial dendritic cell guidance by haptotactic chemokine gradients. *Science.* 2013;339(6117):328-32.
119. Scheinecker C, McHugh R, Shevach EM, Germain RN. Constitutive presentation of a natural tissue autoantigen exclusively by dendritic cells in the draining lymph node. *J Exp Med.* 2002;196(8):1079-90.
120. Miteva DO, Rutkowski JM, Dixon JB, Kilarski W, Shields JD, Swartz MA. Transmural flow modulates cell and fluid transport functions of lymphatic endothelium. *Circ Res.* 2010;106(5):920-31.
121. Martin-Fontecha A, Sebastiani S, Hopken UE, Ugucconi M, Lipp M, Lanzavecchia A, et al. Regulation of dendritic cell migration to the draining lymph node: Impact on T lymphocyte traffic and priming. *Journal of Experimental Medicine.* 2003;198(4):615-21.
122. Thomas SN, Rutkowski JM, Pasquier M, Kuan EL, Alitalo K, Randolph GJ, et al. Impaired humoral immunity and tolerance in K14-VEGFR-3-Ig mice that lack dermal lymphatic drainage. *J Immunol.* 2012;189(5):2181-90.
123. Drummond GR, Vinh A, Guzik TJ, Sobey CG. Immune mechanisms of hypertension. *Nat Rev Immunol.* 2019.
124. Okuda T, Grollman A. Passive transfer of autoimmune induced hypertension in the rat by lymph node cells. *Tex Rep Biol Med.* 1967;25(2):257-64.
125. Olsen F. Transfer of arterial hypertension by splenic cells from DOCA-salt hypertensive and renal hypertensive rats to normotensive recipients. *Acta Pathol Microbiol Scand C.* 1980;88(1):1-5.
126. Guzik TJ, Hoch NE, Brown KA, McCann LA, Rahman A, Dikalov S, et al. Role of the T cell in the genesis of angiotensin II induced hypertension and vascular dysfunction. *J Exp Med.* 2007;204(10):2449-60.
127. Pollow DP, Uhrlaub J, Romero-Aleshire M, Sandberg K, Nikolich-Zugich J, Brooks HL, et al. Sex differences in T-lymphocyte tissue infiltration and development of angiotensin II hypertension. *Hypertension.* 2014;64(2):384-90.
128. Lob HE, Marvar PJ, Guzik TJ, Sharma S, McCann LA, Weyand C, et al. Induction of hypertension and peripheral inflammation by reduction of extracellular superoxide dismutase in the central nervous system. *Hypertension.* 2010;55(2):277-83, 6p following 83.
129. Trott DW, Harrison DG. The immune system in hypertension. *Adv Physiol Educ.* 2014;38(1):20-4.
130. Saleh MA, McMaster WG, Wu J, Norlander AE, Funt SA, Thabet SR, et al. Lymphocyte adaptor protein LNK deficiency exacerbates hypertension and end-organ inflammation. *J Clin Invest.* 2015;125(3):1189-202.
131. Ren J, Crowley SD. Role of T-cell activation in salt-sensitive hypertension. *Am J Physiol Heart Circ Physiol.* 2019;316(6):H1345-H53.
132. Ugur M, Mueller SN. T cell and dendritic cell interactions in lymphoid organs: More than just being in the right place at the right time. *Immunol Rev.* 2019;289(1):115-28.
133. Vinh A, Chen W, Blinder Y, Weiss D, Taylor WR, Goronzy JJ, et al. Inhibition and genetic ablation of the B7/CD28 T-cell costimulation axis prevents experimental hypertension. *Circulation.* 2010;122(24):2529-37.

-
134. Kirabo A, Fontana V, de Faria AP, Loperena R, Galindo CL, Wu J, et al. DC isoketal-modified proteins activate T cells and promote hypertension. *J Clin Invest*. 2014;124(10):4642-56.
 135. Salomon RG, Bi W. Isolevuglandin adducts in disease. *Antioxid Redox Signal*. 2015;22(18):1703-18.
 136. Pons H, Ferrebuz A, Quiroz Y, Romero-Vasquez F, Parra G, Johnson RJ, et al. Immune reactivity to heat shock protein 70 expressed in the kidney is cause of salt-sensitive hypertension. *Am J Physiol Renal Physiol*. 2013;304(3):F289-99.
 137. Tobias A, Mohiuddin SS. Physiology, Water Balance. *StatPearls*. Treasure Island (FL)2019.
 138. Shrimanker I, Bhattarai S. Electrolytes. *StatPearls*. Treasure Island (FL)2019.
 139. Chen JS, Al Khalili Y. Physiology, Osmoregulation and Excretion. *StatPearls*. Treasure Island (FL)2019.
 140. Ogobuiro I, Tuma F. Physiology, Renal. *StatPearls*. Treasure Island (FL)2019.
 141. Palmer LG, Schnermann J. Integrated control of Na transport along the nephron. *Clin J Am Soc Nephrol*. 2015;10(4):676-87.
 142. Cook NR, Cutler JA, Obarzanek E, Buring JE, Rexrode KM, Kumanyika SK, et al. Long term effects of dietary sodium reduction on cardiovascular disease outcomes: observational follow-up of the trials of hypertension prevention (TOHP). *BMJ*. 2007;334(7599):885-8.
 143. He FJ, MacGregor GA. A comprehensive review on salt and health and current experience of worldwide salt reduction programmes. *J Hum Hypertens*. 2009;23(6):363-84.
 144. Sacks FM, Svetkey LP, Vollmer WM, Appel LJ, Bray GA, Harsha D, et al. Effects on blood pressure of reduced dietary sodium and the Dietary Approaches to Stop Hypertension (DASH) diet. DASH-Sodium Collaborative Research Group. *N Engl J Med*. 2001;344(1):3-10.
 145. Weinberger MH, Miller JZ, Luft FC, Grim CE, Fineberg NS. Definitions and characteristics of sodium sensitivity and blood pressure resistance. *Hypertension*. 1986;8(6 Pt 2):II127-34.
 146. Guyton AC. Blood pressure control--special role of the kidneys and body fluids. *Science*. 1991;252(5014):1813-6.
 147. Heer M, Baisch F, Kropp J, Gerzer R, Drummer C. High dietary sodium chloride consumption may not induce body fluid retention in humans. *Am J Physiol Renal Physiol*. 2000;278(4):F585-95.
 148. Titze J, Maillet A, Lang R, Gunga HC, Johannes B, Gauquelin-Koch G, et al. Long-term sodium balance in humans in a terrestrial space station simulation study. *Am J Kidney Dis*. 2002;40(3):508-16.
 149. Rakova N, Juttner K, Dahlmann A, Schroder A, Linz P, Kopp C, et al. Long-term space flight simulation reveals infradian rhythmicity in human Na(+) balance. *Cell Metab*. 2013;17(1):125-31.
 150. Titze J. Water-free sodium accumulation. *Semin Dial*. 2009;22(3):253-5.
 151. Nikpey E, Karlsen TV, Rakova N, Titze JM, Tenstad O, Wiig H. High-Salt Diet Causes Osmotic Gradients and Hyperosmolality in Skin Without Affecting Interstitial Fluid and Lymph. *Hypertension*. 2017;69(4):660-8.
 152. Hofmeister LH, Perisic S, Titze J. Tissue sodium storage: evidence for kidney-like extrarenal countercurrent systems? *Pflugers Arch*. 2015;467(3):551-8.

153. Kopp C, Linz P, Dahlmann A, Hammon M, Jantsch J, Muller DN, et al. ²³Na magnetic resonance imaging-determined tissue sodium in healthy subjects and hypertensive patients. *Hypertension*. 2013;61(3):635-40.
154. Muller S, Quast T, Schroder A, Hucke S, Klotz L, Jantsch J, et al. Salt-dependent chemotaxis of macrophages. *PLoS One*. 2013;8(9):e73439.
155. Karkkainen MJ, Saaristo A, Jussila L, Karila KA, Lawrence EC, Pajusola K, et al. A model for gene therapy of human hereditary lymphedema. *Proc Natl Acad Sci U S A*. 2001;98(22):12677-82.
156. Mäkinen T, Veikkola T, Mustjoki S, Karpanen T, Catimel B, Nice EC, et al. Isolated lymphatic endothelial cells transduce growth, survival and migratory signals via the VEGF-C/D receptor VEGFR-3. *EMBO J*. 2001;20(17):4762-73.
157. Niemeier JE. Telemetry for small animal physiology. *Lab Anim (NY)*. 2016;45(7):255-7.
158. Karlsen TV, McCormack E, Mujic M, Tenstad O, Wiig H. Minimally invasive quantification of lymph flow in mice and rats by imaging depot clearance of near-infrared albumin. *Am J Physiol Heart Circ Physiol*. 2012;302(2):H391-401.
159. Janssen PM, Biesiadecki BJ, Ziolo MT, Davis JP. The Need for Speed: Mice, Men, and Myocardial Kinetic Reserve. *Circ Res*. 2016;119(3):418-21.
160. Reckelhoff JF, Alexander BT. Reproducibility in animal models of hypertension: a difficult problem. *Biol Sex Differ*. 2018;9(1):53.
161. Lerman LO, Kurtz TW, Touyz RM, Ellison DH, Chade AR, Crowley SD, et al. Animal Models of Hypertension: A Scientific Statement From the American Heart Association. *Hypertension*. 2019;73(6):e87-e120.
162. Hartner A, Cordasic N, Klanke B, Veelken R, Hilgers KF. Strain differences in the development of hypertension and glomerular lesions induced by deoxycorticosterone acetate salt in mice. *Nephrol Dial Transplant*. 2003;18(10):1999-2004.
163. Drenjancevic-Peric I, Jelakovic B, Lombard JH, Kunert MP, Kibel A, Gros M. High-salt diet and hypertension: focus on the renin-angiotensin system. *Kidney Blood Press Res*. 2011;34(1):1-11.
164. Kandlikar SS, Fink GD. Splanchnic sympathetic nerves in the development of mild DOCA-salt hypertension. *Am J Physiol Heart Circ Physiol*. 2011;301(5):H1965-73.
165. Lin HY, Lee YT, Chan YW, Tse G. Animal models for the study of primary and secondary hypertension in humans. *Biomed Rep*. 2016;5(6):653-9.
166. Basting T, Lazartigues E. DOCA-Salt Hypertension: an Update. *Curr Hypertens Rep*. 2017;19(4):32.
167. Martus W, Kim D, Garvin JL, Beierwaltes WH. Commercial rodent diets contain more sodium than rats need. *Am J Physiol Renal Physiol*. 2005;288(2):F428-31.
168. Zhao X, Ho D, Gao S, Hong C, Vatner DE, Vatner SF. Arterial Pressure Monitoring in Mice. *Curr Protoc Mouse Biol*. 2011;1:105-22.
169. Carlson SH, Wyss JM. Long-term telemetric recording of arterial pressure and heart rate in mice fed basal and high NaCl diets. *Hypertension*. 2000;35(2):E1-5.
170. Kurtz TW, Griffin KA, Bidani AK, Davison RL, Hall JE, Subcommittee of P, et al. Recommendations for blood pressure measurement in humans and experimental animals. Part 2: Blood pressure measurement in experimental animals: a statement for professionals from the subcommittee of professional and public education of the American Heart Association council on high blood pressure research. *Hypertension*. 2005;45(2):299-310.

171. Wilde E, Aubdool AA, Thakore P, Baldissera L, Jr., Alawi KM, Keeble J, et al. Tail-Cuff Technique and Its Influence on Central Blood Pressure in the Mouse. *J Am Heart Assoc.* 2017;6(6).
172. Salay LD, Ishiko N, Huberman AD. A midline thalamic circuit determines reactions to visual threat. *Nature.* 2018;557(7704):183-9.
173. Taylor CR, Levenson RM. Quantification of immunohistochemistry--issues concerning methods, utility and semiquantitative assessment II. *Histopathology.* 2006;49(4):411-24.
174. Adan A, Alizada G, Kiraz Y, Baran Y, Nalbant A. Flow cytometry: basic principles and applications. *Crit Rev Biotechnol.* 2017;37(2):163-76.
175. Proulx ST, Ma Q, Andina D, Leroux JC, Detmar M. Quantitative measurement of lymphatic function in mice by noninvasive near-infrared imaging of a peripheral vein. *JCI Insight.* 2017;2(1):e90861.
176. Wiig H, Reed RK, Aukland K. Micropuncture measurement of interstitial fluid pressure in rat subcutis and skeletal muscle: comparison to wick-in-needle technique. *Microvasc Res.* 1981;21(3):308-19.
177. Huggenberger R, Siddiqui SS, Brander D, Ullmann S, Zimmermann K, Antsiferova M, et al. An important role of lymphatic vessel activation in limiting acute inflammation. *Blood.* 2011;117(17):4667-78.
178. Huggenberger R, Ullmann S, Proulx ST, Pytowski B, Alitalo K, Detmar M. Stimulation of lymphangiogenesis via VEGFR-3 inhibits chronic skin inflammation. *J Exp Med.* 2010;207(10):2255-69.
179. Kataru RP, Jung K, Jang C, Yang H, Schwendener RA, Baik JE, et al. Critical role of CD11b+ macrophages and VEGF in inflammatory lymphangiogenesis, antigen clearance, and inflammation resolution. *Blood.* 2009;113(22):5650-9.
180. Lachance PA, Hazen A, Sevic-Muraca EM. Lymphatic vascular response to acute inflammation. *PLoS One.* 2013;8(9):e76078.
181. Chakraborty S, Davis MJ, Muthuchamy M. Emerging trends in the pathophysiology of lymphatic contractile function. *Semin Cell Dev Biol.* 2015;38:55-66.
182. Christiansen AJ, Dieterich LC, Ohs I, Bachmann SB, Bianchi R, Proulx ST, et al. Lymphatic endothelial cells attenuate inflammation via suppression of dendritic cell maturation. *Oncotarget.* 2016;7(26):39421-35.
183. Kitada K, Daub S, Zhang Y, Klein JD, Nakano D, Pedchenko T, et al. High salt intake reprioritizes osmolyte and energy metabolism for body fluid conservation. *J Clin Invest.* 2017;127(5):1944-59.
184. Van Beusecum JP, Barbaro NR, McDowell Z, Aden LA, Xiao L, Pandey AK, et al. High Salt Activates CD11c(+) Antigen-Presenting Cells via SGK (Serum Glucocorticoid Kinase) 1 to Promote Renal Inflammation and Salt-Sensitive Hypertension. *Hypertension.* 2019;74(3):555-63.
185. Chachaj A, Pula B, Chabowski M, Grzegorzolka J, Szahidewicz-Krupska E, Karczewski M, et al. Role of the Lymphatic System in the Pathogenesis of Hypertension in Humans. *Lymphat Res Biol.* 2018;16(2):140-6.
186. Lankhorst S, Severs D, Marko L, Rakova N, Titze J, Muller DN, et al. Salt Sensitivity of Angiogenesis Inhibition-Induced Blood Pressure Rise: Role of Interstitial Sodium Accumulation? *Hypertension.* 2017;69(5):919-26.
187. Titze J, Bauer K, Schafflhuber M, Dietsch P, Lang R, Schwind KH, et al. Internal sodium balance in DOCA-salt rats: a body composition study. *Am J Physiol Renal Physiol.* 2005;289(4):F793-802.

188. Ziomber A, Machnik A, Dahlmann A, Dietsch P, Beck FX, Wagner H, et al. Sodium-, potassium-, chloride-, and bicarbonate-related effects on blood pressure and electrolyte homeostasis in deoxycorticosterone acetate-treated rats. *Am J Physiol Renal Physiol*. 2008;295(6):F1752-63.
189. Fuller W, Tulloch LB, Shattock MJ, Calaghan SC, Howie J, Wypijewski KJ. Regulation of the cardiac sodium pump. *Cell Mol Life Sci*. 2013;70(8):1357-80.
190. Doyle D, Smith R, Krozowski ZS, Funder JW. Mineralocorticoid specificity of renal type I receptors: binding and metabolism of corticosterone. *J Steroid Biochem*. 1989;33(2):165-70.
191. Tesch GH, Young MJ. Mineralocorticoid Receptor Signaling as a Therapeutic Target for Renal and Cardiac Fibrosis. *Front Pharmacol*. 2017;8:313.
192. Chadwick JA, Hauck JS, Gomez-Sanchez CE, Gomez-Sanchez EP, Rafael-Fortney JA. Gene expression effects of glucocorticoid and mineralocorticoid receptor agonists and antagonists on normal human skeletal muscle. *Physiol Genomics*. 2017;49(6):277-86.
193. Nishizaka MK, Zaman MA, Calhoun DA. Efficacy of low-dose spironolactone in subjects with resistant hypertension. *Am J Hypertens*. 2003;16(11 Pt 1):925-30.
194. Shibata H, Itoh H. Mineralocorticoid receptor-associated hypertension and its organ damage: clinical relevance for resistant hypertension. *Am J Hypertens*. 2012;25(5):514-23.
195. Rocchini AP, Key J, Bondie D, Chico R, Moorehead C, Katch V, et al. The effect of weight loss on the sensitivity of blood pressure to sodium in obese adolescents. *N Engl J Med*. 1989;321(9):580-5.
196. Alitalo K. The lymphatic vasculature in disease. *Nat Med*. 2011;17(11):1371-80.
197. Aspelund A, Robciuc MR, Karaman S, Makinen T, Alitalo K. Lymphatic System in Cardiovascular Medicine. *Circ Res*. 2016;118(3):515-30.
198. Aebischer D, Iolyeva M, Halin C. The inflammatory response of lymphatic endothelium. *Angiogenesis*. 2014;17(2):383-93.
199. Kim H, Kataru RP, Koh GY. Inflammation-associated lymphangiogenesis: a double-edged sword? *J Clin Invest*. 2014;124(3):936-42.
200. Huggenberger R, Siddiqui SS, Brander D, Ullmann S, Zimmermann K, Antsiferova M, et al. An important role of lymphatic vessel activation in limiting acute inflammation. *Blood*. 2011;117(17):4667-78.
201. Kajiya K, Sawane M, Huggenberger R, Detmar M. Activation of the VEGFR-3 pathway by VEGF-C attenuates UVB-induced edema formation and skin inflammation by promoting lymphangiogenesis. *J Invest Dermatol*. 2009;129(5):1292-8.
202. Liao S, Cheng G, Conner DA, Huang Y, Kucherlapati RS, Munn LL, et al. Impaired lymphatic contraction associated with immunosuppression. *Proc Natl Acad Sci U S A*. 2011;108(46):18784-9.
203. Randolph GJ, Ivanov S, Zinselmeyer BH, Scallan JP. The Lymphatic System: Integral Roles in Immunity. *Annu Rev Immunol*. 2016.
204. Guyton AC, Scheel K, Murphree D. Interstitial fluid pressure. 3. Its effect on resistance to tissue fluid mobility. *Circ Res*. 1966;19(2):412-9.
205. Bates DO, Lodwick D, Williams B. Vascular endothelial growth factor and microvascular permeability. *Microcirculation*. 1999;6(2):83-96.
206. Modi S, Stanton AW, Mortimer PS, Levick JR. Clinical assessment of human lymph flow using removal rate constants of interstitial macromolecules: a critical review of lymphoscintigraphy. *Lymphat Res Biol*. 2007;5(3):183-202.
207. Aldrich MB, Sevick-Muraca EM. Cytokines are systemic effectors of lymphatic function in acute inflammation. *Cytokine*. 2013;64(1):362-9.

-
208. Papadakou P, Bletsas A, Yassin MA, Karlsen TV, Wiig H, Berggreen E. Role of Hyperplasia of Gingival Lymphatics in Periodontal Inflammation. *J Dent Res*. 2017;96(4):467-76.
209. Zhou Q, Guo R, Wood R, Boyce BF, Liang Q, Wang YJ, et al. Vascular endothelial growth factor C attenuates joint damage in chronic inflammatory arthritis by accelerating local lymphatic drainage in mice. *Arthritis Rheum*. 2011;63(8):2318-28.
210. Lahteenvuo M, Honkonen K, Tervala T, Tammela T, Suominen E, Lahteenvuo J, et al. Growth factor therapy and autologous lymph node transfer in lymphedema. *Circulation*. 2011;123(6):613-20.
211. Guyton AC, Coleman TG, Cowley AW, Manning RD, Norman RA, Ferguson JD. A systems analysis approach to understanding long-range arterial blood pressure control and hypertension. *Circ Res*. 1974;35:159 - 76.
212. Palacios C, Wigertz K, Martin BR, Jackman L, Pratt JH, Peacock M, et al. Sodium retention in black and white female adolescents in response to salt intake. *J Clin Endocrinol Metab*. 2004;89(4):1858-63.
213. Schafflhuber M, Volpi N, Dahlmann A, Hilgers KF, Maccari F, Dietsch P, et al. Mobilization of osmotically inactive Na⁺ by growth and by dietary salt restriction in rats. *Am J Physiol Renal Physiol*. 2007;292(5):F1490-500.
214. Titze J, Krause H, Hecht H, Dietsch P, Rittweger J, Lang R, et al. Reduced osmotically inactive Na storage capacity and hypertension in the Dahl model. *Am J Physiol Renal Physiol*. 2002;283(1):F134-41.
215. Titze J, Luft FC, Bauer K, Dietsch P, Lang R, Veelken R, et al. Extrarenal Na⁺ balance, volume, and blood pressure homeostasis in intact and ovariectomized deoxycorticosterone-acetate salt rats. *Hypertension*. 2006;47(6):1101-7.
216. Wiig H, Tenstad O, Bert JL. Effect of hydration on interstitial distribution of charged albumin in rat dermis in vitro. *J Physiol*. 2005;569(Pt 2):631-41.
217. Karlsen TV, Reikvam T, Tofteberg A, Nikpey E, Skogstrand T, Wagner M, et al. Lymphangiogenesis Facilitates Initial Lymph Formation and Enhances the Dendritic Cell Mobilizing Chemokine CCL21 Without Affecting Migration. *Arterioscler Thromb Vasc Biol*. 2017;37(11):2128-35.
218. Scallan JP, Davis MJ. Genetic removal of basal nitric oxide enhances contractile activity in isolated murine collecting lymphatic vessels. *J Physiol*. 2013;591(8):2139-56.
219. Scallan JP, Wolpers JH, Davis MJ. Constriction of isolated collecting lymphatic vessels in response to acute increases in downstream pressure. *J Physiol*. 2013;591(2):443-59.
220. Gashev AA, Davis MJ, Zawieja DC. Inhibition of the active lymph pump by flow in rat mesenteric lymphatics and thoracic duct. *J Physiol*. 2002;540(Pt 3):1023-37.
221. Weissleder R, Pittet MJ. Imaging in the era of molecular oncology. *Nature*. 2008;452(7187):580-9.
222. Mumprecht V, Honer M, Vigl B, Proulx ST, Trachsel E, Kaspar M, et al. In vivo imaging of inflammation- and tumor-induced lymph node lymphangiogenesis by immuno-positron emission tomography. *Cancer Res*. 2010;70(21):8842-51.
223. Kwon S, Agollah GD, Chan W, Sevic-Muraca EM. Altered lymphatic function and architecture in salt-induced hypertension assessed by near-infrared fluorescence imaging. *J Biomed Opt*. 2012;17(8):080504-1.
224. Zawieja SD, Castorena-Gonzalez JA, Scallan JP, Davis MJ. Differences in L-type Ca(2+) channel activity partially underlie the regional dichotomy in pumping behavior by murine peripheral and visceral lymphatic vessels. *Am J Physiol Heart Circ Physiol*. 2018;314(5):H991-H1010.

-
225. Breslin JW, Gaudreault N, Watson KD, Reynoso R, Yuan SY, Wu MH. Vascular endothelial growth factor-C stimulates the lymphatic pump by a VEGF receptor-3-dependent mechanism. *Am J Physiol Heart Circ Physiol.* 2007;293(1):H709-18.
226. Dahlmann A, Dorfelt K, Eicher F, Linz P, Kopp C, Mossinger I, et al. Magnetic resonance-determined sodium removal from tissue stores in hemodialysis patients. *Kidney Int.* 2015;87(2):434-41.
227. Kleinewietfeld M, Manzel A, Titze J, Kvakan H, Yosef N, Linker RA, et al. Sodium chloride drives autoimmune disease by the induction of pathogenic TH17 cells. *Nature.* 2013;496(7446):518-22.

Highlights

- Increase in lymph flow during salt accumulation suggest that lymphatics may contribute in long term regulation of tissue fluid balance and blood pressure by contributing to fluid homeostasis in skin and muscle.
- Recently it has been shown that considerable amounts of Na⁺ can be retained or removed from the body without commensurate water loss, and that the skin can serve as a major salt reservoir contributing in blood pressure regulation.
- We identify lymph clearance as a potential disease modifying factor that might be targeted in conditions characterized by salt accumulation like chronic kidney disease and salt-sensitive hypertension.

Figures

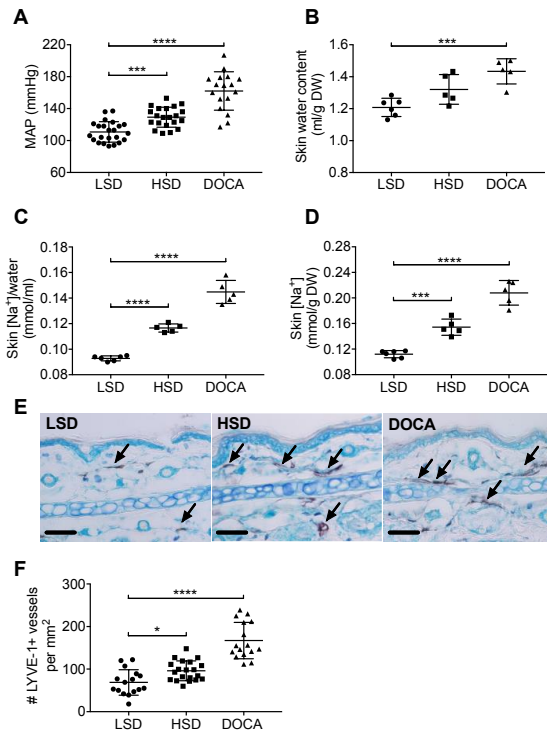


Figure 1. A. Individual values of mean arterial blood pressure measured with tail cuff plethysmography in awake rats after 14 days of either low salt diet (LSD), high salt diet (HSD) or DOCA-salt diet. B. Individual values of skin water content in LSD, HSD and DOCA-salt diet. C. Individual values of skin Na⁺ content relative to skin water in LSD, HSD and DOCA-salt diet. D. Individual values of skin Na⁺ content relative to dry weight in LSD, HSD and DOCA-salt diet. E. Representative ear skin sections showing LYVE-1+ lymphatic vessels in LSD, HSD and DOCA-salt fed rats. Scale bar = 50 μm. F. LYVE-1+ lymphatic vessels were counted in 5-7 consecutive fields per section from 3 rats per group. Also shown mean ± SD. *P<0.05, ***P<0.001, ****P<0.0001 when compared to LSD (ANOVA followed by Dunnett's multiple comparisons test).

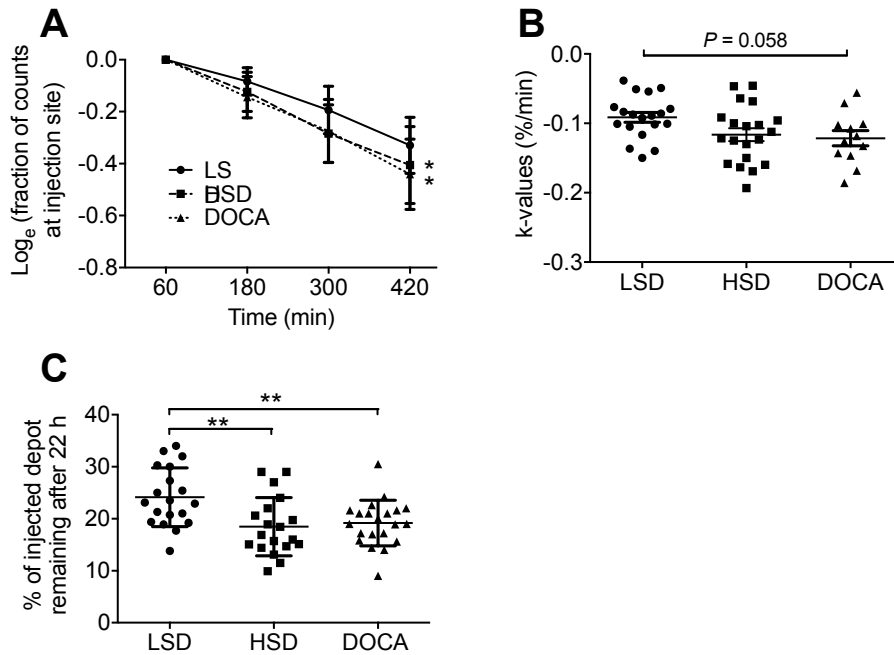


Figure 2. A. Average Log_e fraction of counts remaining in the intradermally injected depot of 3 μ l macromolecular tracer (Alexa680-BSA) in hind paw of rats on LSD (n=19), HSD (n=20) and DOCA-salt diet (n=12). B. Individual rate constants (*k*) calculated as the slope of the monoexponential washout curves for each individual rat in (A) obtained by linear regression analysis. C. Individual values representing the fraction of counts remaining in the intradermal depot 22 hours after injection of 3 μ l Alexa680-BSA in LSD, HSD and DOCA-salt diet. Also shown mean \pm SD. * $P < 0.05$, ** $P < 0.01$ (ANOVA followed by Dunnett's multiple comparisons test).

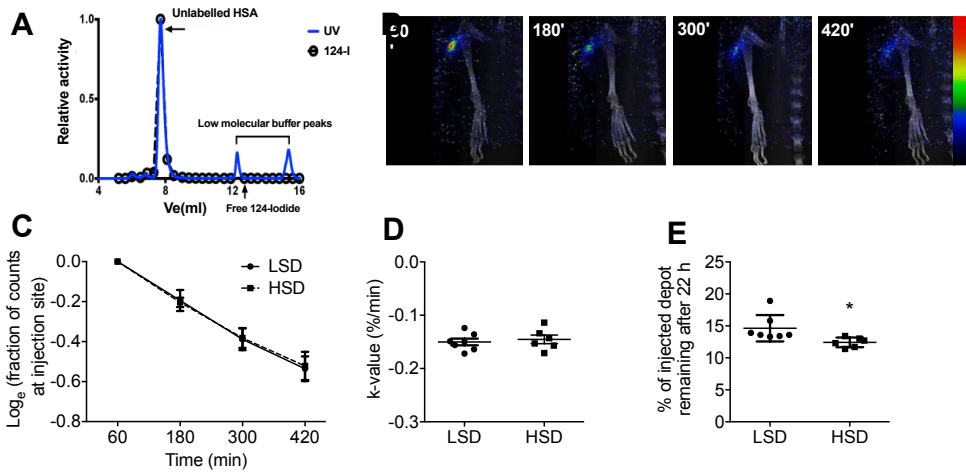


Figure 3. A. HPLC chromatogram of unlabeled native HSA at an ultraviolet (UV) detection of 220 nm compared to elution of ¹²⁴I-labeled HSA counted with a gamma counter. The UV-activity around 12 and 16 ml elution volume represent buffer. Of note, the free ¹²⁴I is zero. B. Representative image of a PET/CT scan showing the time-dependent washout of an intramuscularly injected macromolecular tracer (3 μ l ¹²⁴I-HSA) in thigh muscle. C. Average Log_e fraction of counts remaining in the intramuscularly injected depot of 3 μ l ¹²⁴I-HSA with time in thigh muscle of rats on LSD (n=7) and HSD (n=6). D. Individual rate constants (*k*) calculated as the slope of the monoexponential washout curves for each individual rat in (B) obtained by linear regression analysis. E. Individual values representing the fraction of counts remaining in the intramuscular depot 22 hours after injection of 3 μ l ¹²⁴I-HSA in LSD and HSD. Also shown mean \pm SD. *P<0.05 (unpaired t-test)

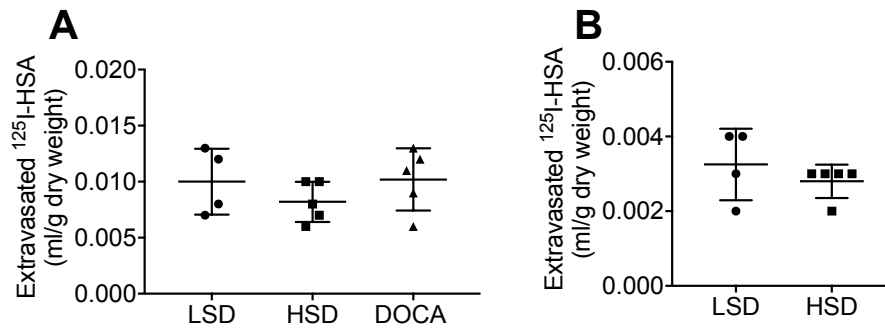


Figure 4. Individual values for extravasation of the radioactive macromolecular tracer ¹²⁵I-HSA from the vasculature into paw skin (A) and thigh muscle (B) after 35 min in LSD, HSD and DOCA-salt diet rats. Five min extravasation of ¹³¹I-HSA was subtracted from these values to correct for any plasma ¹²⁵I-HSA present in the excised tissue at 35 min. Also shown mean \pm SD.

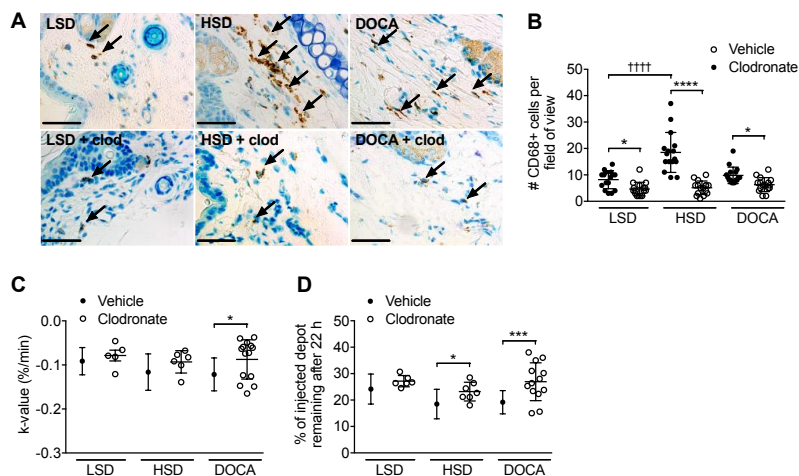


Figure 5. A. Representative staining of MPS cells with CD68 in ear sections from rats fed LSD, HSD and DOCA-salt diet with or without clodronate liposome injection. Scale bar = 50 μm . B. CD68+ MPS cells were counted in 4 consecutive fields per section from 4 rats per group. C. Individual rate constants (k) from skin calculated as the slope of monoexponential washout curves obtained by linear regression analysis for each individual rat in a separate set of experiments where rats on LSD, HSD) and DOCA-salt diet received intraperitoneal liposomal clodronate. Injections (5 mg in 1 ml) every 4th day, started at day 0 of the respective diets, with the last injection at day 12. For comparison, the mean values \pm SD of the rate constants calculated in Fig 2B are also shown, representing k -values from rats on LSD, HSD and DOCA-salt without clodronate injections. D. Individual values representing the fraction of counts remaining in the intradermal depot 22 hours after injection of 3 μl Alexa680-BSA in clodronate injected LSD, HSD and DOCA-salt diet rats. Mean values \pm SD from fig 2C representing rats without clodronate injections are included for comparison. Also shown mean \pm SD for clodronate injected rats. * P <0.05, *** P <0.001, **** P <0.0001 for comparisons within the respective diet groups (unpaired t-tests). †††† P <0.0001 for comparisons between diet groups (ANOVA followed by Dunnett's multiple comparison test).

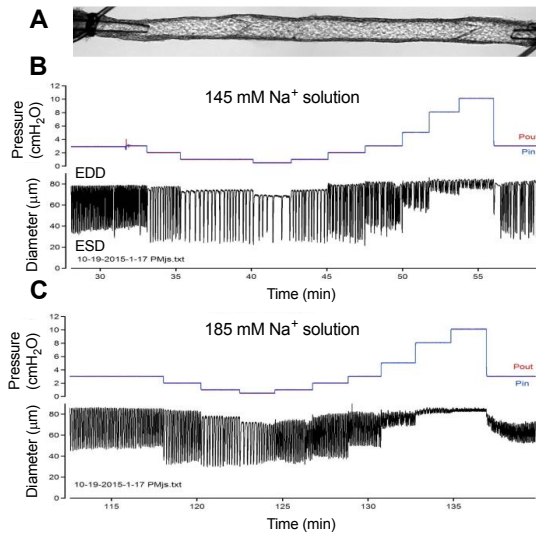
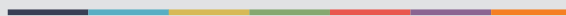


Figure 6. A. An image of a cannulated mouse inguinal afferent lymphatic vessel. B and C. Example recordings showing the pattern of spontaneous lymphatic contractions at each level of pressure (0.5 to 10 cmH₂O) in 145 mmol Na⁺ Krebs solution (B) and 185 mmol Na⁺ Krebs solution (C). Each downward deflection represents a single contraction lasting 3-5 sec. P_{in} and P_{out} are the pressures set by the input and output cannulas, respectively, and were equal throughout the pressure step protocol. Lowering pressure in steps from 3 to 0.5 cmH₂O resulted in a slowing of spontaneous contraction frequency and an increase in contraction amplitude at 1 and 2 cmH₂O but a decrease in amplitude at 0.5 cmH₂O; raising pressure from 0.5 to 10 cmH₂O resulted in an increase in frequency and decrease in amplitude such that only weak contractions were observed at pressures higher than 5 cmH₂O. Exposure of the vessel to 185 Na⁺ Krebs solution produced increases in frequency and slight decreases in amplitude at all pressures (C). Summary of results from 5 vessels exposed to 145, 165 and 185 mmol Na⁺ Krebs solutions and solutions where additional Na⁺ has been replaced by urea. Values mean ± SD. *P<0.05 (ANOVA followed by Bonferroni's multiple comparison tests).



Graphic design: Kommunikasjonsevidlingen, UIB / Trykk: Skjerve Kommunikasjon AS



uib.no

9788230840399 (print)

9788230868379 (PDF)